The Atom Laser

Glenn Michael Moy

A thesis submitted for the degree of
Doctor of Philosophy at
The Australian National University

July 1999

Typeset in Palatino by TEX and LATEX 2ε.

This thesis is an account of research undertaken in the Department of Physics, Faculty of Science, at the Australian National University between March 1995 and August 1998.

This research was supervised by Dr Craig Savage, but unless otherwise indicated, the work presented herein is my own.

None of the work presented here has ever been submitted for any degree at this or any other institution of learning.

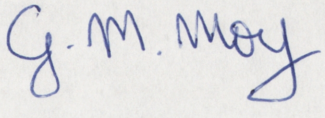

Glenn Michael Moy
1 August 1999

Acknowledgments

'Gratitude is the heart's memory.'

-French Proverb.

I am thankful for the friendship and support of a great number of people during the course of this thesis. Firstly, I would very much like to thank my supervisor, Dr Craig Savage for his constant support and encouragement. His advice and enthusiasm has shaped both this work and my own development as a physicist. I am especially thankful for his ability to see the big picture - both in physics and life in general.

I would also like to thank those who have helped me in producing this thesis. In particular thanks to Geoff Ericksson, Dan Gordon and Joseph Hope for proof reading various parts of this thesis. I have been supported by an Australian Postgraduate Research Award.

Over the course of my PhD I have had the pleasure of sharing my office with Joe Hope and Dan Gordon. I could not have asked for better friends to share the ups and downs of a PhD with. Thank you for many deep conversations, and happy lunches on "the grassy knoll". Our many discussions, both on physics and other topics have greatly influenced the work in this PhD. Thanks also go to other members of the physics department. I have benefited greatly from the helpful insight of Mark Andrews. Thanks also to Jurgen Eschner, Tim Ralph, Allan Baxter, David McClellan, Hans Bachor, Geoff Ericksson, Brett Cuthbertson, PingKoy Lam and Andrew White who have all helped me in various ways through the course of my PhD.

Thanks also to Geoff, Brett, Joe and Dan who taught me that shooting at others with a suitably large cannon is a good stress-management technique and to Ping-Koy and Joe, for inviting me to join in a couple of games of Magic.

There are many other friends both in Canberra and from afar who have provided support during the course of my PhD. My housemates, Tim Surendonk, Paul Wong and Fiona Humphris, along with all my friends from Fenner Hall have greatly contributed to my happiness away from the office. Thanks also to Tony Puclin, Andrew Butterfield and Tim for regular Mountain walks and for allowing me to get to the top first now and then. Thanks also to the members of "the light headed trio" for all the music we shared. I would also especially like to thank those "out of town" friends who kept in touch through many an email, letter or phone call (and to my housemates who had to endure

more than one "short" phone call). In particular, thank you to "Just Norma" for her weekly letters. Many of you helped more than you will ever realize in giving me a sense of perspective throughout this PhD.

Finally, I would like to express my sincerest gratitude to my parents, "Mom" and "Dod" and to my brother and sister, John and Sharon. They have been a constant source of encouragement to me both throughout my PhD and in everything I do.

Abstract

We investigate the pumped and damped atom laser. A rate equation model of the atom laser is presented. This model is based on the geometry of a hollow optical fibre with output coupling achieved through a Raman transition which changes the state of the atoms to an untrapped state. Calculations are presented for overlap elements and transition rates and these lead to rate equations which describe the dynamics of the atom laser. We demonstrate the presence of a threshold in these rate equations and show that Bose-enhancement leads to a large number of bosons accumulating in the ground state mode of the trap.

We give a description of output coupling based on a change of state through Raman transitions. We present an output coupling model based on change of state, and solve this model for the output spectrum and number of atoms in the cavity. We obtain analytic solutions in the limit of broadband coupling. The spectral width of the output spectrum and the shape of the output spectrum is investigated as a function of the coupling strength and of time.

We discuss the use of the Born and Markov approximations in describing the dynamics of an atom laser. We investigate the applicability of the quantum optical Born-Markov master equation for describing output coupling. We discuss conditions for when the Born-Markov approximations are valid for output coupling atoms from a trap. We present results based on an exact method in the regimes in which the Born-Markov approximation fails. The exact solutions in some experimentally relevant parameter regimes give non-exponential loss of atoms from a cavity. We discuss the effects of gravity and atom-atom interactions in the system using a mean field model.

We derive a pump model for an atom laser based on spontaneous emission of atoms into the lasing mode. We show that this is equivalent to other pump models discussed in the context of optical and atom laser theory. We investigate solutions to the input-output equations with the addition of this pumping term and discuss these results in the Born-Markov regime. We also consider the regime where these approximations fail. We extend the mean field model presented earlier to describe the output coupling from a Bose-Einstein condensate. We introduce a phenomenalogical pumping term into this model to provide a mean-field description of a pumped and damped atom laser.

Contents

List of Figures

Chapter 1

Introduction

> Atom - "A hypothetical body, so small as to be incapable of further division."
>
> Laser - "A gum-resin mentioned by Roman writers, obtained from an umbelliferous plant called *laserpicium*."
>
> -Shorter Oxford English Dictionary, 1944.

Atom optics is the study and use of the wavelike nature of atoms. With the development of Bose-Einstein condensates in alkali atoms, there has been enormous progress in this field. Early work in this field led to the development of atom optical devices which are the atomic analogues of optical mirrors, beam splitters, interferometers, and cavities. One of the future goals of atom optics is to develop a source of coherent matter waves which is analogous to the optical laser. The development of a source of coherent matter waves would potentially have as great an influence on atom optics as the development of the optical laser did for quantum optics in the 1960's.

The name which has been most universally used to describe a source of coherent matter waves is "atom laser". Other terms which have been proposed include CAB (Coherent Atomic Beam) [1], MASTA (Matter wave Amplification by Stimulated Transfer of Atoms) and BOSER. These suggestions have been made, in part, to avoid the use of the word "laser" in the name given to a matter wave generator. Originally the acronym "laser" stood for "Light Amplification by Stimulated Emission of Radiation". This definition is clearly not appropriate for a device which does not produce a light beam. Despite this, the strong connection between the physics which describes a coherent atom beam and that of the laser has led to the general acceptance of the term "atom laser". Both the optical laser and the atom laser are devices which produce a beam of bosons (particles with integer spin) with specific properties relating to coherence and intensity. In the former case the bosons are photons, while in the latter case the bosons are atoms.

Optical lasers produce beams of photons with high coherence and spectral brightness. These properties are used in many aspects of our day to day

lives and in almost all fields of scientific endeavor. Optical lasers in modern society occur in devices ranging from supermarket scanners and CD players to laser pointers. They have been used in various surgical techniques and in modern fibre optic communication. Similarly, the use of the laser in scientific disciplines is wide ranging.

Like the optical laser, an atom laser would emit a coherent and spectrally bright beam of bosons. These properties would make the atom laser a useful atomic source for atom optics experiments. However, while atoms are in many ways similar to photons, there are obvious differences. Such differences mean that the atom laser will have uses which are considerably different from those envisioned by comparison with optical devices. Particular areas of atom optics that would benefit from an atom laser include lithography, nanotechnology and atomic interferometry. One of the possible advantages of atoms over photons is that atoms have internal electronic structure. This may lead to practical uses of the atom laser for quantum coding or computation. A further difference between atoms and photons is that they have different dispersion relations. This may lead to different output properties from the atom and photon lasers. Finally, atoms interact with one another, while photons do not.

The experimental feasibility of the atom laser was given a dramatic boost in 1995 with the development of a Bose-Einstein condensate (BEC) in alkali gases [2–5]. To create a BEC, a large number of bosonic atoms are cooled to temperatures of a few nanoKelvin. At sufficiently low temperatures the thermal de Broglie wavelengths of atoms will overlap. A phase transition occurs which leads to a macroscopic number of atoms populating a single mode. This highly populated mode, the condensate mode, bears many similarities to the lasing mode in an optical laser. The BEC is usually assumed to have a global phase due to spontaneously broken gauge symmetry. This is similar to the phase of an optical laser - though there are important differences which we discuss later. In principle a Bose-Einstein condensate, consisting of a single mode which is populated by a large number of atoms with a global phase, could be turned into an atom laser by the introduction of a suitable output coupling mechanism and pump. We discuss these and other related ideas more fully in section 1.4.

1.1 Thesis plan

This thesis is arranged as follows:

In this chapter we will give an overview of the current theory of the atom laser. We will discuss what is required from the output of an atom source for it to be called an atom laser. We also describe the essential elements of an atom laser. Following this we review and compare the main models of atom lasers

which have been proposed to date. We separate these into three main classes based on the theoretical framework on which they are built. These classes are (a) rate equation models, (b) master equation models and (c) mean-field models.

In Chapter 2 we present our rate equation model of an atom laser. We consider a geometry based on a hollow optical fibre. We also model output coupling through a Raman transition, which allows the atoms to change state to an untrapped state. The calculations are done in three dimensions, and overlap elements and transition rates are calculated explicitly. We create rate equations similar to those obtained independently by other groups and we show the presence of threshold behaviour in our model.

The model presented in Chapter 2 allows us to investigate the workings of an atom laser, but gives no information about the quantum statistics, spectrum or other properties of the output beam. In Chapter 3 we begin to consider a fully quantum mechanical model of the atom laser. We present an output coupling model based on change of state, and solve this model for the output spectrum and number of atoms in the cavity. These solutions show results which would not be expected from a standard master equation description of the atom laser.

In Chapter 4 we attempt to reformulate the output coupling theory of Chapter 3 in a master equation context. We show that this is only possible in certain parameter regimes, and that the Born-Markov approximation fails in the case of large output coupling rates. This is due to a combination of factors, including the different parameter regimes appropriate for atoms, the atom dispersion relations and the nature of the atom reservoir. Our solutions in some regimes lead to an atom number in the cavity which does not decay to zero. We present a mean-field theory of our output coupling which includes the effects of gravity on the atoms and show that the atom number does decay to zero for long times in this case. Because of the assumption that the atoms can be described by a mean field it is impossible to use this model to describe the statistics of the output field.

In Chapter 5 we consider the pumping of an atom laser. We derive a pumping term for our atom laser. We find that in the regimes where output coupling leads to a non-zero steady state for the unpumped cavity atom number, the equivalent *pumped* cavity atom number does not reach a steady state, but continues to grow with time. We extend the mean-field model presented in Chapter 4 using a position basis description of the trapped atoms and introduce a phenomenological pumping term into these equations. This approach gives a mean-field model of the pumped and damped atom laser.

1.2 Summary of major results

The primary results of this thesis have been accepted for publication in the following journal articles:

The rate equation model outlined in Chapter 2 appeared in the paper:

- G.M. Moy, J.J. Hope and C.M. Savage: *An atom laser based on Raman transitions*, Phys. Rev. A, **55**, 3631, 1997.

The work outlined in Chapter 3 on the output spectrum obtained by coupling atoms out of a single mode trap has appeared as a Rapid communication:

- G.M. Moy and C.M. Savage: *Output coupling from an atom laser by state change*, Phys. Rev. A, **56**, 1087, 1997.

The work presented in Chapter 4 on the Born and Markov approximations in relation to output coupling from an atom laser has been accepted for publication in the Physical Review A, and is tentatively scheduled for publication as:

- G.M. Moy, J.J. Hope and C.M. Savage: *The Born and Markov approximation for atom lasers*, Phys. Rev. A, 1999.

A further paper, related to the work presented in Chapter 5 is in preparation.

- G.M. Moy, J.J. Hope and C.M. Savage: *A pumped and damped atom laser.*

1.3 The optical laser

In this section we give a brief discussion of the workings of a typical optical laser. This section is included to give readers unfamiliar with optical laser theory a somewhat simplified overview of how an optical laser works. Our approach comes from Siegman [6], in which a detailed semiclassical laser theory is presented. A quantum mechanical theory of the laser can be found in [7]. The quantum theory will be discussed further in the context of atom laser models in later chapters.

The basic elements of a typical laser, as outlined by Siegman [6] are given in Fig. 1.1. The important elements in this figure are (a) the pumping process, (b) the feedback process (optical cavity) and (c) the output coupling. The pumping process is indicated symbolically with the use of arrows and includes a "laser medium". The laser medium typically consists of a collection of atoms, molecules or ions. The pumping process excites this medium into excited states. In a laser, pumping must produce a population inversion in the

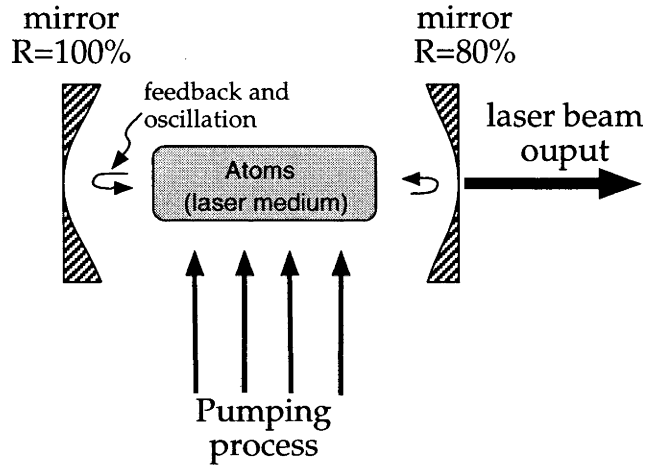

Figure 1.1: Schematic layout of optical laser reproduced from Siegman [6].

laser medium. Population inversion means that a greater number of atoms (we assume the laser medium is atoms here) are in an excited state than in the lower energy level. Atoms in the higher energy levels can relax back to the lower energy level, emitting a photon of electromagnetic radiation in the process. This photon has a particular frequency corresponding to the frequency of the transition between the excited and lower energy levels.

Once a population inversion has been obtained any electromagnetic radiation, with a frequency which is close to this atom transition frequency, can be coherently amplified if it passes through the laser medium. This occurs through Bose enhancement, in which photons (bosons) in a particular mode of a cavity or resonator (and hence with a particular frequency) stimulate the production of further bosons in that mode. The mirrors provide a feedback mechanism so that the additional photons created in the Bose-stimulation are not lost from the system instantaneously, but can themselves stimulate the production of further photons of the same frequency.

The final component of the optical laser system is the output coupler. Output coupling is typically achieved through using a partially transparent mirror on one side of the optical cavity. This allows a bright coherent beam to be emitted from the cavity when lasing occurs. For the laser to operate the net amplification between the mirrors must exceed the net loss of photons from the mirrors and other losses such as scattering.

1.4 What is an atom laser

Before we discuss the atom laser, it is important to consider more closely what is meant by the term "atom laser". This is a topic which has been considered at some length by various authors - most notably by Wiseman [8] and Holland [9]. We will discuss these here. While we present a number of definitions and related ideas here, ultimately we will avoid choosing a particular definition of what qualifies as an atom laser in this thesis. Instead we focus on the various properties that we may require out of an atomic source which may be considered analogous to the optical laser. For instance the rudimentary atom laser produced by output coupling a BEC [4] does not have some of the desirable properties one would require of an atom laser. Nevertheless, it does have properties which are the atomic analogue of a pulsed optical laser. We therefore choose to include this and other similar devices in the term "atom laser".

In the following section we begin by describing the basic components involved in an atom laser scheme, drawing on analogies between these components and the optical laser.

1.4.1 Components of an atom laser

From an experimental point of view the question "What is an atom laser" could be better interpreted as "how do I make an atom laser?" Various schemes have been suggested for atom lasers. Many of these are based on an analogy with the optical laser. There are a number of basic components which all (atom) lasers have. These have been discussed to various degrees by authors producing atom laser models. Here we describe three basic components which are present in all atom laser schemes.

1. A cavity, or resonator.

2. A source of bosons - partially coupled to the resonator.

3. An output mechanism.

These components have analogies in optical (and other) laser systems. These were initially presented at IQEC96 in a talk entitled "The Atom Laser" [10]. A similar classification of the components of an atom laser has been proposed by Wiseman [8]. We discuss each of these in turn in the following sections.

A cavity

The first requirement for a laser is a resonator or cavity. This is required to create the lasing mode. During the operation of a laser the lasing mode is populated with a large number of bosons. In the optical laser, the cavity is typically created using two mirrors. A large number of bosons, (photons in this case) populate a mode or a number of modes of the optical cavity. In an optical laser, the lasing mode is usually a high order mode of the cavity.

In an atom laser, the resonator is usually an atomic trap. In a typical atom laser a large number of bosonic atoms populate the ground state mode of the system. More generally, one could consider populating non-ground state modes for a Bose-Einstein condensate or atom laser [11].

A source

The second requirement for an atom laser is the presence of a source of bosons. That is, a laser requires some form of pumping. In an optical laser, this corresponds to the emission (creation) of photons from an atomic sample. Typically the sample has been pumped so that the atoms undergo population inversion as discussed in section 1.3.

The photons which are created do not all populate the lasing mode, however. Rather there are two possibilities for an excited state in the source. It can irreversibly introduce new photons into the lasing mode, or the excited state may be lost in a spontaneous process.

A final property of an optical source is that it can be depleted. While the source may be continually replenished on some time scale, it is nevertheless not possible to produce an arbitrarily large number of photons in an arbitrarily short time.

These considerations are also required for an atomic source. That is, there must be a finite production of bosonic atoms which are coupled into the lasing mode, along with a loss channel where atoms are not transferred into the lasing mode. At first glance the ability of the atom laser to deplete the source and the presence of a loss channel may seem unimportant. We will see later that these properties are important for the presence of behaviour such as threshold and linenarrowing.

An output coupler

The final requirement for an atom laser is a method of producing the output beam. In optics this consists of having one of the mirrors which form the optical cavity partially transparent. As a result, when a large photon field builds up inside the cavity, some of the photons will be lost through the end mirror in a beam.

For atoms, output coupling may be somewhat more complex. In principle, atoms can tunnel out of atomic cavities. This process is equivalent to optical output coupling through a partially transparent mirror. Unfortunately, in an atom laser, tunneling is not a practical method of getting large output flux out of a trap. This is due to the extremely small tunneling rates which occur for physically realisable confining potentials and the exponential dependence of tunneling rate on trap parameters. Typically, some other method, such as having the atoms undergo an atomic transition, must be employed to transfer the atoms to a non-trapped state. In this state they no longer experience the confining potentials which form the cavity. To create a directed beam of atoms, it may also be necessary to give the atoms a kick. This could be achieved through acceleration due to gravity, or a momentum kick from laser photons.

1.4.2 Experimental progress towards the atom laser

In this section we review experimental progress to date towards producing an atom laser. Currently this work has centred around systems which implement a cavity and an output coupler. Because these schemes do not provide a continuous source of atoms, the atom lasers demonstrated to date are pulsed.

The first experimental "atom laser" was produced at MIT in 1996 [12] with sodium atoms condensed in a magnetic trap. In this experiment, an rf output coupler was used to create Bose condensates in a superposition of trapped and untrapped states. Output pulses of coherent atoms were demonstrated. In the initial experimental work, the issue of the coherence of the output beam was not considered in detail. In the Bose-Einstein condensate produced in the magnetic trap, a macroscopic population of the ground state of the system was achieved.

The output coupling of the atoms was achieved through an rf-induced transition of the atoms into a non-trapped state. Gravitational acceleration gives the output a direction. A simple model of the output coupling process is presented below.

The simplest model of output coupling involves a single two-level system [12]. The system has two states, $|1\rangle$ and $|2\rangle$, with state $|1\rangle$ trapped. The system begins with a BEC of atoms in this state. A resonant rf pulse is applied to the BEC so that states $|1\rangle$ and $|2\rangle$ become coupled. State $|1\rangle$ evolves into the superposition

$$\cos(\omega_R \tau/2)|1\rangle + \sin(\omega_R \tau/2)|2\rangle. \tag{1.1}$$

Here ω_R is the single particle Rabi frequency. For the many particle system, the wavefunction of the system is given by

$$\sum_{n=0}^{N} \sqrt{\frac{N!}{n!(N-n)!}} \cos^{N-n}(\omega_R \tau/2) \sin^{n}(\omega_R \tau/2) \, |N-n, n\rangle, \tag{1.2}$$

where $|N-n,n\rangle$ is the many-particle state with n atoms coupled out into state $|2\rangle$. N is the total number of atoms in the system. From Eq. (1.2) we see that the fraction of atoms coupled out of the condensate oscillates with the single particle Rabi frequency.

In practice the experiment performed by Mewes *et al.* [12] used a three-state system in which the rf radiation coupled the trapped $m_F = -1$ state to an untrapped, $m_F = 0$ state. This, in turn was coupled to the $M_F = 1$ state which is expelled as atoms in the $m_F = 1$ state are strong field seekers and are accelerated away from the trap centre. Experimental results from the output coupler are shown in Fig. 1.2.

Figure 1.2: Image taken after pulsing four bursts of atoms each 5ms apart using the rf output coupler. (Data reproduced from Mewes *et al.* [12]).

1.4.3 Coherence, BECs and the atom laser

So far we have discussed the atom laser by analogy with components found in an optical laser. The reason a laser is an interesting device in physics, however, is due to the nature of its output, and not due to the components which make it up. The output of a laser has a narrow output spectrum, is intense and coherent. Similar properties are required from an atom laser.

The simplest definition of an atom laser, which we introduced earlier, is that an atom laser is a device which emits a coherent beam of atoms. We now discuss what is meant by coherence in the context of an atom beam. To begin with, coherence is not a particle property, but rather a property of fields. Thus, to describe atom-coherence it is useful to use a second quantized description of atoms. By using a second quantized description it is possible to consider an atom field that is formally very similar to the photon field.

Generally, what is meant by coherence depends on the situation in which the term is used. One typical signature of coherence, which is required in classical optics, relates to the ability to produce well defined interference fringes. The visibility of fringes, however relates only to the first-order spatial coherence.

Spatial coherence - theory and experiment

First Order Coherence

As we have discussed above the ability to observe interference fringes is related to the first order coherence function which is defined as

$$g^1(x1,x2) = \frac{G^1(x1,x2)}{\sqrt{G^1(x1,x1)\,G^1(x2,x2)}}, \tag{1.3}$$

where

$$G^1(x1,x2) = \langle \hat{\psi}^\dagger(x1)\hat{\psi}(x2)\rangle. \tag{1.4}$$

In these equations we have used the operator, $\hat{\psi}(x)$ to describe the field annihilation operator at position x. From the definition given in Eq. (1.3) we note that we can achieve fringes with perfect visibility ($g^1(x1,x2) = 1$) for any single mode excitation. This is one of the reasons a "leaky BEC" is a prime candidate for an atom laser. In a BEC a large number of atoms are cooled into a single mode. Theoretically, the first order coherence function of a Bose-Einstein condensate is approximately unity and will show clear interference fringes.

The first order spatial coherence of two freely expanding Bose-Einstein condensates has been observed experimentally by the detection of interference fringes [13]. In this experiment two condensates separated by 40μm were

created in a double-well potential. The potential was switched off and the condensates left to expand over a period of 40ms after which time they overlapped. High contrast matter-wave interference fringes were observed indicating that the BECs were first order coherent. The technical details of this experiment are outlined in Andrews *et al.* [13]. In particular, issues regarding other possible explanations for the interference patterns, such as the fringes being due to density waves of two colliding condensates, were considered. Fig. 1.3 shows the interference pattern of two expanding condensates observed after 40ms time-of-flight. These experiments demonstrate evidence of spatial

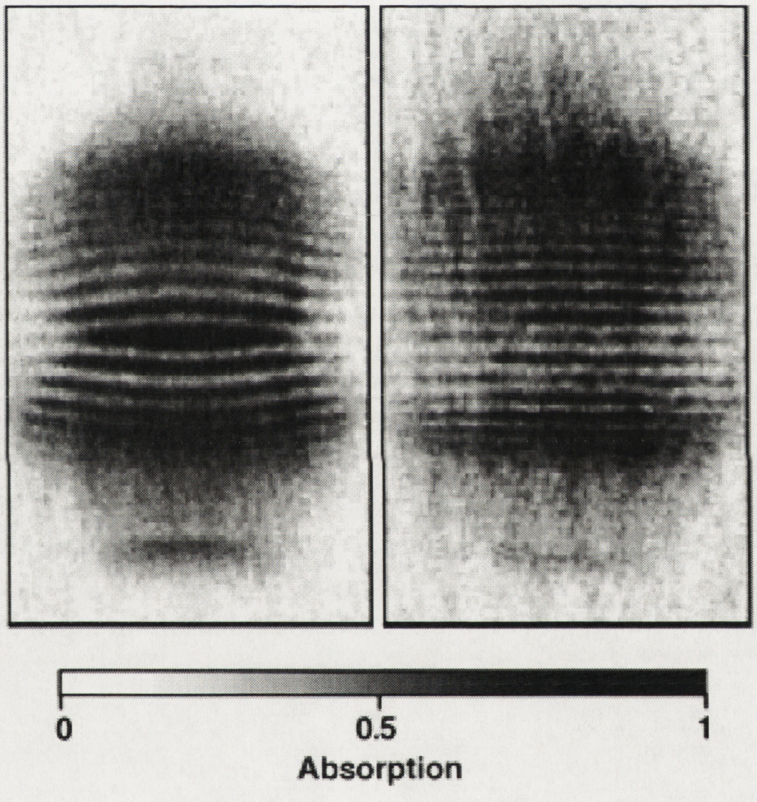

Figure 1.3: Interference pattern of two expanding condensates. The right and left figures correspond to different powers of the argon ion light sheet used to separate the two condensates. (Figure reproduced from Andrews *et al.* [13]).

coherence over the extent of the condensates.

Second Order Coherence

We have noted that fringes with perfect visibility can be achieved from any single mode excitation. In practice this may be all we require from our atom

source. Nevertheless, as for the optical case, the presence of interference fringes does not distinguish a coherent field from a filtered chaotic field of a thermal source.

The second order coherence function is used in optics to describe a correlation between two separate photon detection events. Similarly, for matter waves, the second order coherence function distinguishes between a thermal and coherent source. The second order spatial coherence function is defined as [14]

$$g^2(x1,x2) = \frac{\langle \hat{\psi}^\dagger(x_1)\hat{\psi}^\dagger(x_2)\hat{\psi}(x_2)\hat{\psi}(x_1)\rangle}{\langle \hat{\psi}^\dagger(x_1)\hat{\psi}(x_1)\rangle \langle \hat{\psi}^\dagger(x_2)\hat{\psi}(x_2)\rangle}. \tag{1.5}$$

In particular, the zero separation second order coherence function is given by $g^2(x,x)$. In the case of an homogeneous source, the second order coherence function for a thermal gas is $g^2(x,x) = 2$ and for a BEC or coherent source $g^2(x,x) = 1$. A general discussion of the second order coherence function in the non homogeneous case is given in [15]. Experimentally, the second order coherence of a matter wave source or BEC can be investigated through measuring the atom-atom interaction energy of the condensate [15,16]. This is because for a short-range potential, the interaction energy is proportional to the probability that two atoms are at the same position, which is in turn proportional to $g^2(x,x)$. Experimental evidence summarized in [16] is consistent with $g^2(x,x) = 1.0 \pm 0.2$. This supports the assumption that condensates do suppress local density fluctuations and have second order spatial coherence functions which are approximately unity. In fact, the different spatial distributions of condensate and thermal atoms in a trap mean that the experimental determinations of $g^2(x,x)$ give only its spatial average, and as such may actually underestimate the degree of coherence attainable in an atom laser [15].

Third Order Coherence

Further experimental evidence of higher order coherence in Bose-einstein condensates is given by Burt *et al.* [17]. In this paper a careful comparison of the three-body recombination rate constant in condensed and non-condensed Bose gas provides strong quantitative evidence for the existence of higher-order coherence in Bose-condensed rubidium. In this experiment, the ratio of the $g^3(x,x,x)$ values of a thermal cloud to a Bose-condensed gas was obtained at 7.4 ± 2 in good agreement with the predicted value of 6. This is the first demonstration of the third-order coherence of a Bose-Einstein condensate.

Temporal coherence - theory and experiment

First Order Coherence

Currently only a pulsed source of matter waves has been produced in the laboratory. Ultimately one would want a continuous output beam which is stationary. A stationary beam is one in which the first order temporal coherence, $g^{(1)}(t+\tau,t) = g^{(1)}(\tau)$ does not depend on t. The first order temporal coherence function for an atom laser beam is defined as

$$g^{(1)}(\tau) \equiv g^{(1)}(t+\tau,t) = \frac{\langle a^\dagger(t+\tau)a(t)\rangle}{\sqrt{\langle a^\dagger(t)a(t)\rangle}\sqrt{\langle a^\dagger(t+\tau)a(t+\tau)\rangle}}, \tag{1.6}$$

$$\equiv \frac{\langle a^\dagger(t+\tau)a(t)\rangle}{\langle a^\dagger a\rangle} = \frac{G^{(1)}(\tau)}{\langle a^\dagger a\rangle} \tag{1.7}$$

where we define operators, $a(t), a^\dagger(t)$, at a fixed point in space, such that the operator $I(t) = a^\dagger(t)a(t)$ can be interpreted as the atom-flux at some specified position [8]. The notation used in Eq (1.7) suppresses the t dependence and is valid for a stationary beam. The first order temporal coherence function is a useful measure of phase fluctuations, which we require to be small for a laser like source.

For a laserlike, first order temporally coherent source, $g^{(1)}(\tau) \approx 1, \forall\tau$. This is in contrast to a non-first order coherent source, in which over time the phase of the field gradually becomes decorrelated from its value at time t. That is $g^{(1)}(\tau)$ tends to zero as τ tends to infinity. Currently no continuous matter-wave source has been experimentally built, however even when such a source is built, it is clearly impossible to have a source which has $g^{(1)}(\tau)$ remain approximately unity for an infinite amount of time. We discuss a practical first order coherent criterion put forward by Wiseman in the following section. This would relate to a continuous source of matter waves which could be obtained by continuously pumping a BEC.

Second Order Coherence

As well as first order temporal coherence, a laser beam also requires higher order temporal coherence. The second order temporal coherence function is defined as

$$g^{(2)}(t+\tau,\tau) = \frac{\langle a^\dagger(t)a^\dagger(t+\tau)a(t+\tau)a(t)\rangle}{\langle a^\dagger(t)a(t)\rangle\,\langle a^\dagger(t+\tau)a(t+\tau)\rangle}, \tag{1.8}$$

$$g^2(\tau) \equiv \frac{\langle :I(t+\tau)I(t):\rangle}{\langle I\rangle^2}, \tag{1.9}$$

The second definition, Eq. (1.9) for the second order coherence function is given for a stationary beam in terms of the normally ordered expectation value. The second order coherence function is related to amplitude correlation and is approximately unity for a coherent source. One consequence of having a second order coherent source of matter waves is shown in the arrival times of bosons in the output. As for the optical laser, a filtered thermal beam leads to superpoissonian statistics for the arrival time of bosons, whereas a source with $g^{(2)}(\tau) = 1$ has Poissonian statistics.

In this section we have introduced some concepts of coherence for atom lasers. These indicate that the output from a Bose-Einstein condensate can be regarded as a highly coherent beam of matter waves.

Using notions similar to the ones discussed in these sections, Wiseman [8] has put forward a specific definition of an (atom) laser. While we will not restrict ourselves in this thesis to this definition (for instance it excludes pulsed atom lasers of the style we have discussed above) it provides one clear definition of what properties one may require from a continuous, coherent matter wave source. In its most succinct form, this definition states that a laser is a device which "produces an output which is well approximated by a classical wave of fixed amplitude and phase." Accompanying this are various criteria which elucidate this general principle.

1.4.4 One definition of a laser

The first requirement, suggested by Wiseman [8], for a source to be considered an atom laser is

1. Directionality: The output is highly directional.

This criteria introduces the idea that a laser should produce a beam. This enables one to define a direction of propagation and directions of diffraction. For a laser source, one would normally wish to limit the amount of spreading of the laser beam through diffraction. This can be achieved through waveguides (both for the optical and atomic case). It would be preferable for the output of a laser to have a few, or ideally a single, transverse mode. This can be achieved by employing waveguides with sufficiently narrow confinement in the transverse directions.

The second condition Wiseman discusses regards monochromaticity.

2. Monochromaticity: The longitudinal spatial frequency of the output beam has a small spread.

In principle we would want a source which is perfectly monochromatic,

however in practice this is never possible. As we discussed in section 1.4.3, a large number of atoms populating the lowest energy mode of a system such as in a BEC, is perfectly monochromatic in the sense that the atoms in the BEC have a single well defined energy. When it is coupled out of the trap it will have a range of energies in free space. When we require the beam of atoms to be monochromatic we mean that this spread in energy is as small as possible.

If we consider an output beam with a spread in spatial frequencies, δk about a mean $\bar{k}$ then we want the spread to be sufficiently narrow to give a large coherence length. Here we define the spatial frequency, k in the reference frame in which the laser is at rest. We need to choose this frame as the spatial frequency, k will transform with a change of reference frame under a Galilean transformation. Typically, we want the coherence length to be long on a scale compared with the de Broglie wavelength of the atom beam in this rest frame. Thus we have the condition that $l_{\text{coh}} >> \lambda$, and from $\lambda = 2\pi/\bar{k}$ and $l_{\text{coh}} = 1/\delta k$ we get the condition $\delta k << \bar{k}$, as given by Wiseman. This monochromaticity condition can also be defined in terms of a frequency spread as $\delta\omega << \bar{\omega}$. Here we have defined the frequency, $\bar{\omega}$ in terms of the kinetic energy,

$$\bar{\omega} = \frac{\hbar\bar{k}^2}{2M}, \tag{1.10}$$

where M is the mass of the individual atoms.

This monochromaticity condition discussed must hold for an arbitrary laser - be it a photonic laser or a matter laser. However, for massive particles an extra requirement needs to be considered. An atom wavepacket travelling over time will spread. We define a characteristic lengthscale over which this spreading takes place, the dispersion length. A further condition on the output from the laser is that the dispersion length is much greater than the wavelength of the output. This condition is

$$l_{\text{disp}} >> \lambda. \tag{1.11}$$

The dispersion length, $l_{\text{disp}} = \bar{k}/(2(\delta k)^2)$, is defined as the distance over which the variance of the initial wavepacket doubles. This condition is already guaranteed by the monochromaticity condition given earlier.

The first two of Wiseman's criteria only depend on first order coherence. As discussed in section 1.4.3 this is all that is required if we wish to do atom interferometry with our atom laser beam. However, there are other measurements one could make on a single mode which depends on higher order coherence.

The two final conditions which Wiseman presents as requirements for an atom laser relate to the presence of higher order coherence. The conditions are

3. Well defined intensity: The output intensity fluctuations are small

in the sense that $\forall\tau|\langle: I(t+\tau)I(t) :\rangle - \langle I\rangle^2| << \langle I\rangle^2$

4. Well defined phase: The output phase fluctuations are small in the sense that $\int d\tau|G^1(\tau)| >> 1$.

The term, $G^1(\tau)$, here is the unnormalized version of the first order coherence function, defined in section 1.4.3. Wiseman motivates these two conditions by defining operators, $b(t), b^\dagger(t)$, such that $I(t) = b^\dagger(t)b(t)$ is the atom-flux at some specified position (see section 1.4.3). Conditions 3 and 4 are then obtained from the fundamental principle that for a laser we require the output to be well approximated by a classical wave of fixed intensity and phase. That is that the operator $b(t)$ can be approximated by $\beta e^{-i\omega t}$ with β a complex number. This does not mean that $\langle b(t)\rangle \approx \beta$, however as this expectation value is always zero for an atomic field (see section 1.4.5). Instead Wiseman suggests the criterion that $b(t)$ is be well approximated by $\beta e^{-i\omega t}$ if

$$\langle b^\dagger(t)b(t)\rangle = |\beta|^2, \tag{1.12}$$

and if the fluctuations in $I(t)$ are sufficiently small, as given by the two-time correlation function for $I(t)$. Using the definition given in section 1.4.3, Wiseman's condition that the normally ordered fluctuations in intensity are much less than the average intensity squared is equivalent to saying that $|g^{(2)}(\tau) - 1| << 1$. That is, we require the output of the laser to be (approximately) second order coherent.

The final criterion - that a laser has a well defined phase - is a criterion which is related to the monochromaticity condition mentioned earlier. In section 1.4.3 we mentioned that in practice we cannot have a beam which has $g^{(1)}(\tau) \approx 1$ for all times, τ. The relevant quantity, therefore, is how long it takes for $g^{(1)}(\tau)$ to decay. Wiseman defines the characteristic time for this decay, the coherence time as

$$\tau_{\text{coh}} = \int_{-\infty}^{\infty} |g^{(1)}(\tau)|d\tau. \tag{1.13}$$

This is the time over which the phase of the field is approximately constant. As a result, measurements of phase must be made on a timescale which is smaller than τ_{coh}. To make an accurate measurement we need to have a large number of bosons arrive on this timescale, one requires that $\langle I\rangle \times \tau_{\text{coh}} >> 1$, where I is the output flux of bosons. This is equivalent to condition 4, given by Wiseman.

Furthermore, this condition can be restated in terms of the width of the power spectrum. The power spectrum is defined as

$$P(\omega) = \frac{1}{2\pi}\int e^{i\omega\tau}G^{(1)}(\tau)d\tau. \tag{1.14}$$

Typically this spectrum has a well defined shape (for instance Lorentzian), with a linewidth, $\delta\omega$. The smaller $\delta\omega$ is, the closer the field is to being perfectly monochromatic. The linewidth, $\delta\omega$ is related to the time over which the phase of the field is approximately constant, $\delta\omega = 1/\tau$ so that condition 4 can be written as a further condition on the monochromaticity of the output source, $\delta\omega << \langle I \rangle$. Unlike the earlier monochromaticity condition, condition 4 can not be made more valid by longitudinally accelerating the atom laser beam.

The four conditions discussed above give a detailed definition of an atom laser as presented by Wiseman.

Similar conditions have been put forward by Holland *et al.* [9]. These criteria can be summarized as

1. The atoms have a long temporal coherence length corresponding to a very narrow fluctuation spectrum.

2. The atoms have a long spatial coherence length.

3. The spectral width of the output decreases in direct proportion to the number of intracavity bosons.

4. The source must contain an extremely small band of frequencies and only a very narrow cone of spatial modes.

These criteria are strongly related to those we have already discussed and are again based on the coherence criteria discussed in section 1.4.3. For instance, the first criteria requires the output to have a long coherence time. We have already seen that having a long coherence time, τ compared with the average intensity is equivalent to having a suitably well defined phase. Similarly having a long spatial coherence length leads to the monochromaticity condition. The final two properties were suggested to differentiate the output of a laser from a device which produces a long coherence length by filtering the output field from a high temperature thermal source. One disadvantage of using these criteria is that by mentioning the intracavity number, the definition of the laser depends on both the output field and on the properties of the source.

Finally, it should be noted when considering these definitions that the meaning of atom-laser is most well defined by usage. In optics, there are many example of "lasers" which certainly do not satisfy at least one of the criteria outlined above. With this in mind, we will tend to keep a relatively broad view throughout this thesis of what qualifies a device as an atom-laser.

1.4.5 Differences between atom laser and optical laser

In the preceding sections much of the discussion has centred on the similarities between the atom and optical lasers. While there are many similarities,

the differences between atom and optical lasers are also of considerable interest to those investigating atom lasers. We summarize below some of these differences:

Atoms have mass. As well as affecting their dispersion relation, this means that atoms are accelerated by gravity. A matter wave beam will fall unless supported by a waveguide.

Atoms have a different dispersion relation to photons. This changes the details of the dynamics of the atom laser, along with its coherence properties and mechanisms for its decay and decoherence that are related to the dispersion relation. We discuss this further in Chapter 4.

Atoms interact with each other. Repulsive interactions typically create additional spreading of the output beam. Interactions also tend to destroy coherence properties of the atom laser.

Atom lasers work in different parameter regimes. There are various quantities which are different in the atom case. One example, which we discuss in Chapter 4 is that the system frequency, ω_0 for a typical atom trap is many orders of magnitude smaller than for a typical optical trap. Moreover, atoms populate the ground state single mode of a trap in all atom laser currently proposed, whereas lasers tend to operate on (typically more than one) higher modes of the laser cavity.

The atomic field is not a gauge field. The atom field and the photon field are fundamentally different in nature. In part this is related to the fact that atoms cannot be created or destroyed. While the number of photons in an optical laser is amplified, the same is not true of an atom laser. Rather it is the number of atoms in the lasing mode which is amplified in the atom laser. Furthermore, for an atom field it is impossible for any true mean-amplitude to be generated in a physical process. Thus $\langle a(t) \rangle = 0$ for the atom laser. In fact, this is not a particularly significant difference between optical and atom lasers practically. The result $\langle a(t) \rangle = 0$ is also generally true for photon lasers [18], though photons can be prepared in a superposition of states with different numbers of photons. In the photonic case the result can be understood as a classical average over all possible phases. For atoms, in principle, states with $\langle a(t) \rangle \neq 0$ cannot be generated through any physical process. Nevertheless, in practice spontaneous symmetry breaking assumptions lead to a nonzero expectation value. Making spontaneous symmetry breaking assumptions does not lead to contradictions, and provides a useful framework for understanding the atom laser and Bose-Einstein condensates. A useful discussion

which addresses this question of "why a condensate can be thought of as having a definite phase" is given by Barnett *et al.* in [19]

The significance of each of these differences will be discussed in more detail in later chapters of this thesis.

1.5 Models of atom lasers

A number of proposals for atom laser models have been put forward. The basic operation of these is similar to that outlined above, however the details of the schemes and the theoretical framework on which they are based differs somewhat. We outline the basic models which have been proposed here, before moving on to discuss our own model. We choose to break up our discussion of models of atom lasers into three main groups. These groups categorize the theoretical framework used to describe the atom laser. These are:

1. Rate equation models
2. Master equation (quantum operator) models
3. Mean field models

Each of these approaches has various advantages and disadvantages. Many early atom laser models (including our own model which we discuss in Chapter 2) were based on rate equations. These models analyse the atom laser using an equivalent approach to the semiclassical theory of optical lasers. Like semiclassical optical models, these atom laser models are relatively simple and ignore many of the quantum mechanical features of the laser output. In the regimes where they are valid, they are a useful tool for understanding the basic mechanisms and working regimes of the atom laser. They have the disadvantage, however that they are unable to properly describe the coherence properties of the output from the atom laser. In view of the criteria we previously discussed as to what constitutes an atom laser, this is a serious flaw. Of course, such a criticism can also be made of the rate equation approach for optical lasers. In fact, despite this flaw, rate equations do provide a useful tool for describing aspects of the laser dynamics such as the onset of a threshold, and the role of Bose-enhancement. Despite the inability to model the output spectrum of the atom laser, the output is designed in these approaches to behave like a laser. Indeed, we have already discussed that output coupling atoms from a trap in which a large number of atoms has built up in a single mode leads to coherence properties similar to those found in the laser.

The second approach we discuss involves using a master equation. The master equation is an equation of motion for the reduced density operator,

which describes the quantum state of the atom laser system. This allows the quantum mechanical state of the laser output to be fully investigated. The most obvious disadvantage of these schemes is the requirement for many simplifications in these models to make the analysis possible. A further problem with this approach, which we discuss in Chapter 3, is that the terms commonly used in the master equation treatment involve approximations which are not necessarily valid when output coupling atoms from an atomic trap. For this reason we also discuss general "quantum operator models" which may not use the standard master equation formalism to describe the atom laser.

The final approach is a quantum mean-field approach. Mean field atom laser models are typically based on the modelling of a BEC. The nonlinear Schrödinger equation is used to describe the atom laser. Terms are introduced which describe the pumping and output coupling. These models lie somewhere in between rate equation models and full master equation models in describing the atom laser. The biggest disadvantage of these models is that they, by necessity, assume that the field is in a coherent state. This means that the quantum statistics of the output cannot be obtained - as we have lost information about the quantum field fluctuations by making the mean field approximation. Despite this, the mean-field approach is useful in describing realistic output coupling experiments because it allows atom-atom interactions to be introduced into models. In Chapter 5 we consider a mean field model of a pumped and damped atom laser.

We now present an overview of the published atom laser schemes to date.

1.5.1 Rate equation approach

There are three main rate equation atom laser schemes which have been suggested to date [20–22].

Olshanii *et al.*

In [21], Olshanii *et al.* present an atom laser model in which they show a build up of a large number of atoms in a single mode. They model atoms with initial momenta of the order of or smaller than $\hbar k$ being injected in an atomic cavity in state a with rate R_a. These decay to a lower state, b, and they are then trapped by an external potential forming a 3-dimensional box with a volume V. The magnitude of the momentum of atoms in state b must be less than or equal to $p_0 = 2\hbar k$. The factor of two allows for the photon recoil due to spontaneous emission. Thus, in momentum space the atoms lie in a sphere of radius p_0. Olshanii *et al* work in the regime where V is sufficiently large that a large number of levels can be reached after the decay of an incident atom. They derive rate equations for the number of atoms in various momentum states

and show that the zero momentum state becomes preferentially populated.

The equation of motion for $n_b(p)$, the mean occupation number of atoms in state b with momentum p, is given by

$$\dot{n}_b(p) = -\gamma_b(p)\, n_b(p) \; + \; \frac{\gamma_a}{N_{lev}} N_a(1 + n_b(p)) - \frac{\sigma c}{V} N_\nu n_b(p) \tag{1.15}$$

The first term describes the losses of atoms out of the cavity. The second term describes the feeding of the state $|b, p\rangle$ due to the emission of a photon. This includes the spontaneous and stimulated emission events. The final term describes the opposite process - the reabsorption of emitted photons. σ is the absorption cross-section of a photon. N_μ is the number of photons present in volume V. In the first term, the loss rate γ_b is assumed to be of the form

$$\gamma_b(p) = \gamma_{b0} + \alpha \frac{|p|^2}{p_0^2} \tag{1.16}$$

so that loss is a minimum for $p = 0$. Though they do not model this explicitly, they discuss the use of a velocity selective excitation from b to another untrapped state as a possible mechanism through which this could be employed. Another simplification in these equations is that the decay rates to all accessible levels are assumed to be constant, γ_a/N_{lev}. A more realistic approach, which we discuss in the context of our model in Chapter 2, would have these rates depend on Franck-Condon factors describing the overlap of the initial atomic wavefunction in state a with the trap wavefunctions for the state $|bp\rangle$. Such overlap factors have also been employed by Spreeuw *et al* in the model we discuss in the next subsection.

Two other rate equations are required to describe the atom laser model. These give the rate of change of the number of atoms in state a, N_a and the number of photons N_μ respectively,

$$\dot{N}_a = R_a - \gamma_a N_a \left(1 + \frac{N_b}{N_{lev}}\right) + \frac{\sigma c}{V} N_\mu N_b \tag{1.17}$$

$$\dot{N}_\mu = -\gamma_\mu N_\mu + \gamma_a N_a \left(1 + \frac{N_b}{N_{lev}}\right) - \frac{\sigma c}{V} N_\mu N_b \tag{1.18}$$

where N_b is defined as $N_b = \sum_p n_b(p)$ and γ_μ^{-1} is the time of flight of a photon across the box of volume V.

From the three equations of motion for $n_b(p)$, N_a and N_μ respectively, a steady state solution can be obtained for the number of atoms in the lasing mode, b with momentum p. This steady state solution shows that a threshold condition is obtained if the absorption cross-section is assumed to be zero. Setting $\sigma = 0$ can be justified physically in some situations. This model thus demonstrates that, in principle, atoms can be used to create a system similar

to the optical laser in which, above threshold, a large number of bosons can accumulate in a zero momentum mode.

Spreeuw *et al.*

Spreeuw *et al.* have produced a similar rate equation model based on a resonator created out of blue detuned optical dipole force traps [20]. These can be loaded continuously with laser cooled atoms. These cooled atoms change state into a trapped state which becomes preferentially populated. This population then enhances further transitions into this state. Whereas Olshanii *et al.* work in the regime where $V >> \lambda^3$, Spreeuw *et al.* consider the opposite regime. They present equations of motion for the mean occupation numbers $\bar{N}_\nu$ given by

$$\dot{\bar{N}}_e = r - \Gamma \dot{\bar{N}}_e \left(1 + \sum_\nu S_\nu \bar{N}_\nu\right), \tag{1.19}$$

$$\dot{\bar{N}}_\nu = -\kappa_\nu \bar{N}_\nu + \Gamma \bar{N}_e S_\nu \left(1 + \bar{N}_\nu\right) \tag{1.20}$$

where $\bar{N}_e$ is the mean population of the excited state in their model. $\bar{N}_\nu$ is the mean population in each of the bound levels, labeled by ν, in an optical lattice. The terms, S_ν give Franck-Condon overlap factors with each of the states, ν, and κ_ν describes the loss out of the state labeled by ν. The term r gives the pumping rate into the model. These rate equations lead to a threshold condition in which a large number of atomic bosons populate a single (ground) mode of the resonator.

We have independently considered a rate equation approach to an atom laser [22]. This model is presented, along with various practical considerations, in Chapter 2. In particular, we consider an output coupling based on a change of state, such as is obtained through a Raman transition. We describe a geometry which is based on the implementation of an atom laser in a hollow optical fibre.

1.5.2 Master equation approach

A number of master equation based models of the atom laser have been presented in the literature [1, 9, 23, 24]. These models fall into two basic groups, separated by the mechanism used for transferring atoms from the source to the laser mode. One mechanism involves optical cooling [25–27]. The other uses evaporative cooling [28].

In optical cooling, the kinetic energy of the atoms is reduced through spontaneous emission from an excited internal atomic state. Typically the upper state does not experience a trapping potential, while the lower state is trapped.

This causes an irreversible transfer of atoms into the lower internal state. The chief problem in such schemes is photon re-absorption, in which atoms may be lost from the laser mode. Furthermore optical cooling has not been used to produce a Bose-Einstein condensate to date, though an optical trap has been used to confine a BEC [29].

By contrast, evaporative cooling employs atom-atom collisions to transfer atoms into the ground state. A typical mechanism involves two atoms in the source mode colliding, leading to one atom in the lasing mode and the other in a higher energy mode. The atom in the higher energy mode is lost due to evaporative cooling. This works by selectively removing atoms with higher than average energy. Because this atom is lost the collision process is effectively irreversible. This leads, after rethermalization of the remaining atoms, to a distribution of atoms with successively lower average energy. While this process has already been employed in producing BEC, it is probably not as useful for an atom laser. A BEC is an equilibrium phenomenon whereas an atom laser involves a continuous pumping process. Furthermore, collisions between atoms, which are necessary for such schemes to work, may lead to phase fluctuations and hence an increased linewidth in the output [23]. Due to this, models that involve collisions as part of the lasing mechanism may not be able to produce a true atom laser. Collisions are also present in models which involve optical cooling. In optical cooling schemes, however, it may be possible to reduce the collisional effects while still retaining lasing action.

We now give a brief overview of some of the master equation models presented to date.

Atom lasers based on evaporative cooling

Holland *et al.*

The first atom laser model based on evaporative cooling was proposed by Holland *et al.* [9]. Variations on this model were subsequently suggested by Wiseman *et al.*. The basic proposal of Holland *et al.* is as outlined in Fig. (1.4). Bosonic atoms are confined in an harmonic trap. The pumping mechanism (Fig. 1.4a) involves a thermal atomic source. This has a suitably wide energy spread so as to couple to many eigenstates of the potential. Holland *et al.* then use an evaporative mechanism to remove high energy atoms from the trap and thus allow a steady state output of atoms from the ground state of the trap.

To allow this mechanism to be investigated they consider the simplest model which incorporates the four essential features which occur in the trap. These are

1. the creation of an atom in the trap from the pump field
2. the loss of an atom from a high lying state

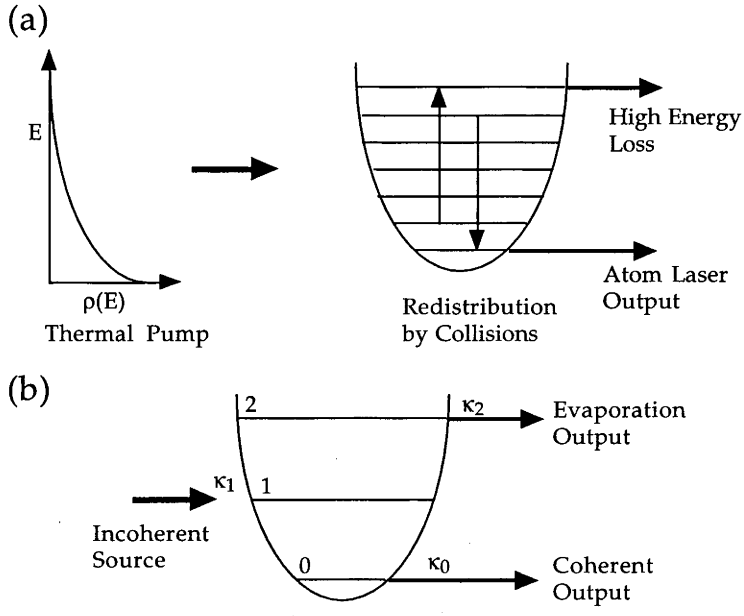

Figure 1.4: Schematic layout of the model of Holland *et al* (Reproduced from Holland *et al.* [9]) .

3. collisions which introduce atoms into the ground state, or scatter atoms out

4. the loss of an atom from the ground state through output coupling

A three level model (see Fig. 1.4(b)) is sufficient to describe these features. Atoms are injected with rate κ_1 in level one and are lost with rates κ_0 and κ_2 from the zeroth level and level two respectively. This system is described by the Hamiltonian

$$\begin{aligned} H &= H_0 + V \\ H_0 &= \sum_{j=0}^{2} \hbar\omega_j \, a_j^\dagger a_j \\ V &= \hbar \sum_{j,k,l,m=0}^{2} g_{jklm} a_j^\dagger a_k^\dagger a_l a_m, \quad j \leq k, l \leq m \end{aligned}$$

where a_j is the second quantized annihilation operator for level j. The coefficients g_{ijkl} correspond to total transfer rates between levels by collisions.

Using this Hamiltonian and a rotating wave approximation, they adiabatically eliminate the second level. The rotating wave approximation ignores some energetically unfavourable processes - such as the annihilation of two ground state atoms to produce two atoms in level 2. These processes may be-

come important at sufficiently high densities. The second level is eliminated as a large damping from this level is assumed for evaporative cooling. This leads to the following Master equation

$$\frac{\partial \rho}{\partial t} = \frac{1}{i\hbar}[V_i, \rho] + \sum_{i=0}^{1} \kappa_i \mathcal{D}[a_i]\rho + \Omega_r \mathcal{D}[a_0^\dagger a_1^2]\rho$$

where

$$V_i = \hbar(a_0^\dagger a_0 - 2n_0)(g_{0000} a_0^\dagger a_0 + g_{0101} a_1^\dagger a_1) + \hbar g_{1111} a_1^{\dagger 2} a_1^2. \tag{1.21}$$

The loss terms are assumed to be of the standard (Born-Markovian) Lindblad form, defined by

$$\mathcal{D}[c] = \mathcal{J}[c] - \mathcal{A}[c], \tag{1.22}$$

$$\mathcal{J}[c]\rho = c\rho c^\dagger \tag{1.23}$$

$$\mathcal{A}[c]\rho = \frac{1}{2}(c^\dagger c\rho + \rho c^\dagger c) \tag{1.24}$$

The effective redistribution rate, Ω_r is obtained from the adiabatic elimination as proportional to $|g_{0211}|^2/\kappa_2$.

This allows equations for the number statistics, $P_{n,k}(t)$, defined as the $\langle nk|\rho(t)|nk\rangle$, to be obtained. Here $|nk\rangle$ describes a state with n atoms in level zero and $k = 0$ or $k = 1$ atoms in level one. Level one is rapidly depleted by the process of two level one atoms colliding to create a level zero atom and a level two atom. The level two atom is lost almost instantaneously from the system. Using this model, results are presented for the evolution of the number statistics for the ground state. Using the initial condition that the trap is empty, they find the population in the trap grows until a balance is reached between the pumping and output coupling. The final number statistics they obtain are Poissonian with mean atom number $2\kappa_1/(3\kappa_0)$. Thus when loss out of the lasing mode is sufficiently small $\kappa_0 << \kappa_1$, a large population can build up in the lasing mode (ground state). This leads to a dense spectrum of de Broglie matter waves.

Holland *et al* also consider the fluctuation spectrum for the ground state. While they use collisions to provide a mechanism for evaporative cooling, these also disrupt the coherence of the ground state. In order to produce a state with a well defined phase they consider parameter regimes where Ω_r is much larger than the frequency shifts in V_i. They produce fluctuation spectra for the case where the nonlinear contribution from V_i is small. They find that, as for an optical laser, linenarrowing occurs as the population of the ground state increases.

However, this result is not possible in a refinement of Holland's model, produced by Wiseman *et al.* Indeed, Wiseman *et al.* shows that in simple mod-

els of an atom laser based on evaporative cooling, the linewidth of the laser output is always broader than the bare linewidth of the laser mode. Thus they claim that evaporative cooling mechanisms may not be able to produce a realistic atom laser, as required by the four definitions discussed earlier in this chapter.

Wiseman *et al.*

Wiseman *et al.* [24] discuss a model which is essentially similar to the one presented above. The first difference between the two models is the description of the irreversible dynamics of mode 1. The approximation that Holland makes involves allowing atoms to leak into the trap, but not out of the trap. This is not possible for an atom laser which is pumped by a thermal reservoir of atoms. We have seen that Holland *et al.* use the form $\kappa_1\mathcal{D}[a_1^\dagger]\rho$ to describe the dynamics of mode 1. Wiseman *et al.* use the more realistic form

$$\dot{\rho} = \kappa_1(N+1)\mathcal{D}[a_1]\rho + \kappa_1 N\mathcal{D}[a_1^\dagger]\rho. \tag{1.25}$$

In fact, there is no limit in which the extra terms introduced by Wiseman *et al.* can be ignored. The extra term is always strictly larger than the term which Holland includes. After proceeding in an identical manner to that discussed above, Wiseman produces the full master equation,

$$\begin{aligned}
\dot{\rho} &= -i[V,\rho] + \sum_{i=0}^{1}\kappa_i\mathcal{D}[a_i]\rho + \kappa_1 N(\mathcal{D}[a_1]+\mathcal{D}[a_1^\dagger])\rho + \Gamma\mathcal{D}[a_0^\dagger a_1^2]\rho, \\
\Gamma &= \frac{\kappa_2|V_{0211}|^2}{(\kappa_2/2)^2+\Delta^2} \\
V &= V_{0000}a_0^{\dagger 2}a_0^2 + V_{0101}a_0^\dagger a_1^\dagger a_0 a_1 + V_{1111}a_1^{\dagger 2}a_1^2 + v a_0^\dagger a_1^{\dagger 2} a_0 a_1^2.
\end{aligned} \tag{1.26}$$

where we have now used a notation introduced by Wiseman, V_{ijkl} which is equivalent to the coefficients, g_{ijkl} discussed above. The coefficient Γ is related to Ω_r presented earlier and $v = (\Delta/\kappa_2)\Gamma$. These processes are shown diagrammatically in the figure, Fig. 1.5 reproduced from [24].

If it is assumed that $\kappa_0 << \kappa_1$, there are two distinct parameter regimes depending on the relative size of Γ and κ_0. These two regimes, termed the strong and weak collision regimes by Wiseman, correspond to $\Gamma >> \kappa_0$ and $\Gamma << \kappa_0$ respectively.

In the strong collision regime, $\Gamma >> \kappa_0$ the number of atoms in the source mode will be small. If the pumping is sufficiently weak it is possible to assume that there are at most two atoms in the source mode at any given time. Using this simplification analytic results for the atom laser in the strong collision, with weak pumping regime are obtained. Wiseman finds intensity fluc-

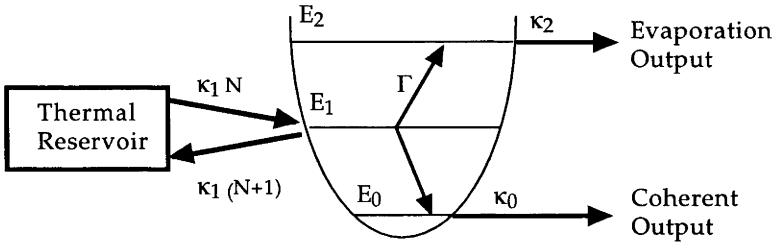

Figure 1.5: Schematic layout of the model of Wiseman *et al* (Reproduced from Wiseman *et al.* [24]) .

tuations which become Poissonian far above threshold. However, the phase diffusion rate is greater than the output flux of atoms. This makes the use of the term "atom laser" somewhat inappropriate in this regime. If the collisions are very strong, the assumption that there is at most two atoms in the source mode can be made even if the pumping is not weak. This leads to similar results to those obtained by Holland *et al.* in their model. The relative magnitude of the phase fluctuations in this case are found to be better than for the preceding case. The linewidth, however, which is dominated by the excess phase diffusion, is always greater than the bare linewidth

In the weak collision regime, $\Gamma << \kappa_0$ it is only possible to get a large population in the laser mode if $N >> 1$. Physically this says that if the collisions are weak then we need a strong pumping of the source mode so as to populate the laser mode. As both the source and laser mode will have a large population Wiseman makes the assumption of a well-defined amplitude for these modes. A P function representation is used which leads to a Fokker-Planck equation. An analysis of the power spectrum and fluctuation spectrum leads to results which are considerably worse than an ideal laser. The linewidth, in particular, is much greater than an ideal laser above threshold and in fact, is larger than the bare linewidth of the lasing mode. However, in this regime, the phase diffusion rate may still be slow in the sense of being much less than the total loss rate of atoms from the round mode of the trap. Nevertheless, these poor results for laser linewidths leads Wiseman to suggest that for an atom laser in which collisions play an essential role (such as through evaporative cooling) it may not be possible to have a laser with close to ideal (narrow) linewidth. In other models of lasers which do not rely on collisions these problems may be avoided - as, at least in principle, steps could be made to reduce the effects of collisions.

Before going on to discuss a model proposed for an atom laser based on op-

tical cooling we discuss briefly another proposal for an atom laser which uses inelastic atom-atom interactions as the lasing mechanism. While this model is similar to the general proposal of Holland and Wiseman discussed above the details of this proposal are quite different.

Guzman *et al.*

In [1], Guzman *et al.* discuss a proposal for an atom laser (or Coherent Atomic-Beam generator). A schematic representation of the matter wave resonator scheme they propose is shown in Fig. 1.6.

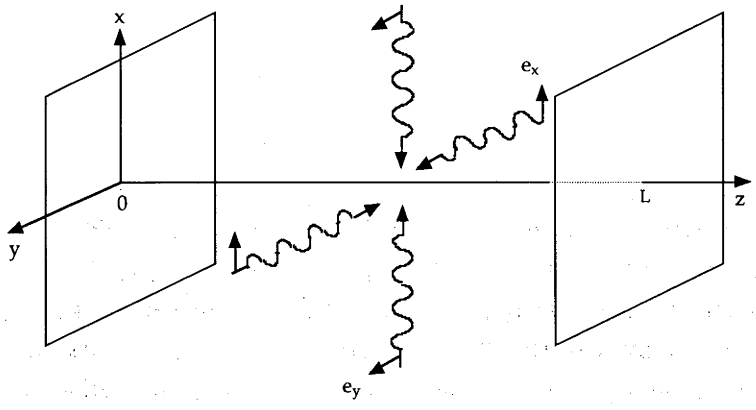

Figure 1.6: Schematic layout of the model of Guzman *et al* (Reproduced from Guzman *et al.* [1]) .

The scheme achieves longitudinal confinement of matter waves via a Fabry-Perot for atoms. They suggest that the end mirrors (see Fig. 1.6) may be formed using focussed laser beams or by evanescent waves. The transverse confinement is achieved through laser cooling beams. They consider the case of large detunings between atomic transition and the light fields. This is essential in an atom laser to reduce spontaneous heating. It also allows the excited atomic states to be adiabatically eliminated.

The model which Guzman *et al* propose for the atom laser is based on two-body collisions to achieve a transfer of atoms into the lasing mode. The dominant source of atom-atom interactions is expected to be near resonant dipole-dipole interactions in the regime they consider. They assume the atoms are in an electronic ground state, and also consider them to remain in the ground state for transverse motion. The states are thus labeled by the longitudinal mode of motion. By considering the dipole interaction, they show that energy levels in the atomic resonator are predominantly coupled within manifolds separated in momentum by the wave number $(\sqrt{2}/2)k_L$, where k_L is the wave

number of the cooling laser. Since the coupling between manifolds is weak, Guzman *et al.* consider a single manifold as a first step.

The model is described by a four-level system. The "pump" level, $|3\rangle$ is taken to be the highest bound level of the resonator. It is assumed that this is pumped by a process which is state selective, and pumping into other levels is ignored. As we mention above, this level $|3\rangle$ is predominantly coupled to a manifold of levels separated in momentum by integers of $(\sqrt{2}/2)k_L$. Level $|2\rangle$ is the lasing level. The dynamics is dominated by collision processes satisfying the resonance condition with the smallest energy defects. The processes which dominate thus correspond to, for example, the annihilation of two atoms from state $|3\rangle$ followed by the creation of an atom in the state $|4\rangle$ and an atom in the resonator bound state $|2\rangle$. Since the levels in the manifold with energy higher than that of level $|2\rangle$ are, by construction, continuum levels, they make the assumption that atoms excited to the continuum are lost irreversibly from the system. Similarly, the other process which dominates the dynamics corresponds to the reverse process in which two atoms are annihilated from $|2\rangle$ and created in $|3\rangle$ and $|1\rangle$ respectively. Again, level $|1\rangle$ is treated as being part of a reservoir. Thus, the effective model they describe is a two level model where the pump level $|3\rangle$ and atom laser level, $|2\rangle$ are coupled to each other and two reservoirs symbolically labeled $|1\rangle$ and $|4\rangle$ via near resonant dipole-dipole collisions. The pump level is selectively pumped. Linear losses are included in the two levels, $|2\rangle$ and $|3\rangle$. By adiabatically eliminating the reservoirs in the Born-Markov approximation Guzman *et al.* obtain a master equation.

$$\begin{aligned}\frac{d\rho}{dt} &= \frac{-i}{\hbar}[V_{dd12},\rho] + \alpha_1\mathcal{D}[c_3^\dagger c_2^2]\rho + \alpha_4\mathcal{D}[c_2^\dagger c_3^2]\rho + \beta_2\mathcal{D}[c_2]\rho + \\ &\quad [\Lambda_3+\beta_3]\,\mathcal{D}[c_3]\rho + \Lambda_3\mathcal{D}[c_3^\dagger]\rho \end{aligned} \tag{1.27}$$

Solving this equation, Guzman *et al* find typical lasing phenomena, including the presence of a "threshold". The atom statistics of the laser change from super-Poissonian to approximately Poissonian as the laser is pumped above threshold. The threshold transition is not particularly sharp, however, due to the limited size of the system they consider.

Atom Lasers based on optical cooling

Wiseman *et al.*

The first model of an atom laser which used a master equation approach but did not involve evaporative (or collisional) cooling was proposed by Wiseman in 1995 [23]. This atom laser model relied on dark state cooling. A dark state is a state which is not excited in an optical field, due to quantum interference. Hence it is not subject to heating by cycles of stimulated absorption fol-

lowed by spontaneous emission. Instead the atoms remain in the dark state. A non-dark state atom, however, may absorb a photon followed by spontaneous emission into the dark state.

The model Wiseman proposed is outline schematically in Fig. 1.7. The

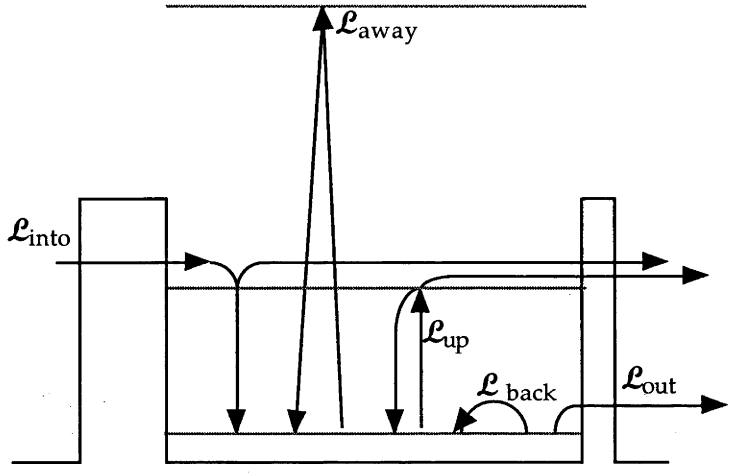

Figure 1.7: Schematic layout of the model of Wiseman *et al* (Reproduced from Wiseman *et al.* [23]) .

master equation describing the model contained five terms which correspond to the five processes outlined in the figure. Thus we have

$$\dot{\rho} = (\gamma/l^2)(\mathcal{L}_{\text{into}} + \mathcal{L}_{\text{up}} + \mathcal{L}_{\text{out}} + \mathcal{L}_{\text{back}} + \mathcal{L}_{\text{away}})\rho \tag{1.28}$$

where

$$\mathcal{L}_{\text{into}} = \frac{1}{2}\left\{(n_s + \mathcal{J}[a^\dagger])(n_s + \mathcal{A}[a^\dagger])^{-1} - 1\right\} n_r \tag{1.29}$$

describes an atom entering an upper mode and either condensing ($\mathcal{J}[a^\dagger]$) or tunneling out again (n_s). The term,

$$\mathcal{L}_{\text{up}} = \frac{1}{2}\left\{(n_s + \mathcal{J}[a^\dagger])(n_s + \mathcal{A}[a^\dagger])^{-1}\mathcal{J}[a] - \mathcal{A}[a]\right\}, \tag{1.30}$$

describes an atom excited from the ground mode and either returning ($\mathcal{J}[a^\dagger]$) or tunneling out (n_s). The term $\mathcal{L}_{\text{out}}$ describes the output of atoms assumed to be of the usual Born-Markov form,

$$\mathcal{L}_{\text{out}} = \lambda\mathcal{D}[a] \tag{1.31}$$

The term $\mathcal{L}_{\text{back}}$ describes the phase diffusion,

$$\mathcal{L}_{\text{back}} = \frac{3}{16l}\mathcal{D}[a^\dagger a] \tag{1.32}$$

Finally, the term (far above threshold)

$$\mathcal{L}_{\text{away}} = \frac{1}{2}(\mathcal{J}[a^\dagger]\mathcal{A}[a^\dagger]^{-1}\mathcal{J}[a] - \mathcal{A}[a]) \tag{1.33}$$

deals with transitions from the ground mode into the high energy states. Far above threshold this term just adds to the phase diffusion.

Using this model Wiseman obtains various properties of the laser model. The output of the laser is found to have a linewidth, which while above the fundamental limit, is narrower than the bare linewidth. This is an improvement on models based on evaporative cooling discussed above. The output is also found to be second order coherent.

1.5.3 Mean-field approach

Ballagh *et al.*

A third approach to modelling atom lasers is based on the modelling of a BEC and has currently been used to consider a "pulsed" atom laser. In this approach, the atom laser is modelled using a Gross-Pitaevskii equation (GPE). Ballagh *et al.* consider an output coupler in the limit of strong coupling [30]. They do not strictly discuss their model in the context of atom lasers, however Steck *et al.* consider a similar system as a pulsed atom laser. One of the advantages of the GPE technique is it leads to the relatively easy inclusion of the spatial effects of atom-atom interactions. The model used by Ballagh *et al.* is two coupled GP equations for the mean fields $\psi_1(r,\tau)$ and $\psi_2(r,\tau)$ of the two states:

$$\frac{\partial\psi_1}{\partial\tau} = i\nabla^2\psi_1 - \frac{i}{4}r^2\psi_1 - iC(|\psi_1|^2 + 2|\psi_2|^2)\psi_1 + iV\psi_2 \tag{1.34}$$

$$\frac{\partial\psi_2}{\partial\tau} = i\nabla^2\psi_2 - \frac{ik}{4}r^2\psi_2 - iC(|\psi_2|^2 + 2|\psi_1|^2)\psi_2 + iV\psi_2 - i\Delta\psi_2 \tag{1.35}$$

Here r and τ, the spatial and temporal coordinates, are scaled in harmonic oscillator units. The nonlinearity parameter, C is given by $C = NU_0/\hbar\omega$ where N is the number of atoms and U_0 is the s-wave scattering effective interaction strength. They later consider a one dimensional version of this problem so the exact definition of C needs careful consideration. They show using this model that from an initial trapped single component state, a second component can be generated which may escape from the trapping region. Because it is as-

sumed in the mean field approach that the atoms are in a coherent state, it is not possible to find out information about the quantum statistics of the model.

Steck *et al.*

Steck *et al.* also consider a pulsed atom laser using a Gross-Pitaevskii equation [31]. Their laser model consists of an interacting BEC in a magnetic trap and an additional rf field which transfers atoms to an untrapped Zeeman sublevel. A three component Gross-Pitaevskii equation is used. The system of equations for the wavefunction $\bar{\psi}_m(t) = e^{-im\omega_{rf}t}\langle\hat{\psi}_m(t)\rangle$ is given by

$$\begin{aligned} i\hbar\frac{\partial}{\partial t}\bar{\psi}_m(r,t) &= \left(-\frac{\hbar^2\nabla^2}{2M} + V_m(r) + \hbar m\omega_{rf} + U|\bar{\psi}(r,t)|^2\right)\bar{\psi}_m(r,t) \\ &\quad +\hbar\Omega\sum_{m'}\left(\delta_{m,m'+1} + \delta_{m,m'-1}\right)\bar{\psi}_{m'}(r,t), \end{aligned} \tag{1.36}$$

where m and m' range over $-1, 0, 1$ and the equations are in the rotating wave approximation. They consider the case of weak output coupling. This allows them to calculate properties of the system such as the number of atoms in the cavity mode, the dynamics of its chemical potential and the velocity of the output atoms. We consider a similar model to this in the context of our input-output theory discussed in Chapters 3,4 and 5.

Zhang *et al.*

Zhang *et al.* [32] present details of an output coupler from a Bose-Einstein condensate . As with the work of Steck *et al.* and Ballagh *et al.* they do not describe a continuous atom laser. However, the output coupling presented is directly applied to describe the pulsed atom laser experiment of Mewes *et al* [12].

A schematic diagram of the system considered by Zhang *et al* is shown in Fig. 1.8. This shows the three Zeeman levels, $m_F = -1$, $m_F = 0$ and $m_F = 1$. The BEC is initially prepared in level $m_F = -1$ which is trapped. An rf field is applied to the system, which includes a spin-flip transition to the other two Zeeman levels. The untrapped condensate components will leave from the trapping regime under due to gravity.

They describe the system using a three-component vector field,

$$\psi(\mathbf{r},t) = \sum_{m_F=-1}^{m_F=1}\psi_{m_F}(\mathbf{r},t)\,|F=1,m_F\rangle. \tag{1.37}$$

The operator, $\psi_{m_F}(\mathbf{r},t)$ corresponds to the atomic field component in the magnetic Zeeman level, m_F. Using a Hamiltonian which describes the coupling

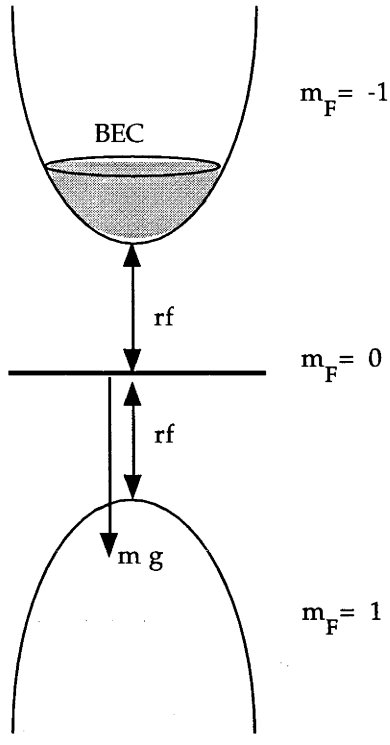

Figure 1.8: Schematic diagram of the model of Zhang *et al* (Reproduced from Zhang *et al.* [32]) .

of the atomic field to the rf field, Zhang *et al.* obtain three coupled nonlinear Schrödinger equations for ψ_1, ψ_2 and ψ_3 respectively. These are written in the interaction picture. Using these equations they numerically simulate the output coupler for the pulsed atom laser demonstrated by Mewes *et al* [12]. They investigate the Rabi oscillations and collective dynamics in this system and find quantitative agreement with the experiment of Mewes *et al.*

Kneer *et al.*

Kneer *et al.* [33] describe a generic model of an atom laser using the Gross-Pitaevskii equation with the inclusion of a pump and loss term. We present related work which does not involve the assumption of exponential loss in Chapter 5. The modified G-P (Gross-Pitaevskii) equation for the mean field,

$\psi = \psi(\mathbf{r})$ of the Bose-condensed atoms of mass m in a trap potential $V(\mathbf{r})$ is

$$i\hbar\frac{\partial\psi}{\partial t} = -\frac{\hbar^2}{2m}\nabla^2\psi + V(r)\psi + U_0|\psi|^2\psi + H_{\text{gain}}\psi + H_{\text{loss}}\psi, \quad (1.38)$$

where

$$H_{\text{gain}}\psi = \frac{i\hbar}{2}\Gamma N_u\psi, \quad (1.39)$$

$$H_{\text{loss}}\psi = -\frac{i\hbar}{2}\gamma_c\psi. \quad (1.40)$$

The first three terms in Eq. (1.38) are the standard G-P equation. The nonlinear term, $U_0|\psi|^2\psi$ takes into account two particle s-wave scattering. The parameter U_0 can be written in terms of the s-wave scattering length, a_0 as $U_0 = 4\pi\hbar^2 a_0/m$. Kneer *et al.* add to the standard G-P equation the loss and gain term, given by Eq. (1.39) and Eq. (1.40) respectively. γ_c is the loss rate of atoms from the condensate and leads to an exponential decay in the number of atoms in the condensate. The quantity N_u in the gain term is the number of atoms outside the condensate. Γ is the rate of transition for these atoms into the condensate. In this model, along with Eq. (1.38), a rate equation is used to describe the number of uncondensed atoms, N_u,

$$\frac{dN_u}{dt} = R_u - \gamma_u N_u - \Gamma N_c N_u. \quad (1.41)$$

The term, R_u describes a source which pumps the un-condensed state at rate R_u. The term $\gamma_u N_u$ describes atoms lost from the system, but not trapped in the condensed state. The final term describes the loss of atoms into the condensed state.

In this model, the loss term, γ_c is spatially homogeneous. Kneer *et al* investigate the one dimensional case for a harmonic potential, and find undamped collective excitations, with the final mean field depending on the initial mean field. The solution to Eq. (1.41) and Eq. (1.38) they find in this case oscillates around the stationary solution of the G-P equation.

To avoid this, Kneer *et al.* describe an improved model which describes a spatially dependent decay rate, so that γ_c is a function of position, $\gamma_c(\mathbf{r})$. In this case they achieve a single lasing mode as the spatially dependent loss leads to a natural mode selection. Using this model, they derive a modified Thomas-Fermi solution for the steady state mean field and compare this with the usual Thomas-Fermi solution. This model describes the laser threshold and the build up of the coherent mean field of the condensate.

In this model, the loss term is a phenomenological exponential decay term. In Chapter 5 we discuss a similar model to this which describes the pumped and damped atom laser using a modified Gross-Pitaevskii equation. In our

model, the damping is described by coupling the trapped atoms to free space.

Chapter 2

An atom laser based on Raman transitions

Overview

In this chapter we present our rate equation model of an atom laser. The laser uses spontaneous emission to transfer atoms irreversibly into the lasing mode. The output coupling mechanism is also considered explicitly. We consider a method for output coupling based on changing the internal atomic state of the atoms using a Raman (two photon) transition in a spatially localized region. Using this model we produce rate equations which are analogous to the optical laser rate equations. These are equivalent to atom-laser rate equations developed independently in work by Olshanii *et al.* [21] and Spreeuw *et al.* [20]. The rate equations show the presence of a threshold pumping condition. We propose an implementation of our atom laser scheme using hollow optical fibres. This work has been published in the Physical Review [22]

2.1 Introduction

As we mention in Chapter 1, rate equations do not describe the atom statistics of an atom laser. Nevertheless, as for optical lasers, rate equations can give a useful practical guide to the workings of the atom laser. In particular, we focus in this proposal on some practical aspects of the atom laser, such as the output coupling mechanism. Previous proposals had not considered aspects of the atom laser, such as output coupling, explicitly. Early suggestions for an output coupling mechanisms included quantum mechanical tunneling [23] and periodically turning off the cavity mirrors [1]. Wiseman *et al.* [23] find that any physically realizable optical potential barrier confining the atoms leads to an extremely small tunneling rate. Turning off the cavity mirrors, while effective for output coupling, will not provide a continuous beam.

In this work we model the geometry of an optical fibre. This has several advantages, including providing a directed output beam, and minimization of

the reabsorption of spontaneously emitted photons. The calculations are performed in 3D for various different geometries, however in all cases we assume the hollow fibre leads to strong transverse confinement. The rate equations which describe this atom laser model also lead to the presence of a threshold as would be obtained in an optical laser.

2.2 Atom laser scheme

In this section we present an overview of our atom laser scheme. The details are discussed in the following sections.

2.2.1 Model

The model consists of atoms with four energy levels, as outlined in Fig. 2.1. Level $|1\rangle$ is the input pump level, level $|2\rangle$ is the lasing level and level $|4\rangle$ is the

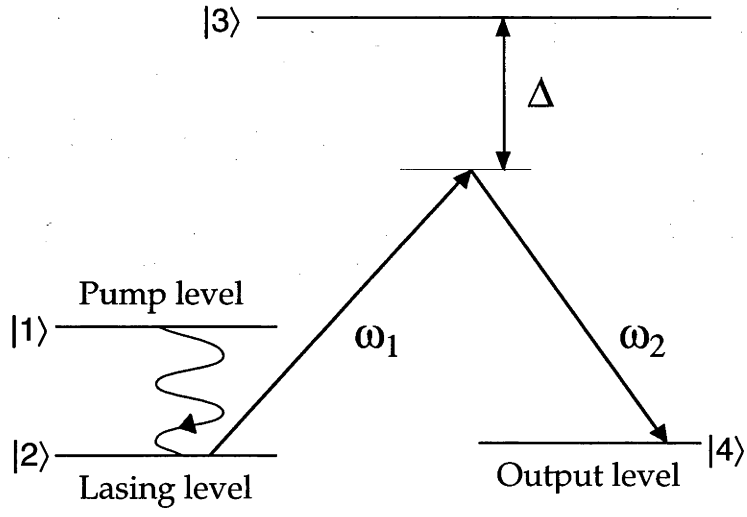

Figure 2.1: Schematic diagram of atomic states and output coupling lasers.

output level. Level $|3\rangle$ mediates the output coupling Raman transition. There are two atomic cavities for confining atoms in states $|1\rangle$ and $|2\rangle$. One of these cavities, the lasing cavity, traps atoms in the level $|2\rangle$. Only a single mode of this cavity becomes populated as we show in section 2.6. We wish to build up a large number of atoms in this ground state mode, in an analogous way to the standard optical cavity in a laser. The other cavity, the pump cavity, traps a large number of atoms in the internal metastable level $|1\rangle$. The two cavities are spatially overlapping, see Fig. 2.2.

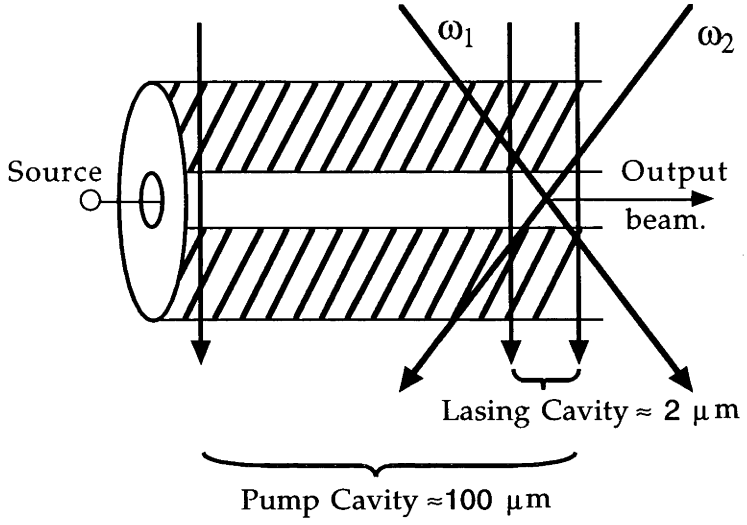

Figure 2.2: Schematic diagram of possible implementation of our atom laser model using hollow optical fibre.

2.2.2 Getting atoms into the lasing mode

Initially the atoms are prepared in level $|1\rangle$, cooled and injected into the pump cavity. Injection could be achieved by a number of methods. These methods would depend on the exact implementation of the pump cavity which we discuss in more detail later. For example, a partially reflecting atomic cavity mirror could be employed. Such atomic mirrors can be produced using the repulsive potentials created by blue detuned laser beams [34]. The transmittivity of such a mirror may be very small for a practical cavity [23], however extremely large input fluxes of atoms are possible allowing useful numbers of atoms into the cavity. Another possible input mechanism would be to inject the atoms into the cavity in a non-trapped atomic state and then employ a change of atomic state (for example using a Raman transition) to the trapped state. This reverses our output coupling method. Perhaps the most simple method of input couple could be achieved if the pump cavity is a hollow-optical fibre gravitational cavity [35]. In this case, the atoms are constrained by gravity and the geometry of the fibre. Thus atoms can enter the cavity unhindered, but cannot leave due to gravity.

Atoms change from the pump level $|1\rangle$ to the lasing level, $|2\rangle$ at a rate r_{12} in the absence of Bose-enhancement. Atoms which make this change of level, however, do not necessarily become trapped in the ground state of the lasing cavity - the lasing mode. However the wavefunction overlap with this ground state is larger than the overlap with other higher energy states. Tunneling losses out of this state are also lower. Atoms that do transfer to the ground

state of the lasing cavity are trapped, and so further transitions to this state will be enhanced by a factor of $(N_{21}+1)$ where N_{21} is the number of atoms in atomic level $|2\rangle$ and the ground state of the cavity. With suitably large pumping rate of atoms into the system, a large number of atoms will build up in this single quantum mechanical state of the combined atomic and cavity system. For the parameters considered in this paper (section 2.3) other higher energy modes of the cavity state are not significantly populated.

2.2.3 Getting atoms out of the lasing mode

A Raman transition couples atoms out of the system. Two lasers transfer the atoms from level $|2\rangle$ to a final atomic level $|4\rangle$. The lasers are confined to the lasing cavity, and are shone diagonally across the cavity so that they are counter-propagating in one direction (the longitudinal direction) and co-propagating in the transverse direction, Fig. 2.2. Thus a momentum kick is imparted on atoms in the longitudinal direction, but no net momentum kick occurs in the transverse direction. The longitudinal momentum kick pushes the atoms out of the interaction region. If the rate at which atoms leave the system due to this kick is much larger than the Raman transfer rate then we have an effective irreversible transfer of atoms from the lasing mode out of the system.

In section 2.3 we present an implementation of the scheme using a hollow optical fibre to create the transverse confinement for the atoms, and focussed laser light to form the longitudinal atomic mirrors. For a fibre with a hole of diameter $\approx 2\mu$m it is appropriate to model the confining potential in the transverse direction as a harmonic oscillator potential. In the longitudinal direction we model the confining lasers for the pump cavity as a square well, and those of the lasing cavity as a harmonic oscillator. One possible problem with coupling the pump and lasing cavity by spontaneous emission is photon reabsorption. A simple argument suggests that reabsorption might reduce the number of atoms in the ground trap state. Reabsorption can be reduced, however, by ensuring that the lasing cavity is smaller than the mean free path of a photon. This assumption is made in the models of Spreeuw *et al* and Olshanii *et al* [20,21]. The rate of reabsorption depends on the gas density and the absorption cross section of the atoms for photons at a particular frequency. The rate of reabsorption, dR/dt is given by [21]

$$\frac{dR}{dt} = \frac{dN_\nu}{dt} = -\frac{\sigma c}{V} N_\nu N, \tag{2.1}$$

where c is the speed of light, σ is the absorption cross section, N_ν is the number of photons within volume, $V \approx L^3$ and N is the total number of atoms in the ground state which could absorb a photon. To ignore reabsorption we require that, for a single spontaneously emitted photon ($N_\nu = 1$), the average number

of absorption events in the time it takes for the photon to leave the cavity (L/c) is much less than unity. Using Eq. (2.1) we can approximate this condition by $\sigma \bar{N} L << 1$, where $\bar{N} = N/V$ is the atom number density. Typical numbers of atoms in a BEC may range up to 10^6, in a volume, $V = (2\mu\text{m})^3$, so that $\bar{N}L \approx 10^{17}\text{m}^{-2}$. Thus the assumption to ignore the reabsorption of photons in this case assumes the absorption cross section, $\sigma < 10^{-17}\text{m}^2$. Typical values of σ range from 10^{-13}m^2 to 10^{-20}m^2 [6] depending on parameters including the wavelength of the emitted photon, the width of the atomic resonance. Thus, the assumption to ignore reabsorption will be valid for some gas samples.

Furthermore, however, Cirac and Lewenstein [36] have shown that under certain conditions reabsorption will actually increase the number of atoms in the ground state. They show that while a simple phenomenalogical theory predicts that reabsorption will destroy a BEC, a more careful investigation shows that this is not necessarily the case.

2.3 Implementation

In this section we discuss in more depth the details of the proposal outlined in the previous section. In particular we propose one possible implementation of this atom-laser model using hollow optical fibres. A schematic diagram of this is shown in Fig. 2.2. To begin with, we give a brief review of hollow optical fibres.

2.3.1 Hollow optical fibres

Single mode hollow optical fibres, with holes of about 1.5μm have been proposed for guiding atoms [37,38] and multimode fibres have already been demonstrated experimentally to guide atoms [39–41]. A review of the theory behind these waveguides and the earlier experiments has been produced by Dowling and Gea-Banacloche [42].

The hollow fibre acts as a waveguide for atoms. However in contrast to the optical case, the longitudinal atomic motion along the fibre decouples from the transverse motion, so there is a continuum of longitudinal plane wave modes which atoms can couple into. A detailed development of the theory of hollow optical fibre waveguides is given by Marksteiner *et al.* [37]. There are two basic mechanisms by which hollow optical fibres may guide atoms. These involve red detuned light and blue detuned light respectively.

A laser field will produce a potential when it is highly detuned from an electronic transition in an atom. The potential, V is inversely proportional to the detuning, Δ and proportional to the intensity of the light, given by the

square of the Rabi frequency, Ω of the laser field,

$$V = \frac{\hbar\Omega^2}{4\Delta}. \tag{2.2}$$

Thus, when the detuning is negative ("red" detuning) atoms are attracted to regions of high laser intensity. When the detuning is positive ("blue" detuning) atoms are repelled from more intense regions of light. This is the dipole force.

In the red detuning scheme for guiding atoms down a hollow optical fibre, red detuned light is guided down the centre of a hollow optical fibre. The intensity of the light is maximum in the hollow centre, so that atoms are attracted to the centre and guided by the fibre. This scheme was first suggested by Ol'Shanii *et al* [43]. Experimentally, guiding of atoms using a red-detuned hollow fibre scheme was first achieved at JILA [44] in 1995. In this experiment rubidium atoms were guided down a 3cm length of glass capillary tube with a hole of diameter 40μm. Atoms were found to be strongly guided for some detunings with an atomic flux increase of a factor of approximately three for best guiding over the large detuning limit.

An alternative method for guiding atoms down hollow optical fibres using blue detuned light was proposed by Savage [38] and Marksteiner [37]. In the blue-detuning scheme, light is carried in the glass surrounding the hole in the fibre. This leads to an evanescent field which penetrates the hole in the centre and repels atoms away from the walls of the fibre. The first demonstration of atom guiding using a blue-detuned evanescent field was performed at JILA, again using rubidium atoms. The fibre had a hole diameter of 20μm, and similar to the red detuning experiments led to an enhancement of the atom flux by a factor of approximately three times the ballistic flux. Laser guiding of rubidium atoms using blue-detuned light was also observed by Ito *et al.* [41]. An enhancement of 20 times the ballistic flux was observed, indicating the guiding of atoms down a fibre. Moreover, in these experiments two fibres were used with diameters of only 7μm and 2μm respectively. Such small holes lead to a well spaced transverse structure. Indeed these diameters are close to the regime where only a single transverse mode may be populated. Another feature of this experiment was that the atomic guiding was sufficiently sensitive to detuning that it was possible to guide atoms in a state selective manner - that is the F=2 and F=3 hyperfine levels or rubidium could be guided independently.

Probably the main advantage of hollow fibres for an atom laser is the relatively simple method of producing transverse confinement, and the ability to transfer the output atoms as a beam away from the atom laser device. Their effective 1D geometry makes them an obvious candidate for an atom laser. Ultimately, the use of an atom laser will lie in using the atom laser beam for

particular experimental purposes. However, if one wishes to keep the coherence of the atoms - thus allowing applications such as interferometry - it is necessary to avoid collisions of the atom laser beam with background gas. That is, the atoms must be kept in a vacuum. Hollow fibres have already been demonstrated to be able to easily be evacuated. The fibres can be flushed with helium. The helium then diffuses through the glass leaving the hole of the fibre in a vacuum.

Problems with hollow optical fibre waveguides

In the atom laser proposal we discuss here, we use such hollow optical fibres to both guide the output beam from the atom laser, and also to provide transverse confinement for atoms in the lasing and pump states. As with any such proposal, this is not without experimental difficulties. One of these is the presence of Casimir-Polder forces through which the glass walls may attract atoms. This reduces the effective optical potential. However, this problem can be avoided by having a suitably high repulsive potential confining the atoms. Another possible limitation on the use of hollow optical fibres for atom guidance would be atomic excitation due to stimulated Raman scattering and stimulated Brillouin scattering. This is discussed by Hope *et al* in [45]. They find that for the parameters given by Agrawal [46], a length of fibre of size $\approx$ 1m would be too short for stimulated Brillouin and Raman scattering to occur. This is a typical size which might be considered in a practical experiment. Probably the main practical limitation on hollow optical fibres is spontaneous emission of photons by atoms in the evanescent field.

Spontaneous emission is a generic problem with using optical potentials to confine atoms. When atoms experience an optical field, such as we suggest above to create a guiding potential, the atoms will be partially excited, and thus subject to spontaneous emission. Spontaneous emission leads to the loss of coherence of atoms. The loss of coherence due to a single spontaneous emission event has been studied in Metastable Helium atoms [47]. A spontaneous emission event in a random direction induces a random shift on the phase of the atom which leads to a destruction of interference.

The loss of coherence through spontaneous emission by atoms in the confining light field is particularly a problem in those experiments that use red-detuned light. In these cases atoms continuously experience the light field, being attracted to regions of high intensity. However, for the blue detuned case the atoms only interact with the light field when they approach the inner wall of the hollow fibre. The effect of spontaneous emission while the atoms are in this light field can be reduced by increasing the detuning of the light field from the atomic resonance.

We estimate here the amount of spontaneous emission one would obtain

for atoms in the evanescent field which we use to confine the atoms. We assume confining light with maximum blue detuning of $\Delta_{\max} = 2\pi \times 50\text{THz}$. We assume a typical linewidth of $\gamma = 2\pi \times 6\text{kHz}$ for an (unspecified) upper level $|e\rangle$. The spontaneous emission rate is given by the usual formula,

$$\Gamma_{\text{se}} = \gamma\Omega^2/4\Delta^2, \tag{2.3}$$

where the Rabi frequency is determined by the intensity of the light field, and hence the required potential height. As discussed by Hope and Savage [48] we assume that the minimum excited state population is limited by the maximum possible detuning, rather than by the available laser power. Then the minimum possible spontaneous emission rate is given by Eq. (14) of Hope and Savage [48]

$$\Gamma_{\text{se,min}} = \frac{\gamma(k_b T)}{\hbar\Delta_{\max}}. \tag{2.4}$$

The required potential height has been expressed in terms of Boltzmann's constant k_b and the atom temperature T. With a temperature of $T = 200\text{nK}$ these parameters give a spontaneous emission rate of approximately $3.0 \times 10^{-6}\text{s}^{-1}$. Thus a typical atom must spend a time of order $3 \times 10^5\text{s}$ inside the confining light fields before a spontaneous emission event is likely. Note that this time is an upper bound since we have assumed that the atom always experiences the maximum field. Nevertheless it is possible to further reduce this spontaneous emission rate by a factor of almost 100, to $6.0 \times 10^{-5}\text{s}^{-1}$, by using the Raman scheme of Hope and Savage [48] to create the potential.

In the case where a large number of atoms are being confined in a single condensate mode, these rates will actually be increased by the effects of Bose-enhancement . However, these "atom stimulated" events do not lead to a destruction of the condensate as in this situation atoms are being "atom stimulated" into the lasing mode. The actual magnitude of this stimulated effect is discussed as a function of velocity of atoms, and the direction of the sponataneously emitted photon by Hope *et al.* in [49].

Thus in principle, optical confinement which has very small spontaneous emission rates is possible. In practice, blue-detuned lasers have already been used in experiments to plug holes in a BEC or create a double-well potential [13]. These experiments demonstrate the use of light beams to create a potential barrier for atoms in a Bose-condensed state without leading to the destruction of the condensate through spontaneous emission.

2.3.2 Implementing the cavities in a hollow optical fibre

We have discussed the hollow fibre in terms of producing a waveguide. However, for an atom laser we need to provide longitudinal confinement as well

to produce a cavity. We discuss methods of producing the pump and lasing cavity inside a hollow optical fibre.

The pump cavity

The walls of a hollow optical fibre are made of glass. This allows laser beams to be shone across the fibre (see Fig. 2.2). If the laser beams are blue detuned the atoms will be repelled away from the potential created by the laser beams. That is, they will act as an atomic mirror. This uses the same confinement mechanism as the evanescent beam which provides transverse confinement.

The pump cavity is assumed to be long and narrow, compared with the width of the fibre. As a result, the transverse mode energy level spacings are much larger than the longitudinal mode spacings. Due to the length of the pump cavity longitudinally, it would be possible to bend into a "well" shape the hollow optical fibre. This would lead to another method of producing the pump cavity - a gravitational cavity [35]. The flexibility of the fibre would give one freedom to choose the cavity geometry. In particular a cycloid shape is found by Harris *et al.* [35] to produce a simple harmonic oscillator potential longitudinally.

We see later that the exact details of the pump cavity and its energy levels are not critical in this laser scheme. If we use laser beams shone across the fibre to create longitudinal confinement, then the pump cavity is best modelled longitudinally as a square well. Alternatively a gravitational cavity may be modelled longitudinally as an harmonic oscillator for a cycloid shaped fibre. Transversely, the pump cavity is confined by the evanescent field of the fibre in either case.

The lasing cavity

In principle, the lasing cavity may be produced by either of the two methods discussed above. However, the lasing cavity requires a tighter confinement than the pump cavity. This means that a gravitational cavity would require too great a bend in the fibre to be practical. Moreover, it is not possible to create both pump and lasing cavity from the same fibre if we use gravitational cavities.

Hence, the lasing cavity is produced in the fibre by using two blue detuned lasers. These are much closer together than in the pump cavity. Due to the large overlap of the lowest pump cavity modes with the ground state of the lasing cavity only the ground state becomes significantly populated (see section 2.6).

Previously, we proposed that the pump cavity could be modelled by a box potential longitudinally if laser beams were used to provide longitudinal confinement. This effectively treats the light sources which create the cavity walls

as having no width. This is valid for the pump as the walls are well separated and an atom will spend most of its time away from the laser beams. In contrast, the lasing cavity has a longitudinal confinement which is small. Typically this is of the same scale as the transverse confinement. Because of this we must consider the effect of the width of the light beams which form the potential walls. Having two beams with only a couple of microns of darkness between them is close to the optical diffraction limit, thus assuming that the resulting optical potential in this case is a square well is not realistic. In practice such a small cavity will always be close to harmonic. Therefore, we model the longitudinal lasing cavity potential as harmonic. This will lead to an increased chance of spontaneous emission due to the atoms being present in the light field. This problem was discussed in the context of the transversely confining beams previously. In both cases (longitudinal and transverse confinement) the potential barrier is provided by the dipole force and the dimensions of the cavity are very small so that light will leak into the cavity. The discussion on spontaneous emission in the previous section, however, assumed (as an overestimate) that the atoms were constantly in the presence of the far detuned light field. Thus, the amount of spontaneous emission from the longitudinal confinement will be at most of similar order to the effect considered there.

It should be noted, in concluding this section on forming the pump cavity that throughout this discussion we have considered two blue-detuned lasers focussed to form the lasing cavity. In practice, a single laser in a donut mode may be shone across the fibre to produce the longitudinal confinement. Such donut modes have already been demonstrated to confine atoms as a waveguide. As an experimental practicality, it may be possible to use a single laser source to produce a donut mode of blue detuned light. A beam splitter could then be used to couple some of the light into the glass of the hollow optical fibre (creating the evanescent field which confines transversely) and to shine some of this blue-detuned light across the fibre (creating the narrow longitudinal lasing confinement).

With such a lasing cavity, and a gravitational pump cavity atoms could be cooled down in an atom trap. They could then be injected or allowed to diffuse into the optical fibre where they would become confined into the pump cavity by gravity. After making the atomic transition from the excited "pump" state to the "lasing" state the atoms would then see the potential which forms the lasing cavity. We show later that a large number of atoms will build up in the ground state mode under suitable conditions. This can then be coupled out as the atom laser output. The process of populating the lasing mode is considered in the next section.

2.4 Population of the lasing mode

Atoms enter the system from a thermal source. We consider an initial rate of atoms entering the system which we call the pump rate, r_1. The coupling between the pump and laser cavity occurs through spontaneous emission. The rate of transfer of atoms from the pump cavity to the lasing cavity depends both on this atomic transition rate, r_{12}, and on the average wavefunction overlap between the pump atoms and the lasing cavity. The pump atoms are cooled. However, they will occupy a large number of modes of the pump cavity. The average overlap between the pump cavity and the jth mode of the lasing cavity, g_j, is equal to the sum over all the pump cavity states of the probability of finding an atom in that state, multiplied by the overlap between it and the jth energy state of the lasing cavity,

$$g_j = \sum_{i=0}^{\infty} n_i g_{ij} / N_1, \tag{2.5}$$

where N_1 is the number of atoms in level $|1\rangle$ in any pump cavity state. g_{ij} is the value of the wavefunction overlap between the ith energy state of the pump cavity and the jth energy state of the lasing cavity. This overlap includes the effect of the random momentum kick from the spontaneously emitted photon. n_i is the number of atoms in the ith pump cavity state. The exact nature of the pump cavity distribution does not affect the qualitative behaviour of the atom laser scheme, so for calculational purposes we will assume that the population of states is a Bose-Einstein distribution,

$$n_i = \frac{z \exp\left[-E_i/k_b T\right]}{1 - z \exp\left[-E_i/k_b T\right]}, \tag{2.6}$$

where E_i is the energy of the ith cavity state, k_b is the Boltzmann constant and T the temperature. z is the fugacity, which is related to the chemical potential, and can be found by solving the equation $\sum_{i=0}^{\infty} n_i = N_1$. The total rate R_{12j} at which atoms transfer from the pump cavity to the jth mode of the lasing cavity is given by

$$R_{12j} = (N_{2j} + 1) N_1 \, r_{12} \, g_j, \tag{2.7}$$

where $(N_{2j} + 1)$ is the Bose-enhancement factor due to the presence of N_{2j} bosons in level $|2\rangle$ and the jth state of the lasing cavity. g_j is given by Eq. (2.5). We present details of the calculation of g_{ij} below.

2.4.1 Wavefunction overlap between cavities

The overlap, g_{ij} between an atom in the ith state of the pump cavity and the jth state of the lasing cavity is given by

$$g_{ij} = \int_0^{\pi} \frac{d\phi}{4\pi} \int_{-\pi}^{\pi} d\theta \, \sin(\phi) \times \left| \int d\mathbf{r} \, \phi_i^*(\mathbf{r}) \psi_j(\mathbf{r}) \, \exp\left[i\mathbf{k}.\mathbf{r}\right] \right|^2, \tag{2.8}$$

where the domain of the k space integrals is a spherical shell of radius k_0. This accounts for the spontaneous emission of a photon with wavevector k of magnitude k_0. For simplicity we assume that spontaneous emission is isotropic. Other emission distributions are found to give similar overlap results for a particular k_0. ϕ_i and ψ_j are the wavefunctions of atoms in the ith and jth energy states of the pump and lasing cavity respectively.

The lasing states are modelled in this paper as the eigenstates of three dimensional harmonic oscillators. The transverse mode structure of the pump cavity is likewise modelled as harmonic oscillators, while the longitudinal states depend on the exact physical situation we are using. If we consider a cavity formed by blue detuned light beams then the most appropriate model for the longitudinal states are eigenstates of a square well. For a gravitational cavity, harmonic oscillator states are appropriate.

The initial spatial wavefunction for atoms in the pump cavity state is thus given by

$$\phi_{n_x n_y n_z}(x, y, z) = \phi_{n_x}(x) \, \phi_{n_y}(y) \, \phi_{n_z}(z), \tag{2.9}$$

where the transverse modes, ϕ_{n_x} and ϕ_{n_y},

$$\phi_{n_x}(x) = \frac{1}{\sqrt{2^{n_x} \, n_x!}} \, H_{n_x}\left(\sqrt{\frac{m\omega_x^{(1)}}{\hbar}} x\right) \, \phi_0(x). \tag{2.10}$$

are the one-dimensional energy eigenstates for an harmonic oscillator. In the above expressions, $H_{n_x}(x)$ is an Hermite polynomial, m is the mass of the atom, and $\omega_x^{(1)}$ is the harmonic oscillator angular frequency in the x direction for the pump cavity. The ground state wavefunction, ϕ_0 is given by

$$\phi_0(x) = \left(\frac{m\omega_x^{(1)}}{\pi\hbar}\right)^{1/4} \exp\left[\frac{-m\omega_x^{(1)} x^2}{2\hbar}\right]. \tag{2.11}$$

A similar expression to Eq. (2.10) holds for ϕ_{n_y}. For the pump cavity, the longitudinal mode ϕ_{n_z} will also be as given in Eq. (2.10) if a harmonic cavity is considered. If the cavity is formed from two atomic mirrors using blue-detuned light, a square well is a more appropriate model for the longitudinal (z) dimension of the pump cavity. In this case, the eigenstates in the z direction are

given approximately by

$$\psi_{n_z}(z) = \begin{cases} \sqrt{\frac{2}{a}} \sin\left(\frac{n_z \pi (z+a/2)}{a}\right) & \text{if } -a/2 < z < a/2 \\ 0 & \text{if } |z| > a/2 \end{cases} \tag{2.12}$$

We can evaluate the overlap between an atom in the ith state of the pump cavity and the jth state of the lasing cavity by writing Eq. (2.8) as

$$g_{ij} = \int_0^\pi \frac{d\phi}{4\pi} \int_{-\pi}^{\pi} d\theta \, \sin(\phi) \, g_x g_y g_z, \tag{2.13}$$

where g_x, g_y and g_z are 1-Dimensional overlap factors, given by, for instance,

$$g_x = \int_{-\infty}^{\infty} \phi_i^*(x) \psi_j(x) \, e^{ik_x x}. \tag{2.14}$$

Here, it has been possible to break up the three dimensional wavefunction into the tensor product of 1-dimensional wavefunctions because the potential which is confining the atoms can be written as $V = V_x + V_y + V_z$ [50]. In these expressions, the momentum kick, k is given by

$$k_x = k_0 \sin\phi \cos\theta \tag{2.15}$$

$$k_y = k_0 \sin\phi \sin\theta \tag{2.16}$$

$$k_z = k_0 \cos\phi. \tag{2.17}$$

Once written in this form, the wavefunction overlap between the pump and lasing states for our model can be calculated analytically, or by numerically evaluating the integrals in Eq. (2.14). In the transverse directions, x and y, the potential is assumed to be harmonic with frequency $\omega_x = \omega_y = \omega$. This describes the trapping from the evanescent field of the hollow optical fibre. The 1-Dimensional overlap, g_x, between the mth level of the pump cavity with the nth level of the lasing cavity, including the effect of a momentum kick, k is calculated to be

$$O^x_{mn} = \exp(k_x^2 \, l^2/2) \sqrt{\frac{2^n m!}{2^m n!}} \left(\frac{ik_x l}{\sqrt{2}}\right)^{n-m} L_m^{n-m}(-k_x^2 l^2), \tag{2.18}$$

$$l = \sqrt{\frac{\hbar}{2m\omega}}, \tag{2.19}$$

$$L_m^{n-m}(u) = \sum_{r=0}^{m} \frac{u^r}{r!} \frac{n!}{(m-r)!(n-m+r)!}. \tag{2.20}$$

A similar expression can be obtained for g_y. The overlap in the longitudinal direction depends on our model of the pump cavity and the lasing cavity. We as-

sume the lasing cavity to be approximately harmonic with frequency ω_z. If we further assume the pump cavity is also approximately harmonic, with angular frequency $\omega_p \neq \omega_z$ (for instance a gravitational cavity discussed above) we obtain the overlap between the nth level of the pump cavity with the ground state of the lasing mode to be

$$g_z = \frac{2(-1)^n(\omega_p\omega_z)^{1/2}\,(\omega_p-\omega_z)^n}{2^n n!(\omega_p+\omega_z)^{n+2}} \times \exp\left[\frac{-m\omega_p\bar{z}^2}{\hbar} - \frac{\hbar(k_z - im\omega_p\bar{z}/\hbar)^2}{m(\omega_z+\omega_p)}\right] \times H_n^2\left[\frac{i(k_z - im\omega_p\bar{z}/\hbar)\sqrt{\hbar\omega_z}}{\sqrt{m}(\omega_p^2-\omega_z^2)^{1/2}}\right]. \tag{2.21}$$

In this expression k_z is the z component of the momentum kick which occurs in changing state to the lasing state, given by Eq. (2.17). $\bar{z}$ is the relative displacement in the longitudinal (z) direction of the pump and lasing cavities. This allows for the possibility that the lasing cavity may be situated at the edge of the pump cavity rather than in the centre. We have only considered the overlap with the ground state, here, as it is the population of this mode, the lasing mode, which most concerns us in the atom laser model. Furthermore, the overlaps with higher states cannot be evaluated analytically. A program was developed which numerically evaluated the overlap factors with higher lasing states.

Eq. (2.21) describes the overlap factors with the lasing mode for the case in which the pump cavity is harmonic in the longitudinal direction. This could describe, for instance, a gravitational cavity. The other possible method of creating the pump cavity would be with the use of lasers to create a potential barrier for the atoms in the pump electronic state. In this case, the longitudinal potential is better described as a square well, of length l_p. The lasing cavity is still harmonic, with frequency ω_z, however we define $l_z = \sqrt{\hbar/(2m\omega_z)}$ for convenience. For this model the appropriate overlap amplitude between the nth pump level and the mth lasing level is given by

$$g_z = \sqrt{\frac{1}{2^{m-1}m!l_p}}\left(\frac{1}{2\pi l_z}\right)^{1/4} \times \int_{-l_p/2}^{l_p/2} \sin\left(\frac{n\pi(z+l_p/2)}{l_p}\right) H_m\left[\frac{z-\bar{z}}{\sqrt{2}l_z}\right] \times \exp\left[\frac{-(z-\bar{z})^2}{4l_z^2} + ik_z z\right] dz. \tag{2.22}$$

The integral in Eq. (2.22) must be evaluated numerically, in general. Analytic results however can be obtained for the overlap of the nth pump state with the ground state of the lasing mode,

$$g_z = \sqrt{\frac{\pi l_z}{2l_p}}\left(\frac{1}{2\pi}\right)^{1/4} i\exp\left[\frac{-l_z^2(k_z l_p + n\pi)^2}{l_p^2} + ik_z\bar{z}\right] \times \tag{2.23}$$

$$\Bigg[\exp[4k_z l_z^2 n\pi/l_p]\; e^{-i(n\pi(1/2+\bar{z}/l_p))} \times$$
$$\left(\mathrm{erf}\left[\frac{l_p + 4ik_z l_z^2 - 4il_z^2 n\pi/l_p + 2\bar{z}}{4l_z}\right] + i\,\mathrm{erf}\left[\frac{l_p - 4ik_z l_z^2 + 4il_z^2 n\pi/l_p - 2\bar{z}}{4l_z}\right]\right)$$
$$- e^{i(n\pi(1/2+\bar{z}/l_p))} \times$$
$$\left(\mathrm{erf}\left[\frac{l_p + 4ik_z l_z^2 + 4il_z^2 n\pi/l_p + 2\bar{z}}{4l_z}\right] + i\,\mathrm{erf}\left[\frac{l_p - 4ik_z l_z^2 - 4il_z^2 n\pi/l_p - 2\bar{z}}{4l_z}\right]\right)\Bigg].$$

For a given pump model, we can therefore use the above results to obtain the overlap factors, g_{ij} between the ith pump and jth lasing state. Using these expressions in Eqs. (2.5-2.7), we can obtain the total rate at which atoms are transferred into the jth mode of the lasing cavity. We will discuss the rate equations which we derive for the atom laser model in section 2.6. Below we discuss a particular set of parameter values which are typical of those one would obtain from the overlap calculations outlined above.

2.4.2 Parameter values

Before presenting the full rate equations, we discuss parameter values for the quantities involved in our atom laser model. The figures and rate equation values presented later will use the values we discuss below.

We consider in this work the overlap factors obtained with the pump cavity modeled as a square well with sides of length 100μm in the longitudinal direction. The lasing cavity is modeled as a three dimensional harmonic oscillator. The oscillator frequencies ω_i are specified in terms of the ground state width, d_i

$$d_i = 2\sqrt{\frac{\hbar}{2m\omega_i}}. \tag{2.24}$$

In the longitudinal direction the width of the lasing cavity is $d_i \approx 2\mu$m. Transverse confinement for both cavities is modeled by oscillators in the transverse directions with widths of $d_i = 1.5\mu$m. The lasing cavity is displaced a distance $\bar{x}$ from the center of the pump cavity. For definiteness, we consider a spontaneous emission kick from the $|1\rangle \rightarrow |2\rangle$ transition of magnitude $k_0 = 10^6$ m^{-1} which corresponds to an infrared transition. Modeling a lasing cavity placed at the edge of the pump cavity, $\bar{x} = 48\mu$m, we calculate the average overlap for a spontaneous emission kick of magnitude 10^6 m^{-1} to be $g_1 = 0.00571$. The overlaps, g_j with the higher exited states ($j > 1$) are smaller, with the next greatest overlap, $g_2 = 0.00362$ occurring with the state $n_x = 1$, $n_y = n_z = 0$. In the analysis leading to Fig. 2.3, later, we use these values, and consider the six lowest energy states of the lasing cavity. All of these apart from the first are found to have negligible population in steady state because of their weaker overlap

with the pump cavity modes, and due to the Bose-enhancement of transitions into already populated states. In the rate equations which describe pumping we also use an atomic transition rate, r_{12}, given by the inverse lifetime of the initial atomic level, $|1\rangle$. For definiteness we assume that $r_{12} = 0.1\ \mathrm{s}^{-1}$, corresponding to $|1\rangle$ being quite long lived.

In the next section we calculate the rate of loss of atoms from the lasing mode through output coupling by state change.

2.5 Output coupling

We discuss here a method of switching the atomic state of the atoms, using a Raman transition, to allow output coupling from the system. A pair of lasers at frequencies ω_1 and ω_2 induce a Raman transition from level $|2\rangle$ to the output level $|4\rangle$ of the atom, see Fig. 2.1. This output level is not trapped.

The lasers may be oriented as discussed in section 2.2 so as to impart a net momentum kick to the atoms of magnitude $2\hbar k_z$ in a particular direction, z. For the hollow fibre situation discussed in section 2.3, the z direction is the longitudinal fibre direction, so that the atoms are pushed out of the fibre. The lasers are on resonance with the Raman $|2\rangle \leftrightarrow |4\rangle$ transition. They are far detuned from the $|2\rangle \rightarrow |3\rangle$ and $|4\rangle \rightarrow |3\rangle$ resonances to reduce excitation to level $|3\rangle$. The Raman transition from level $|2\rangle$ to level $|4\rangle$ has a transition rate that depends on the Rabi frequencies, Ω_1 and Ω_2, of the two lasers for their respective transitions $|2\rangle \rightarrow |3\rangle$ and $|4\rangle \rightarrow |3\rangle$. This rate also depends on the detuning of the two lasers from level $|3\rangle$. This transition rate can be found from scattering theory [51]. We discuss this below.

2.5.1 Transition rate

We estimate the output coupling rate at which atoms change from the lasing state, $|2\rangle$ to the output state, $|4\rangle$ and are lost from the system. In our model atoms change state through a Raman transition to an untrapped state. An alternative method would involve an RF transition. In either case, if the coupling is left on the atoms may undergo Rabi oscillations in and out of the trapped state. Here we wish to model a process whereby the majority of atoms which change state in the Raman transition are irreversibly lost from the system. For a continuous coupling, one method by which this occurs would be through a further change of electronic state. Here however, we consider state $|4\rangle$ to be metastable. Instead the Rabi oscillations are damped through the atoms exiting the physical interaction region defined by the Raman lasers. If the atoms leave the interaction region, then they can no longer couple back into the trap. Loss from the interaction region in this way is essentially analogous to having

a "temporally dependent" output coupler in that some time after the atoms change state the interaction is effectively turned off. We note in passing that if the output transition involved an r-f transition, it may not be possible to produce a spatially localized interaction region. We discuss these issues in more detail in Chapter 4 in the context of the Born-Markov approximation.

The Raman transition rate, r_{24}, depends on the intensity of the lasers and the effective loss rate from the system of atoms in level $|4\rangle$. This result can be understood by considering a simple two level atom system. In this simple system, atoms are pumped into the upper level, level $|2\rangle$ by a laser at some rate R. Thus we can write $\dot{\rho}_{22} = -\gamma_2\rho_{22} + R$, where γ_2 is a loss rate from level $|2\rangle$. This equation has a steady state, given by $R = \gamma_2\rho_{22}$. However, it can be shown that in steady state $\rho_{22} \approx \Omega^2/\gamma_2^2$ where Ω is the Rabi frequency of the atom transition and we have assumed that the detuning of the lasers from the atomic transition is small. This leads to the rate of transfer of atoms from the initial to final level of $R = \Omega^2/\gamma_2$. By analogy, for the Raman transition we expect the transfer rate to be given by $r_{24} \approx \Omega^2/\Gamma_4$. Here Γ_4 is the loss rate of atoms from the output level, and Ω is now an equivalent two-photon Rabi frequency, given by $\Omega = \Omega_1\Omega_2/(2\Delta)$, with Δ now the single photon detuning of the lasers from the level which mediates the Raman transition. Normally, these equations are derived with γ_2 in the 2-level system (and hence our Γ_4) given by the spontaneous decay rate of the final level. Here however we have broadening due to the finite interaction time of the atoms with the light beams. This is transit time broadening [6]. We assume that the spontaneous emission rate is small in comparison to this as the final state, $|4\rangle$ is metastable.

The equations for the output transition rate, r_{24}, which we have motivated above can also be derived from Bloch equations or from scattering theory [51]. Fermi's golden rule for transitions can be used to obtain the transition rate in terms of photon fields as

$$\begin{aligned}
\frac{1}{\tau} &\approx \frac{2\pi e^4}{\pi\hbar^4}\left|\frac{\epsilon_s.D_{fi}\ \ \epsilon.D_{i1}}{\omega_i-\omega}\right|^2 \times \\
&\quad \times\left(\frac{\hbar}{2\epsilon_0 V}\right)^2 \omega\omega_s\bar{n}(\bar{n}_s+1) \times \frac{\Gamma_f}{(\omega_f-\omega-\omega_s)^2+\Gamma_f^2} \qquad (2.25)\\
&\approx \frac{\omega\omega_s\bar{n}\bar{n}_s e^4}{2\hbar^2\epsilon_0^2 V^2\Gamma_f} \times \left|\frac{\epsilon_s.D_{fi}\ \ \epsilon.D_{i1}}{\omega_i-\omega}\right|^2 \qquad (2.26)\\
&= \frac{\Omega_{i1}^2\Omega_{fi}^2}{8\Delta^2\Gamma_f}\mathrm{s}^{-1} \qquad (2.27)
\end{aligned}$$

In Eq. (2.25) - Eq. (2.27) we have used a notation typical of that used for scattering problems [51]. Eq. (2.25) begins by describing the Raman transition as a two-photon scattering process. ϵ and ϵ_s are the unit polarization vectors of the incident and scattered photons respectively. D_{fi} is the electric dipole matrix

element of the atom between the final and intermediate level which mediates the Raman transition. Similarly, D_{i1} is the matrix element between the intermediate and initial level of the Raman transition. ω and ω_s are the frequencies of the absorbed and scattered photons in Raman process, respectively. $\hbar\omega_f$ and $\hbar\omega_i$ give the energy of the final atomic level and intermediate atomic level in the Raman transition. Γ_f is the linewidth of the final level, which includes broadening effects such as Doppler broadening and transit time broadening. Typically, here, we will consider parameter regimes where this linewidth is dominated by transit time broadening. In contrast, the initial level is assumed to be the ground state or another long lived state with a very narrow linewidth. In Eq. (2.26) $\bar{n}$ and $\bar{n_s}$ are the number of photons of frequency ω and ω_s respectively in a box of volume, V. These lead to the n-photon Rabi frequencies, Ω_{i1} and Ω_{fi}.

Eq. (2.27) is equivalent to the transition rate motivated previously using the two-atom picture. We rewrite this equation in a notation which is consistent with that used throughout the rest of this chapter as:

$$r_{24} = \frac{\Omega_1^2\Omega_2^2}{8\Delta^2\,(1/t_0)}. \tag{2.28}$$

Here, $\Delta = \omega_{32} - \omega_1$ is the detuning (see Fig. 2.1). $\hbar\omega_{32} = \hbar(\omega_3 - \omega_2)$ is the energy of the level which mediates the Raman transition minus the ground state energy. t_0 is the time scale on which atoms are irreversibly lost from the system due to the momentum kick. The atoms that are lost from the system due to this momentum kick are the atom laser output. We assume that the total momentum kick is purely in the longitudinal direction, z. We are also assuming that $1/t_0 > \gamma_4$, where γ_4 is the linewidth of level $|4\rangle$. This is a good approximation if γ_4 is metastable and hence has a long lifetime. Here, t_0 is estimated by

$$t_0 = \frac{l_z}{2\hbar k_z/m}, \tag{2.29}$$

where m is the mass of the atom, l_z is the length of the light-atom cavity interaction region in the z direction and $2\hbar k_z$ is the size of the momentum kick.

To calculate this transition rate, we have implicitly assumed that the system is governed by an irreversible rate process, and that atoms which leave the interaction region do not return to the system. This irreversibility condition is given by:

$$\frac{\Omega_1\Omega_2}{\Delta} < \frac{1}{t_0}. \tag{2.30}$$

2.5.2 Practical considerations

In the previous section we discuss the output coupling rate, r_{24} which we obtain from using a Raman transition to change the state of our lasing atoms into an untrapped output state. For the atom laser, however, we require that the output coupling is coherent. As we have mentioned previously a rate equation description does not provide any information about the quantum statistics of the atom laser. We will discuss a fully quantum description of this in later chapters. For now, however, we note that if a single mode of the lasing cavity is populated with a coherent state, then to couple this out into a coherent atom laser beam requires a unitary coupling mechanism.

In practice, we therefore require a coherent transfer of the population from level $|2\rangle$ to level $|4\rangle$ for our atom laser output. To ensure that the transfer is unitary we require negligible spontaneous emission from level $|3\rangle$. More specifically, we require that the rate at which atoms populate and then spontaneously emit from level $|3\rangle$ is much less than the rate at which atoms leave the system coherently, $N_{21}r_{24}$. This constraint is given by

$$\frac{\Omega_1^2}{\Omega_1^2+\Delta^2}\frac{N_{21}\Gamma_3}{2} << N_{21}r_{24}. \tag{2.31}$$

We have only considered in this expression the population of $|3\rangle$ due to atoms in level $|2\rangle$. The population due to level $|4\rangle$ atoms is negligible compared to this, as the number of atoms in state $|4\rangle$ is always small, (see section 2.6). We now consider typical values of the quantities involved in these expressions and show that condition Eq. (2.30) and Eq. (2.31) are satisfied for the values we later use.

The physical situation we consider is output coupling achieved by shining two lasers diagonally across the lasing cavity. This has the dual purpose of localizing the interaction region, as well as providing a total momentum kick, $2\hbar k_z$, directed along the longitudinal axis of the optical fibre (the transverse components cancel). The atoms move out of the interaction region due to the momentum kick, thus forming the atom laser beam. For definiteness we use a value of $2k_z = 1.31 \times 10^7$ m^{-1} in this work. This value could be achieved using lasers with wavelengths $\lambda = 480$ nm oriented at 60^0 to the long axis of the fibre. It is possible to produce light of this wavelength with a frequency doubled titanium-sapphire laser. Assuming a typical atomic mass $m = 10^{-26}$ kg and size of the interaction region, $l_x = 2 \times 10^{-6}$ m, we find that the timescale on which atoms leave the system due to the momentum kick is given by Eq. (2.29) to be $t_0 = 1.5 \times 10^{-5}$ s. Using this value for t_0, we find that constraint (2.30) can be fulfilled using large detunings, and relatively small Rabi frequencies. If state $|3\rangle$ has a linewidth of $\Gamma_3 = 2\pi \times 1.6$ MHz then both constraints (2.30) and (2.31) can be satisfied with the output lasers detuned by an amount, $\Delta =$

$2\pi \times 1.6$ GHz and Rabi frequencies, $\Omega_1 = 2\pi \times 50$ kHz and $\Omega_2 = 2\pi \times 1.6$ MHz. With these values the single atom rate constant, r_{24} is given by Eq. (2.28) to be $r_{24} = 0.125\ \mathrm{s}^{-1}$. The total rate at which atoms leave the system as the atom-laser beam is then given by $N_{21} r_{24}$.

In the discussion above we assumed that the lasers impart a fixed momentum kick of magnitude $2\hbar k_z$ to the atoms. This assumption corresponds to modelling the lasers as plane waves. Atoms undergo a Raman transition, absorbing a photon from one of the beams and emitting into the other. The final state of the atoms will, in general, have a non-zero mean momentum as the atoms will obtain a longitudinal momentum kick from the Raman lasers. In the transverse direction, the output state of the atoms remains the ground state mode of the hollow optical fibre. This is achieved using output coupling lasers with a sufficiently narrow linewidth compared with the separation of the lasing cavity transverse energy levels. By suitably tuning such Raman lasers to the output atomic level it is impossible for the atoms to excite into a higher transverse mode of the fibre, as the energy required to change internal atomic levels and excite the atoms to a higher transverse mode is higher than the available energy from the Raman photons. For a fibre approximately 2μm in diameter this requires the Raman lasers to have a linewidth of only a few kHz, which can be achieved by active stabilization.

In the longitudinal direction, the output atoms in state $|4\rangle$ are no longer trapped. The atoms couple to a continuum of momentum eigenstates. Since the initial wavefunction is an energy eigenstate of the lasing cavity the atoms do not have a definite momentum, due to the position-momentum uncertainty principle. When the atoms leave the trap they have a momentum distribution with some width $\hbar\Delta k$. Based on the time-energy uncertainty relation we expect the output linewidth to be narrower for slower output coupling. We can obtain an upper bound for the output width by considering fast output coupling. By fast we mean that the internal state of the atom is changed without time for the spatial wavefunction to evolve. Then the spread in momentum due to the presence of a momentum distribution in the cavity is identical to the momentum spread one would obtain from a pulsed atom beam created by removing the walls of the cavity as suggested by Guzman *et al.* [1]. We discuss the nature of the output in the more appropriate context of the full many-particle theory of output coupling in Chapter 3.

For the parameters considered above the longitudinal kick is of the order of $2k_z \approx 1.3 \times 10^7\ \mathrm{m}^{-1}$, in comparison to the momentum spread of the atoms in the lasing mode of length 2μm of $\Delta k \approx 10^6 \mathrm{m}^{-1}$. In practice, the laser beams are not plane waves and will also contribute to the final momentum spread of the atomic beam. This will depend on the shape of the Raman laser beams. The size of this spread can be reduced by increasing the waist size of the laser beams. For instance, we can estimate the size of this spread by considering a

Gaussian laser beam focussed down to a waist of size $w_0 = 2\mu$m. This corresponds to focusing onto an interaction region of the size of the laser cavity that we consider in section 2.3. The gaussian transverse wavevector spread has standard deviation $\sigma = 5 \times 10^5 \text{m}^{-1}$. Thus the lasers impart a range of kicks which is somewhat smaller than the spread in the momentum in the cavity, Δk. In fact, the assumption of plane wave lasers can be made arbitrarily good by increasing the waste size. This, however, may lead to a decreased output coupling rate as the interaction region which the atoms have to leave becomes larger. This problem, however, can be avoided by increasing the momentum kick imparted on the atoms.

2.6 The atom laser rate equations

The advantage of the rate equation approach to describing an atom laser lies in the ability to demonstrate clearly certain properties one would expect from an atom laser. In particular, we show here the existence of a laser threshold in our model. Above this pumping threshold, our rate equations show that a large number of bosons build up in a single mode of the lasing cavity - a behaviour which is expected of a "laser" by analogy with the optical device. Rate equations such as these, while failing to describe the full quantum nature of a laser, provide a useful practical tool to understand the workings of a laser - be it atom, optical or other.

Our model of the atom laser contains analogous elements to those found in the optical laser and thus the rate equations we present have many similar elements. One of the differences is in the pumping process. Here our pumping consists of the loading of the pump cavity. In an optical laser, pumping involves exciting atoms which then emit photons. This difference is a consequence of the inability to create atoms in a manner analogous to creation of photons. Instead, atoms must be transferred from different states to the lasing state. Another difference is that the output coupling of our atom laser also involves changing the state of the atoms.

One important characteristic of the optical laser that is observed in our atom laser model is the presence of a threshold condition. This threshold condition occurs in an optical laser when the net amplification between the mirrors for a single photon circulating the cavity equals the loss at the mirrors. Similarly for the atom laser threshold, we consider atoms injected into an otherwise empty system ($N_{2j} = 0$). The threshold condition occurs when the single atom input rate into the lasing cavity, $g_1 r_{12}$, is just sufficient to dominate the loss rate, r_{24}. We thus expect a threshold when $r_{12} = r_{24}/g_1$. This threshold condition can in turn be expressed in terms of the injection rate into the pump cavity, r_1, using the fact that for the empty system considered for the onset of

threshold, $r_1 \approx r_{12}$ at steady state. This gives the threshold condition in terms of the rate of input into the pump cavity as $r_1 \approx r_{24}/g_1$.

We now present rate equations for an atom laser scheme. Similar equations were investigated independently by Spreeuw *et al.* as outlined in section (1.5.1), though the overlap factors g_j, and rates, r_{12} and r_1 in our equations are different due to physical differences between the schemes. Spreeuw *et al.* consider only irreversible output coupling and so have no equation which is equivalent to Eq. (2.34). We begin, for generality, with the inclusion of level $|4\rangle$ and consider an unspecified output coupling method which may allow atoms to transfer back into the lasing mode at rate r_{42}. For the parameters and output coupling method discussed in section 2.4.2, however, our output coupling is irreversible. In this regime we do not have to consider a separate output atomic level and we eliminate Eq. (2.34) from the system of equations. We do this to obtain Eq. (2.35) and the later results in this section for the model we have described earlier.

These rate equations allow us to investigate the number of atoms in the modes of the lasing cavity as a function of the pumping rate and of time, and to verify the threshold condition. Using the notation presented earlier for transition rates between the various levels, rate equations for each of the atom laser levels are obtained.

In these equations r_{24} describes a general coupling rate between level $|2\rangle$ and $|4\rangle$. This rate is not, in general, correctly given by the values presented earlier in this chapter. These values correspond specifically to irreversible output coupling. For irreversible coupling the back coupling rate from level $|4\rangle$ to $|2\rangle$ must also be set to zero for consistency and level $|4\rangle$ can be eliminated from the system. We do this to obtain Eq. (2.35). In general, however, the rate equations are given by

$$\frac{dN_1}{dt} = r_1 - \sum_j g_j(N_{2j}+1)r_{12}N_1 - (1-\sum_j g_j)r_{12}N_1, \tag{2.32}$$

$$\frac{dN_{2j}}{dt} = g_j r_{12}N_1(N_{2j}+1) - r_{24}N_{2j} + G_j(N_{2j}+1)N_4 r_{42}, \tag{2.33}$$

$$\frac{dN_4}{dt} = \sum_j N_{2j}r_{24} - \sum_j G_j(N_{2j}+1)N_4 r_{42} - N_4\frac{1}{t_0}. \tag{2.34}$$

Eq. (2.32) describes the pump level. The first term gives the input rate into the pump level. The second term corresponds to the transfer of atoms from the pump cavity to the lasing modes as described in Eq. (2.7). This term includes the bosonic enhancement of transitions into lasing states due to the presence of N_{2j} bosons. The final term gives the loss from level $|1\rangle$ into states which are not in the laser cavity. Eq. (2.33) describes the population of the various modes

of the lasing cavity. The first term corresponds to the Bose enhanced input into the levels of the lasing cavity from the pump. The second term describes the loss from the lasing states into the output level, $|4\rangle$. The final term describes a coupling of atoms from level $|4\rangle$ back into the lasing state. Finally, Eq. (2.34) describes the population of the output level, $|4\rangle$. N_4 is the number of atoms in level $|4\rangle$ which are still confined to the system. The first term describes the gain in level $|4\rangle$ due to atoms transferring from the lasing states. The last two terms describe losses out of level $|4\rangle$ due to coupling back to the lasing cavity and out of the system respectively.

The notation, $|4\rangle$ for the output level only describes the internal state of the atoms. Atoms in level $|4\rangle$ can be described with manifold of states $|4,j\rangle$, where state $|4,j\rangle$ corresponds to an atom that has made a Raman transition from the jth mode of the lasing cavity to the electronic level $|4\rangle$. Each of these $|4,j\rangle$ states can, after further free space evolution couple back to any of the $|2,k\rangle$ states. However, for the coupling rates considered here the coupling between $|4,j\rangle$ to $|2,j\rangle$ dominates. We consider this in more detail in Chapter 5 where we consider the output states in the position basis. Here, for simplicity of notation, we have not considered separate equations for the states $|4,j\rangle$. Instead, we define a coupling constant, G_j, for transitions between $|4\rangle$ and $|2,j\rangle$. $G_j = N_{4j}/N_4$ is the probability that an atom with an electronic level $|4\rangle$ is in the state $|4,j\rangle$. We approximate $G_j \approx N_{2j}/N_2$ in the numerical calculations discussed below, however it is found that the results are insensitive to the value of G_j as this back-coupling term is small in the regime defined by inequality (2.30) where we consider irreversible output coupling. This approximation for G_j is based on the fact that the lasing atoms transfer to level $|4\rangle$ at a rate which is independent of the lasing mode from which they come. Since the lasing atoms are the only source for $|4\rangle$, the number of atoms in each of the $|4,j\rangle$ states depends only on the number of atoms in the corresponding $|2,j\rangle$ state of the lasing cavity.

From Eq. (2.32)-Eq. (2.34), the steady state population of the lasing mode N_{21} can be obtained. For the values we discuss in section 2.4.2, the output coupling is irreversible and all atoms which transfer into level $|4\rangle$ are rapidly lost from the system. In this case, we eliminate Eq. (2.34) from the system and a relatively simple analytic solution for the steady state atom number can be obtained. In this regime the steady state is given by

$$N_{2j} = \frac{1}{2g_j}\left[\left(R_j - (1+\sum_{j'\neq j} g_{j'}N_{2j'})\right) + \left(\left(R_j - (1+\sum_{j'\neq j} g_{j'}N_{2j'})\right)^2 + 4R_j g_j\right)^{\frac{1}{2}}\right], \tag{2.35}$$

where the R_j are dimensionless pumping rate parameters, given by

$$R_j = \frac{r_1 g_j}{r_{24}}. \tag{2.36}$$

The time dependent solutions of Eqs. (2.32)-(2.34) can be found numerically. Fig. 2.3 shows a logarithmic plot of the number of atoms in the lasing mode as a function of time, for an input pumping rate of $r_1 = 1000\ \mathrm{s}^{-1}$. For the

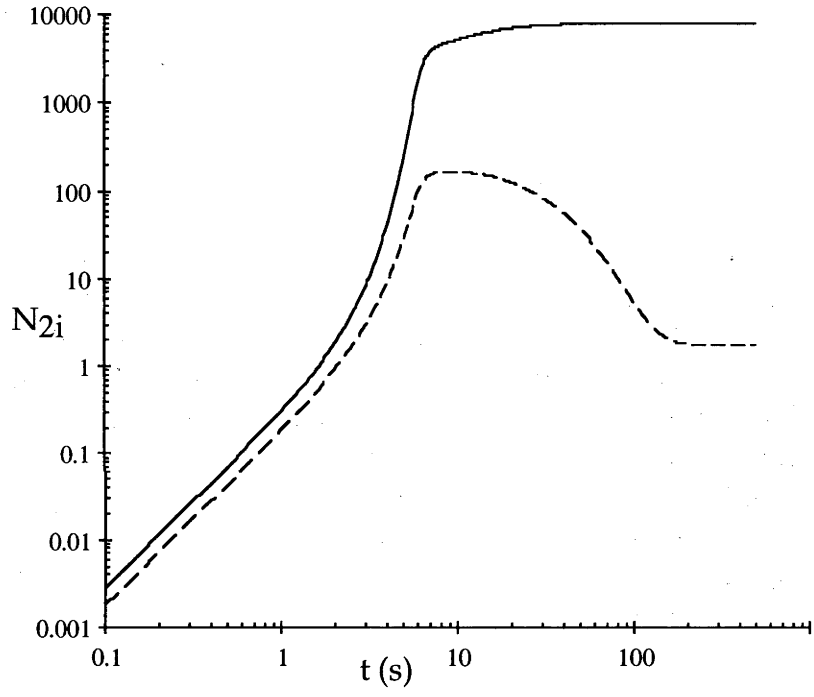

Figure 2.3: Plot of number of atoms in lasing mode, N_{21} (solid line) and in the next highest energy mode N_{22} (dashed line) of the lasing cavity as a function of time, t.

parameters of section 2.3 it takes a time on the order of 10 seconds for a large number ($\gg 1$) of atoms to build up in the lasing mode. After this time the number of atoms reaches a steady state value and remains constant. The number of atoms populating the next highest energy state of the lasing cavity is also plotted in Fig. 2.3. In this plot we see that due to gain competition and the Bose-enhancement of transitions into the highly populated ground state mode the steady state population of the next highest mode is negligible. All higher modes are also found to have negligible population. In the regime where the populations of all but the ground state mode are negligible, the steady state

equations given in Eq. (2.35) reduce to the form

$$N_{21} = \frac{1}{2g_1}\left[(R_1 - 1) + \sqrt{(R_1 - 1)^2 + 4R_1 g_1}\right]. \tag{2.37}$$

This result is analogous to the standard laser population equation [6] and equivalent to results of Spreeuw *et al.* [20]. In the limit of strong pumping $r_1 \to \infty$ the number of atoms in the lasing mode, N_{21}, increases linearly with the pumping rate R_1, with a slope of $1/g_1$. We assume numerical values for the transition rates, $r_{12} = 0.1\ \mathrm{s}^{-1}$, $r_{24} = 0.125\ \mathrm{s}^{-1}$ and for the wavefunction overlap, $g_1 = 0.00571$. A logarithmic plot of the number of atoms at steady state in the lasing cavity, N_{21}, as a function of the dimensionless pumping rate R_1 is given in Fig. 2.4. The threshold pumping rate is $R_1 = 1$, which corresponds to an

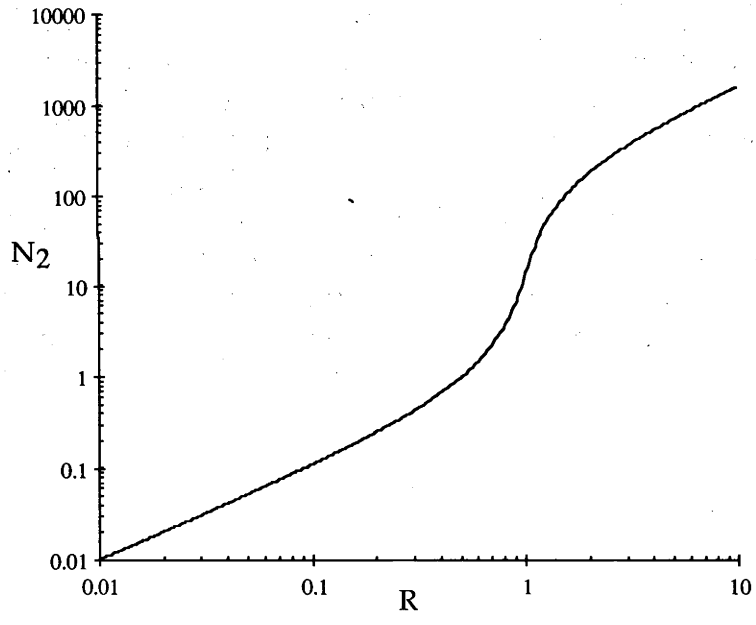

Figure 2.4: Plot of the steady state number of atoms in the lasing mode, N_{21} as a function of the dimensionless pumping rate, R_1.

input pumping rate, $r_1 \approx 21.9\ \mathrm{s}^{-1}$. The general behaviour of these plots does not depend on the particular parameters or details of our model however, for definiteness, we have chosen here parameters which are discussed earlier in relation to our hollow optical fibre model.

2.7 Conclusions

In this chapter we have analyzed an atom laser model and calculated values for the lasing population using an implementation of the scheme based on hollow optical fibres. We have proceeded by analogy with the photon laser and have described a device that will produce a large number of atoms in a single atomic state and a method of coherently coupling a beam of atoms out of this device.

In a strict sense we have not shown that such a device is an "atom laser" as we defined it in Chapter 1. Indeed, such a proof is not possible with a rate equation model. Instead, this model for an atom laser provides a similar role to rate equation models for optical lasers. This is to give an overview of the mechanisms involved in building a large number of bosons in a single mode of a trap and coupling them out. This also allows a number of practical issues involved in creating an atomic beam out of atoms trapped in a single mode to be considered. This model may be called an atom laser in a similar sense to the first experimental atom laser. That is, we have a single mode of a cavity being coupled to the outside world through a change of state. An important advantage of the Raman scheme over switching the cavity walls or the RF scalpel techniques used in experiments to date, is that atoms can be let out continuously. In principle the mechanisms are the same, however. In the experiments the RF fields only act on the atoms for a certain time because they are pulsed. Here the lasers act continuously, but still they effectively act on the atoms for a finite time, as the atoms leave the interaction region. In our case, this is due to the Raman transition giving the atoms a longitudinal momentum kick. In general, however, gravity could also be used to accelerate the atoms away from the interaction region.

We found that the output energy spread is bounded by the momentum spread of the atoms in the lasing cavity in the fast change of state limit. For large coupling rates, the Raman output coupling gives an output spectral density similar to that produced by dropping the walls of the cavity. This is because an atom making the Raman transition changes to a non-trapped state where the atom is no longer affected by the confining potential. We discuss the effects of general (slow) output coupling on the spectrum in more detail in Chapter 3

Other atom laser schemes [23] have found large output linewidths due to collisions. This may increase the linewidth of our atom laser, though as our linewidth is already broad we do not expect this to be a limiting factor and have not considered this in our model. We assume large blue detuning to minimize the excited state population due to the confining light. The Raman transition scheme of Hope and Savage [48] for generating mechanical potentials provides a method for further reducing spontaneous emission.

Chapter 3

Output coupling for an atom laser by state change

Overview

This chapter describes a theory of output coupling based on change of state. We calculate the spectrum of a beam of atoms output from a single mode atomic cavity. The output coupling uses an internal state change to an untrapped state. We present an analytical solution for the output energy spectrum from a broadband coupler of this type. An example of such an output coupler, which we discuss in detail, uses a Raman transition to produce a non-trapped state.

Initially, we rewrite the equations describing output coupling through Raman coupling in a general form. Using the second quantized Hamiltonian for our system we can obtain Heisenberg equations of motion. A general solution of such equations can be found in terms of inverse Laplace transforms. For our particular system we are able to obtain analytic solutions in the limit of broadband coupling.

3.1 Introduction

The previous chapter presented a model for an atom laser which is based on a rate equation description. This model was based on populating a single mode of an atom trap with a large number of bosonic atoms. The essential elements of the atom laser process involve pumping atoms into the single mode of the trap and output coupling the atoms from this mode.

Here we wish to investigate more carefully the output coupling mechanism of the atom laser, and the properties of the output atom field. In this work, we do not specify the exact nature of the trap which confines the atoms. In principle it could be an optical trap created in a hollow optical fibre such as we discuss in Chapter 2. In this work, however, it is perhaps experimentally more

relevant to consider a magnetic trap, similar to those in which Bose Einstein Condensates have been produced to date. We ignore for now the pumping of the trap. By ignoring this, we make the assumption that at some early time we have a large number of bosonic atoms populating a single mode. This restricts us to describing a pulsed atom laser. Nevertheless, this understanding provides a framework for understanding output coupling when pumping is included. In Chapter 5 we will come back and discuss possible methods of continuous pumping of this mode.

Here, we restrict our discussion to the output coupling of a Bose Einstein Condensate - a pulsed atom laser. Experiments in which a Bose Einstein Condensate (BEC) has been produced in the lab are now routine [2–5]. Some experimental advances have also been made on coupling the atoms in a BEC out of a trap. While initial experiments have succeeded in coupling atoms out of a BEC by changing the internal state of the atoms to a non-trapped state [4, 12], there is still much to be understood about the output beam.

There are a number of possible ways in which atoms can be coupled out of a trap. These include

- Turning off the trap
- Quantum mechanical tunneling
- Change of internal state

The simplest method of output coupling is to turn off the trap. This idea has the advantage of simplicity as suggested in an early atom laser paper by Guzman [1]. The result of rapidly turning off the trap, if we are to ignore atom-atom interactions is to reproduce the BEC wavefunction in free space. In particular, the wavefunction momentum width is conserved. As a result, the atoms have the corresponding range of energies in free space and the monoenergetic nature of the original BEC is lost. Indeed, the situation in practical experiments is worse than this as the interaction energy between the atoms repels them away from each other, further increasing the momentum width.

Fortunately, energy conserving output coupling is possible. One example is quantum mechanical tunneling of atoms through the trap walls. This is the atomic analogue to the use of partially transparent mirrors on an optical laser. Such a process has been considered in a model of an atom laser proposed by Wiseman [23]. It would be difficult in practice, however, to use tunneling to produce sufficient fluxes of atoms due to the exponential dependence of the tunneling rate on the trap potential barrier.

The final approach to output coupling that we list above is to change the internal state of the trapped atoms to an untrapped state. Experimentally such a method has been used by implementing radio-frequency pulses to induce

spin flips on trapped atoms in a BEC [4, 12]. Another possible method of inducing a change of state is through a Raman transition. This is the method which we suggest in Chapter 2 for our rate equation model of the atom laser. A Raman transition can have an extremely narrow linewidth so that lasers can be tuned so as to only couple atoms from a particular trap mode, due to energy conservation.

A generic model can be used to describe output coupling which does not specify a particular method out of those discussed above. We present such a model in the next section, and show how this corresponds to a particular, Raman, output coupling method.

3.2 Model

We consider an atomic cavity, the modes of which have annihilation (creation) operators denoted by a_j ($a_j^\dagger$). This cavity is output coupled to a continuum of free modes, indexed by the momentum $\hbar k$, with annihilation (creation) operators denoted by b_k ($b_k^\dagger$). Later we will assume that only the ground state mode, a_0 of the atomic cavity is populated and will ignore the higher modes. We ignore the effects of interactions between the atoms so that the "ground state mode" corresponds to the single particle ground state mode of the trap. In practice, the presence of atom-atom interactions mean that the atoms populate a self consistently defined condensate mode.

We can write the Hamiltonian which describes the cavity and the external modes, respectively, as

$$H_{\mathrm{A}} = H_{\mathrm{sys}} + H_{\mathrm{ext}}, \tag{3.1}$$

$$H_{\mathrm{sys}} = \sum_j \hbar\omega_j \, a_j^\dagger a_j, \tag{3.2}$$

$$H_{\mathrm{ext}} = \int \mathrm{dk}\, \hbar\omega_k \, b_k^\dagger b_k. \tag{3.3}$$

In these equations, $\omega_k = \hbar k^2/2M$ and M is the mass of the atom. The final part of our general model describes the interaction between these two subsystems. The most general form of interaction term is given by

$$H_{\mathrm{int}} = H_{\mathrm{ab}} + H_{\mathrm{aa}} + H_{\mathrm{bb}}, \tag{3.4}$$

$$H_{\mathrm{ab}} = -i\hbar \sum_j \int_{-\infty}^{\infty} dk \, (\kappa_j(k) b_k a_j^\dagger - \kappa_j^*(k) b_k^\dagger a_j), \tag{3.5}$$

$$H_{\mathrm{aa}} = \sum_{j,l} \kappa_{jl} a_j^\dagger a_l, \tag{3.6}$$

$$H_{\mathrm{bb}} = \int dk_1 \int dk_2 \, \kappa(k_1, k_2) b_{k_1}^\dagger b_{k_2}. \tag{3.7}$$

In this equation, the term involving H_{ab} describes the interaction between the internal mode, a_j and the external continuum, b_k. This is the term which describes the output coupling. The other terms included here describe processes in which atoms change between the various modes of the atom trap (H_{aa}) or the various modes of the continuum (H_{bb}) respectively. In each of these, κ describes an interaction strength. The most significant of these is $\kappa_j(k)$ which the shape and strength of the coupling between the jth mode of the trap and the kth mode of the continuum. Different coupling methods correspond to different choices of the shape and strength of $\kappa_j(k)$. For instance broadband coupling has $\kappa_j(k) =$ constant, with the value of the constant dictating the strength of the coupling.

The Hamiltonian terms presented above are general. Later we will simplify this model with some assumptions about the particular output coupling we are considering. In the next section, however, we reconsider output coupling through change of state which we introduced in Chapter 2. Using this output coupling method we show how the Hamiltonian may be written in the general form presented above.

3.2.1 Output coupling through Raman transition

We consider a three level atom model to describe output coupling through a Raman transition. Here we use a single particle description to obtain an effective two level system by adiabatically eliminating level $|3\rangle$ [52]. By second quantizing this we obtain an interaction Hamiltonian of the form (Eq. 3.1-Eq. 3.7). Consider an atom initially in the ground state, $|1\rangle$. We consider using a Raman transition which is mediated by level $|3\rangle$ to transfer the population into the output state $|2\rangle$ as outlined in Fig. 3.1. The interaction Hamiltonian which describes the interaction of atoms with light is given in the single atom picture by $H_{int} = -\mathbf{d}.\mathbf{E}$ where $\mathbf{d}$ is the electric dipole moment operator, and $\mathbf{E}$ is the electric field. This leads to the interaction Hamiltonian which describes the change of state between $|2\rangle$ to $|1\rangle$ through level $|3\rangle$ being given by

$$\begin{aligned} H_{int} &= \Big(\hbar\Omega_1\, f_1(\mathbf{r})\, e^{i(\mathbf{k}_{1L}.\mathbf{r}-\omega_{1L}t)}\, |3\rangle\langle 1| + \\ &\quad \hbar\Omega_2\, f_2(\mathbf{r})\, e^{i(-\mathbf{k}_{2L}.\mathbf{r}-\omega_{2L}t)}\, |3\rangle\langle 2|\Big) + \text{h.c} \end{aligned} \tag{3.8}$$

We have assumed that the interaction occurs through the dipole interaction with two different light beams. There are two lasers, as shown in Fig. 3.1 with frequencies given by ω_{1L} and ω_{2L} respectively. The wavevectors which correspond to these are $\mathbf{k}_{1L}$ and $\mathbf{k}_{2L}$ respectively. Ω_1 and Ω_2 are the Rabi frequencies of the two lasers for their respective transitions $|1\rangle \rightarrow |3\rangle$ and $|2\rangle \rightarrow |3\rangle$. The functions f_1 and f_2 describe the shape of the interaction region.

These equations are written in three dimensions. For simplicity, however

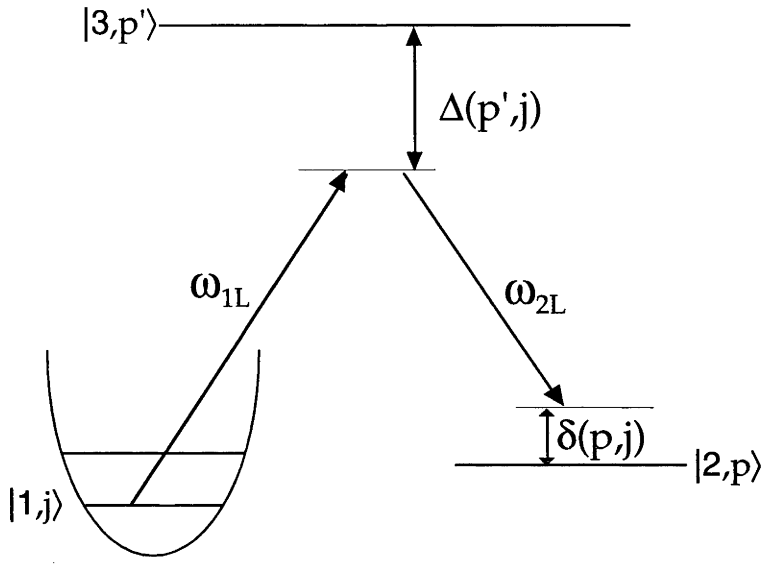

Figure 3.1: Schematic diagram of energy levels and detunings.

we will from here on consider a situation in which we are only interested in one dimension. One example where this is appropriate is in a hollow optical fibre. In this case two dimensions remain tightly constrained both before and after the change of state. In the transverse direction, atoms remain in a single mode and we only need to consider the longitudinal, z direction. Writing the equations in a one-dimensional form is not necessary however it does make the subsequent discussion more simple as we can consider k_{1L} and k_{2L} as wavenumbers. This also helps notationally by reducing the three integrals over k space in later equations to a single integral.

In this picture we can write the non-interaction part of the Hamiltonian as the sum of the energies of the atoms in each of the three states, $|1\rangle$, $|2\rangle$ and $|3\rangle$. We assume that atoms in state $|1\rangle$ are trapped, so we chose a basis for these which are the eigenstates of the trap, labeled by j. The external motion of states $|2\rangle$ and $|3\rangle$ is free, and so we label these by their momentum, p. Thus the free Hamiltonian in this picture is given by

$$\begin{aligned} H_A &= \sum_j (\hbar\omega_1 + E_j)\,|1,j\rangle\langle 1,j| + \int (\hbar\omega_2 + \frac{p^2}{2M})\,|2,p\rangle\langle 2,p|dp \\ &\quad + \int (\hbar\omega_3 + \frac{p^2}{2M})\,|3,p\rangle\langle 3,p|dp \end{aligned} \tag{3.9}$$

To further proceed, we note that we can rewrite the interaction Hamilto-

nian in terms of momentum eigenstates using the equality

$$e^{\pm ikz} = \int_{-\infty}^{\infty} dp\ |p\rangle\langle p \mp \hbar k|. \tag{3.10}$$

This equality is relevant in the case where the interaction regime can be approximated as extending across all space. For now, we continue to include the spatially dependent term, $f_j(z)$ so that we use

$$f(z)e^{ikz} = \int dp_1 \int dp_2 \int dz\ f(z)e^{-i(p_1-p_2-\hbar k)z/\hbar}\ |p_1\rangle\langle p_2|. \tag{3.11}$$

This allows the single particle interaction term to be written in the form

$$\begin{aligned} H_{int} &= \hbar\Omega_1 e^{-i\omega_{1L}t} \int dp \int dp_2\ g(p_2 + \hbar k_{1L} - p)\ |3,p\rangle\langle 1,p_2| \\ &+ \hbar\Omega_2 e^{-i\omega_{2L}t} \int dp \int dp_2\ g(p_2 - \hbar k_{2L} - p)\ |3,p\rangle\langle 2,p_2| + \text{h.c}, \end{aligned} \tag{3.12}$$

where

$$g(\hbar k) = \int f(z)e^{ikz}dz. \tag{3.13}$$

It should be noted that as $f(z)$ becomes increasingly broad in space, we can approximate $g(p)$ increasingly well by $\delta(p)$, the Dirac delta function. This allows considerable simplification of this and the following equations. Also, because atoms in state $|1\rangle$ experience a trapping potential, it will be convenient to consider the basis states $|j\rangle$, the eigenstates of the trap, rather than the momentum eigenstates used above.

The interaction term, as presented above involves a two step change of state. We wish to obtain an effective interaction Hamiltonian which describes the change of state in a similar manner to the generic form given in Eq. (3.1)-Eq. (3.7). To do so we begin by moving into an interaction picture with the Hamiltonian, H_A. This allows the Hamiltonian to be written as

$$\begin{aligned} \tilde{H}_{int} &= \sum_j \int dp\ \hbar\Omega_1\ e^{it\Delta(p,j)} \int dp'\ g(p' - p + \hbar k_{1L})\psi_j(p')|3,p\rangle\langle 1,j| \\ &+ \int dp \int dp'\ \hbar\Omega_2 e^{it(\Delta(p,j)+\delta(p',j))} g(p' - \hbar k_{2L} - p)|3,p\rangle\langle 2,p'| \\ &+ \text{h.c.} \end{aligned} \tag{3.14}$$

We have introduced the detuning of the laser, ω_{1L} from the upper level, $|3\rangle$ by the definition (see Fig. 3.1)

$$\Delta(p,j) = \left[(\omega_3 - \omega_1) + (\frac{p^2}{2m\hbar} - \frac{E_j}{\hbar})\right] - \omega_{1L}, \tag{3.15}$$

and the two photon detuning of the lasers by

$$\delta(p,j) = \left(\frac{E_{gj}}{\hbar} - \omega_{21} - \frac{p^2}{2m\hbar}\right) - (\omega_{2L} - \omega_{1L}). \tag{3.16}$$

The function, $\psi_j(p)$ is the momentum wavefunction of the jth eigenstate of the trap for the atoms in state $|1\rangle$.

To proceed further we consider the evolution of a general state, expressed in terms of the basis states corresponding to the three atomic levels by

$$|\psi_I(t)\rangle = \sum_j b_{1j}(t)|1,j\rangle + \int dp\, b_2(p,t)\,|2,p\rangle + \int dp\, b_3(p,t)\,|3,p\rangle \tag{3.17}$$

We consider the evolution of the general state expressed above under the interaction given by H_{int}, Eq. 3.12. This allows equations for the three levels, b_1, b_2 and b_3 to be obtained as follows

$$i\hbar\dot{b}_{1j}(t) = \int dp\, \hbar\Omega_1 e^{-it\Delta(p,j)} \int dp' g^*(p'-p+\hbar k_{1L})\psi_j^*(p')\, b_3(p,t) \tag{3.18}$$

$$i\hbar\dot{b}_2(p,t) = \int dp'\, \hbar\Omega_2 e^{-it(\Delta(p')+\delta(p))} g^*(p-p'-\hbar k_{2L})\, b_3(p,t) \tag{3.19}$$

$$\begin{aligned} i\hbar\dot{b}_3(p,t) = \sum_j \int dp' \Big(&\hbar\Omega_1 e^{it\Delta(p,j)} g(p'-p+\hbar k_{1L})\psi_j(p')\, b_{1j}(t) + \\ &+ \hbar\Omega_2 e^{it(\Delta(p)+\delta(p'))} g(p'-p-\hbar k_{2L})\, b_2(p',t)\Big) \end{aligned} \tag{3.20}$$

We now wish to adiabatically eliminate the third level, $b_3(p,t)$ from these equations. If $\Delta >> \Omega_1, \Omega_2, \delta$ then we can ignore the time dependence of $b_1(p,t)$ and $b_2(p,t)$. That is, we assume b_1 and b_2 oscillate more slowly than the detuning, Δ. We can solve for $b_3(p,t)$ by integrating the third equation above, making errors of order $t\Omega^3/\Delta^2$ and $t\Omega^2\delta/\Delta^2$. This is small in the limit of large single photon detuning, Δ, with small two photon detuning, δ. Substituting this solution in to the equations for b_1 and b_2 we obtain an effective two level system, with the third level b_3 remaining empty. We thus write our state in the form

$$|\psi_I(t)\rangle = \sum_j b_{1j}(t)|1,j\rangle + \int dp\, b_2(p,t)|2,p\rangle, \tag{3.21}$$

which evolves under the effective (Schrödinger picture) Hamiltonian

$$\begin{aligned} H_{\text{int}}^{\text{eff}} = &\sum_{j,l} h_{11}(j,l)\,|1,j\rangle\langle 1,l| + \sum_j \int dp\, h_{12}(j,p)\,|1,j\rangle\langle 2,p| + \\ &+ \sum_j \int dp\, h_{21}(j,p)\,|2,p\rangle\langle 1,j| + \int dp \int dp'\, h_{22}(p,p')\,|2,p\rangle\langle 2,p'|. \end{aligned}$$

(3.22)

The terms given by h_{jl} for $j,l = 1,2$ are given for the situation we have discussed above by

$$h_{11}(j,l) = \int dp \int dp' \int dp'' \frac{-\Omega_1^2 \hbar g(p' - p - \hbar k_{1L}) \times g(p'' - p + \hbar k_{1L})}{\Delta(p,l)} \times \psi_j^*(p'')\psi_l(p'), \tag{3.23}$$

$$h_{12}(j,p) = \int dp' \int dp'' \frac{-\Omega_1 \Omega_2 \hbar e^{-it(\omega_{2L}-\omega_{1L})} g(p - p' - \hbar k_{2L})}{\Delta(p') + \delta(p)} \times g^*(p'' - p' + \hbar k_{1L})\psi_j^*(p''), \tag{3.24}$$

$$h_{21}(p,j) = \int dp' \int dp'' \frac{-\Omega_2 \Omega_1 \hbar e^{it(\omega_{2L}-\omega_{1L})} g(p'' - p' + \hbar k_{1L})}{\Delta(p',j)} \times \times g^*(p - p' - \hbar k_{2L})\psi_j(p''), \tag{3.25}$$

$$h_{22}(p_1,p_2) = \int dp' \frac{-\Omega_2^2 \hbar g(p_2 - p' - \hbar k_{2L}) \times g^*(p_1 - p' - \hbar k_{2L})}{\Delta(p') + \delta(p_2)}. \tag{3.26}$$

In equations, Eq. (3.22)-Eq. (3.26) we have adiabatically eliminated the level which mediates the Raman transition to produce a two level interaction Hamiltonian in the single particle picture. This ignores the interactions between the various atoms. We can write this effective Hamiltonian in the second quantized picture [53]. If we define the operators a_j and b_k as the annihilation operator for an atom in state $|1\rangle$ in the jth mode of the trap, and the annihilation operator for an atom in state $|2\rangle$ in the momentum eigenstate labeled by k respectively then we obtain the interaction Hamiltonian which describes the action of the Raman lasers given by

$$H_{\text{int}} = \sum_{j,l} h_{11}(j,l)\, a_j^\dagger a_l + \sum_j \int dk\, \hbar h_{12}(j,\hbar k) a_j^\dagger b_k + \sum_j \int dk\, \hbar h_{21}(\hbar k, j) b_k^\dagger a_j + \int dk_1 \int dk_2\, \hbar^2 h_{22}(\hbar k_1, \hbar k_2) b_{k_1}^\dagger b_{k_2} \tag{3.27}$$

with the Hamiltonian describing the trap and free energy given by

$$H_A = H_s + H_r = \sum_j \hbar(\omega_1 + \omega_j) a_j^\dagger a_j + \int dk\, \hbar(\omega_2 + \omega_k) b_k^\dagger b_k. \tag{3.28}$$

The total effective Hamiltonian in the many particle picture is $H_{\text{eff}} = H_{\text{A}} + H_{\text{int}}^{\text{eff}}$. The Hamiltonian, Eq. (3.27) and Eq. (3.28), presented above are in the form of Eq. (3.4) and Eq. (3.1) respectively which describe a general interaction

between two states.

3.2.2 Simplifications

The interaction Hamiltonian presented above is in a form which is somewhat more complex than is typically considered in optical or atom input-output theory. The optical input-output theory begins with an interaction which involves only a single mode of the cavity and terms of the form $b(\omega)a^\dagger$ [7]. Similarly an equivalent atomic formulation of equations of motion by Hope [54] begins with a simplified form of the Hamiltonian we present above.

Here we discuss the physical grounds on which these simplifications are made for our model. The first of these concerns the lasers which provide the Raman transition. In our expression, Eq. (3.27) there are terms of the form $a_j^\dagger a_l$ with $j \neq l$. These terms describe a process in which an atom starts in level $|1\rangle$ and then absorbs and reemits a photon back into level $|1\rangle$, in the process changing trap state. Such processes cannot occur from energy conservation if the Raman lasers are eigenstates of energy with a well defined k value. For instance, if the lasers are modeled as plane waves with a precise k, then the function $g(p)$ is a Dirac delta function, and $h_{jl} = 0$ for $j \neq l$. While the output from a laser cannot be described as a plane wave with a single k number, the contribution from the terms $a_j^\dagger a_l$ ($j \neq l$) is small for typical laser waist sizes. For now we make the approximation that the lasers are sufficiently broad in position space that their momentum uncertainty if effectively negligible on the scale of the wavefunction momentum spread. In this case, $g(p)$ is well approximated by a Dirac delta function and $h_{22}(\hbar k_1, \hbar k_2)$ can be simplified as

$$h_{22} = \frac{-|\Omega_2|^2 \hbar \tilde{\delta}(k_1 - k_2)}{\Delta(\hbar k_2 - \hbar k_{2L}, j) + \delta(\hbar k_2, j)}, \tag{3.29}$$

where we have used $\tilde{\delta}$ to represent the Dirac delta function to avoid confusion with the detuning, δ.

A further simplification comes from considering the form of $\Delta(p, j)$ and $\delta(p, j)$. These are defined in terms of the difference between the lasing energy, $\hbar\omega_{1L}$ and the energy difference between atoms in level $|1\rangle$ in the jth eigenstate of the trap and atoms in level $|2\rangle$ in the momentum eigenstate labeled by p. If we suppose that the atomic energy difference, $\omega_3 - \omega_1$ is much greater than the energy due to motion, $p^2/2m\hbar$ then we can treat the detunings $\Delta(p, j) \approx \Delta$. Similarly $\delta(p, j) \approx \delta$.

Finally we assume that only a single state of the trap is populated, both initially and for later times. In the case of a Bose Einstein condensate being coupled out of the trap this is a natural single mode assumption, which ig-

nores the populations of other modes due to the large build up of bosons in the ground state. Similarly, for an atom laser working above threshold we have seen from the earlier rate equation model that we would expect only a single mode of the trap to be populated by our pump, and further transitions are stimulated preferentially into this occupied state. In Chapter 5 we will reintroduce the higher modes of the trap into a model of output coupling. There we also find that higher order modes do not become significantly populated.

Making the approximations discussed above, we write the Hamiltonian, Eq. (3.27-3.28), in the simplified form

$$H_{\text{eff}} = H_{\text{sys}} + H_{\text{ext}} + H_{\text{int}}, \tag{3.30}$$

$$H_{\text{sys}} = \hbar\tilde{\omega}_0\, a^\dagger a, \tag{3.31}$$

$$H_{\text{ext}} = \int \mathrm{dk}\, \hbar\tilde{\omega}_k\, b_k^\dagger b_k, \tag{3.32}$$

$$H_{\text{int}} = -i\hbar \int \mathrm{dk}\ \left(\kappa(k,t)\, b_k a^\dagger - \kappa^*(k,t)\, b_k^\dagger a\right), \tag{3.33}$$

with

$$\tilde{\omega}_0 = \omega_1 + \omega_0 - \frac{\Omega_1^2}{\Delta_1}, \tag{3.34}$$

$$\tilde{\omega}_k = \omega_2 + \frac{\hbar k^2}{2m} - \frac{\Omega_2^2}{\Delta_2}, \tag{3.35}$$

$$\kappa(k,t) = \Gamma^{\frac{1}{2}} \left(-ie^{-i(\omega_{2L}-\omega_{1L})t}\psi^*(k - k_{1L} - k_{2L})\right), \tag{3.36}$$

$$\Gamma^{\frac{1}{2}} = \frac{\Omega_1\Omega_2}{\Delta_1}. \tag{3.37}$$

The single trap mode is described by the creation operator, $a^\dagger = a_0^\dagger$ and is coupled by the Raman lasers to a continuous spectrum of external modes described by creation operators, $b_k^\dagger$. $\hbar\omega_1$ ($\hbar\omega_2$) is the energy of the trap (output) atomic state. $\hbar\omega_0$ is the ground state trap energy. m is the mass of the trapped atoms. $\hbar k_{1L}$ and $\hbar k_{2L}$ are the momenta of the two lasers inducing the Raman transition, with frequencies ω_{1L} and ω_{2L} respectively. Thus $\hbar(k_{1L} + k_{2L})$ is the total momentum kick received by atoms making the Raman transition. Ω_1 (Ω_2) is the Rabi frequency of the transition between the trapped (output) state and the excited state which mediates the Raman transition. Δ_1 and Δ_2 are the detunings of the two Raman lasers from the excited state. We have assumed these are large to obtain an effective two level Hamiltonian by adiabatically eliminating the upper level. If the lasers are tuned close to the two-photon resonance ($\delta = 0$) then $\Delta_1 \approx \Delta_2$. $\psi(k)$ is the momentum space wavefunction of the ground mode of the trap. Γ is related to the coupling strength, given here in terms of the Rabi frequencies and single photon detuning.

The form of the Hamiltonian, Eq. (3.31) - Eq. (3.33) is valid for an arbi-

trary output coupling through state change from a single mode system to a continuous spectrum of external modes. This is the same form as used in a general theory of optical input-output and a more recent atom input-output theory. Eq. (3.34) - Eq. (3.37) give the general quantities in terms of parameters relevant for change of state through Raman transition for definiteness. The results, however, can be extended to a general output coupler with the coupling strength, $\Gamma^{1/2}$, and the energies $\hbar\tilde{\omega}_0$ and $\hbar\tilde{\omega}_k$ suitably defined. For instance, a change of state in which an RF field induces a spin flip on the atoms and allows them to leave the trap will have a Hamiltonian which is formally the same as the one presented above. Some differences may be that the momentum kick obtained will be zero (or small). This however can be achieved by assuming $k_{1L} = -k_{2L}$ — a Raman transition.

3.3 Equations of motion and solutions

In the atom laser we are interested in the properties of the output field. For instance, we wish to obtain expressions for the output energy spectrum, $\langle b_k^\dagger b_k \rangle$ which is the mean population density of the continuum of free space momentum eigenstate modes, labeled by the momentum $\hbar k$.

Solutions for the output field can be obtained from the Heisenberg equations of motion. For the Hamiltonian given in Eq. (3.30)-Eq. (3.33) the Heisenberg equations of motion lead to the following equations for the annihilation operators, a and b_k respectively

$$\frac{da(t)}{dt} = -i\tilde{\omega}_0 a(t) - \int \kappa(k) b_k(t) dk \tag{3.38}$$

$$\frac{db_k(t)}{dt} = -i\tilde{\omega}_k b_k(t) + \kappa^*(k) a(t). \tag{3.39}$$

These equations can be solved formally by integration, leading to

$$a(t) = a(0)e^{-i\tilde{\omega}_0 t} - \int_0^t \int \kappa(k)\, b_k(t')\, e^{-i\tilde{\omega}_0(t-t')} dk dt' \tag{3.40}$$

$$b_k(t) = b_k(0)e^{-i\tilde{\omega}_k t} + \int_0^t \kappa^*(k) a(t') e^{-i\tilde{\omega}_k(t-t')} dt', \tag{3.41}$$

where we have introduced the initial conditions $a(0)$, $b_k(0)$ as the Heisenberg operators at time $t = 0$. From these equations, we see that if the solution for $b_k(t)$, Eq. (3.41) is substituted into the solution for $a(t)$, Eq. (3.40) then we obtain

$$a(t)e^{i\tilde{\omega}_0 t} = a(0) - \int_0^t dt' \int \kappa(k) e^{i(\tilde{\omega}_0 - \tilde{\omega}_k)t'} b_k(0)$$

$$-\int_0^t dt' \left[\int_0^{t-t'} dt'' \int |\kappa(k)|^2 e^{i(\tilde{\omega}_0 - \tilde{\omega}_k)t''} \right] a(t') e^{i\tilde{\omega}_0 t'}. \quad (3.42)$$

At this point we have simply reproduced equations of motion and formal solutions which are valid for any coupling of the form of our Hamiltonian above. In particular, this is the formal solution which is given by Collet in the optical input-output theory. In the optical case the integrals over k in the above equations are normally written as integrals over ω due to the linear dispersion relation $\tilde{\omega}_k = c_L|k|$ which holds for photons, where c_L is the speed of light. These integrals can be approximated and evaluated to give the standard optical input output theory. In the atom case the dispersion relation is different, $\tilde{\omega}_k \propto k^2$ so new methods of solving these equations and finding the output fields, $b_k(t)$ are required. While work on the atom input-output theory has been developed collectively in our group, the general solution to the above equation was developed by Hope [54]. These equations are linear Volterra equations of the convolution type. By taking the Laplace transform of Eq. (3.42) and using a convolution theorem Hope showed that the general solution for $a(t)$ is given by

$$a(t) = e^{-i\tilde{\omega}_0 t} \mathcal{L}^{-1} \left\{ \frac{a(0) - \mathcal{L}\left[\int \kappa(k) e^{i(\tilde{\omega}_0 - \tilde{\omega}_k)t} b_k(0)\right](s)}{s + \mathcal{L}[\int |\kappa(k)|^2 e^{i(\tilde{\omega}_0 - \tilde{\omega}_k)t}](s)} \right\}(t). \quad (3.43)$$

Here, we have used our own notation, which differs slightly from that used by Hope. A further point to note is that in obtaining this solution from Eq. (3.42) we have taken a Laplace transform of both sides and then the inverse Laplace transform. For this reason, Hope's solution is strictly only valid if the inverse Laplace transform exists. In fact, the inverse Laplace transform does not exist for some functions which correspond to practical output coupling mechanisms. In these cases, the equations may still be solved using a general Volterra equation solver (see Appendix A). Here, however, we consider the inverse Laplace transform to be well defined.

Having obtained an equation for $a(t)$, given by Eq. (3.43) we can substitute this into Eq. (3.41) to obtain solutions for $b_k(t)$ solely in terms of $b_k(0)$ and $a(t')$. Taking the expectation value of this solution, $\langle b_k^\dagger(t) b_k(t) \rangle$ in the case where initially the external modes are empty gives

$$\langle b_k^\dagger(t) b_k(t) \rangle = |\kappa(k,t)|^2 \ \langle a^\dagger(0) a(0) \rangle \ |M_k(t)|^2, \quad (3.44)$$

with

$$M_k(t) = \mathcal{L}^{-1} \left\{ \frac{1}{(s + \mathcal{L}(f')(s)) \ (s + i\delta_k)} \right\}(t), \quad (3.45)$$

$$f'(t) = \int \mathrm{dk}\, |\kappa(k,t)|^2\, e^{-i\delta_k t}, \tag{3.46}$$

$$\delta_k = \widetilde{\omega}_k - \widetilde{\omega}_0 + \omega_{1L} - \omega_{2L} = \frac{\hbar k^2}{2m} - \omega_0. \tag{3.47}$$

The final equality holds for our particular Raman coupling model in the case when the lasers are tuned to the two photon resonance in free space, which we assume here. $\mathcal{L}$ and $\mathcal{L}^{-1}$ are the Laplace transform and inverse Laplace transform respectively. The $|M_k(t)|^2$ term in Eq. (3.44) determines the time dependence of the spectrum evolution. We have written this term as it appears when formally solving the Heisenberg equations. This, however, makes it somewhat difficult to see how the time dependence of the output spectrum relates to the internal system operators, $a^\dagger(t), a(t)$. It is more illuminating to write $M_k(t)$ in the form

$$|M_k(t)|^2 = \frac{\int_0^t dt' \int_0^t dt'' \langle a^\dagger(t') a(t'')\rangle e^{-i\omega_k(t'-t'')}}{\langle a^\dagger(0) a(0)\rangle}. \tag{3.48}$$

This has been obtained by evaluating $\langle b_k^\dagger(t) b_k(t)\rangle$ directly from Eq. (3.41). This shows that the time dependence of the output spectrum is given by a Fourier transform of the system two-time correlation function $\langle a^\dagger(t') a(t'')\rangle$.

We have seen that we can obtain a solution for $a(t)$, and $a^\dagger(t)$ in terms of an inverse Laplace transform, given by Eq. (3.43). From this solution, along with Eq. (3.41) all higher order correlations and information about the quantum statistics of the atoms can be obtained. While this is true in principal, in practice the inverse Laplace transforms required to obtain $a(t)$ or $M_k(t)$, and hence the output spectrum, cannot be obtained analytically for most physical situations. Moreover, numerical solutions are unstable and can only be obtained in the limits of short time, or small coupling strength.

In the next section we present an analytic solution for $a(t)$, and for the spectrum, $\langle b_k^\dagger(t) b_k(t)\rangle$ in the limit of broadband coupling. Later we will discuss the parameter regimes in which the broadband approximation is found to be valid.

3.4 Solution method

Together, Eq. (3.44) and Eq. (3.45) give the output spectrum in terms of parameters which are found in the Hamiltonian. We now evaluate the spectrum for the Hamiltonian discussed above, Eq. (3.30) - Eq. (3.33). For simplicity, we consider here the case where the total momentum kick from the Raman lasers is very small. That is we assume $k_{1L} \approx -k_{2L}$. This is analogous to the MIT output coupling experiments in which the atoms receive a negligible momentum kick in changing state [4, 12].

The shape of $\kappa(k,t)$ is given in terms of the ground state momentum wavefunction of the trap, $\psi(k)$ in Eq. (3.36). We consider here a harmonic trap, with a gaussian ground state of standard deviation σ_k in wavenumber space, given by

$$\psi(k) = \left(2\pi\sigma_k^2\right)^{-1/4} \exp\left[-k^2/\left(4\sigma_k^2\right)\right] \tag{3.49}$$

Using the function, $f'(t)$ as defined in Eq. (3.46) we can take the Laplace transform to obtain

$$\mathcal{L}(f')(s) = \int_{-\infty}^{\infty} \mathrm{dk}\, \frac{|\kappa(k,t)|^2}{s+i\delta_k}. \tag{3.50}$$

Substituting Eq. (3.49) and Eq. (3.36) into Eq. (3.50) and evaluating the integral we obtain

$$\mathcal{L}(f')(s) = \Gamma c \frac{\sqrt{i}}{\sqrt{s-i\omega_0}}\, G(r), \tag{3.51}$$

where

$$G(r) = \exp[r^2]\,(1-\mathrm{Erf}[r])\,, \tag{3.52}$$

$$r = \sqrt{-im(s-i\omega_0)/\left(\hbar\sigma_k^2\right)}, \tag{3.53}$$

$$c = -i\left(\frac{m\pi}{\hbar\sigma_k^2}\right)^{1/2} \tag{3.54}$$

and Erf is the error function. We must simplify this expression for $\mathcal{L}(f')(s)$ in order to evaluate Eq. (3.45). We first note that we can approximate $G(r) \approx 1$ if $|r| << 1$. Noting that the abscissa of convergence [55] for the inverse Laplace transform, Eq. (3.45), is zero, we can set the real part of s to any small, real positive number in the inverse Laplace transform. We now make the broadband approximation by assuming here that σ_k is sufficiently broad that $\omega_0 << \hbar\sigma_k^2/m$. Typically ω_0 is of the order of hundreds of Hertz for atomic traps, with the atomic mass of order 10^{-26}kg, thus this inequality will hold for broadband coupling with $\sigma_k >> 2 \times 10^5 \mathrm{m}^{-1}$. The approximation $|r| << 1$ then holds in the regime where $\mathrm{Im}(s) << \hbar\sigma_k^2/m$. Using the approximation $G(r) \approx 1$ to calculate $M_k(t)$ is, thus, equivalent to smoothing over high ($> \hbar\sigma_k^2/m$) frequency components in the time dependence of $M_k(t)$. As we increase the width of the coupling in momentum space, given by σ_k, our solution for $M_k(t)$ becomes valid for increasingly high frequencies, $\mathrm{Im}(s)$. For an infinitely broad coupling, the approximation $G(r) = 1$ becomes exact.

We substitute Eq. (3.51) for $\mathcal{L}(f')(s)$ with $G(r) = 1$ into the equation for $M_k(t)$ given in Eq. (3.45). Thus, in the broadband approximation the time de-

pendence of the spectrum is given by

$$M_k(t) = \mathcal{L}^{-1}\left\{\frac{1}{\left(s+\frac{\Gamma c\sqrt{i}}{\sqrt{s-i\omega_0}}\right)(s+i\delta_k)}\right\}(t). \tag{3.55}$$

To evaluate this inverse Laplace transform analytically, we must first write it in a suitable form, using some general theorems. The first of these is the shift theorem, which states for a general function, $g(s)$ that

$$\mathcal{L}^{-1}\left\{g(s-i\omega_0)\}\right)t) = e^{i\omega_0 t}\mathcal{L}^{-1}\left\{g(s)\right\}(t). \tag{3.56}$$

Using this we can write $M_k(t)$ as

$$M_k(t) = e^{i\omega_0 t}\mathcal{L}^{-1}\left\{\frac{1}{\left(s+i\omega_0+\frac{\Gamma c\sqrt{i}}{\sqrt{s}}\right)(s+i\omega_0+i\delta_k)}\right\}(t) \tag{3.57}$$

$$= e^{i\omega_0 t}\,\mathcal{L}^{-1}\left\{h(s^{1/2})\right\}(t), \tag{3.58}$$

where we have introduced the function,

$$h(p) = \frac{p}{(p^2+i(\omega_0+\delta_k))(p^3+i\omega_0 p+\Gamma c\sqrt{i})}. \tag{3.59}$$

We have chosen to write the inverse Laplace transform in the above form, Eq. (3.58), so as to make use of the following general theorem for inverse Laplace transforms. The theorem states that for a function, $g(s)$ with inverse Laplace transform given by $\mathcal{L}^{-1}\left\{g(s)\right\}(t) = f(t)$, the inverse Laplace transform, $\mathcal{L}^{-1}\left\{g(s^{1/2})\right\}(t)$ is given by

$$\mathcal{L}^{-1}\left\{g(s^{\frac{1}{2}})\right\}(t) = \frac{1}{2}\pi^{-\frac{1}{2}}\,t^{-\frac{3}{2}}\int_0^\infty u e^{-u^2/(4t)}\,f(u)\,du \tag{3.60}$$

Using this in Eq. (3.58) above, we have

$$M_k(t) = \frac{e^{i\omega_0 t}}{2}\pi^{-1/2}t^{-3/2}\int_0^\infty u e^{-u^2/(4t)}\,\mathcal{L}^{-1}\left\{h(s)\right\}(u)\,du. \tag{3.61}$$

The function, $h(u)$ is given in Eq. (3.59). We can write this function in the form

$$h(u) = \frac{u}{(u^2+i(\omega_0+\delta_k))\left((u-\alpha)(u-\beta)(u-\gamma)\right)}, \tag{3.62}$$

where α, β and γ are the three roots of the cubic in Eq. (3.59). In this form we obtain, after some further work, the inverse Laplace transform of $h(u)$ as

$$\mathcal{L}^{-1}\left\{h(u)\right\}(t) = U(\alpha,\beta,\gamma)+U(\beta,\alpha,\gamma)+U(\gamma,\alpha,\beta)+$$

$$+\frac{(-\alpha\beta\gamma + i(\alpha+\beta+\gamma)\times(\omega_0+\delta_k))\times\cos[\sqrt{i(\omega_0+\delta_k)}t]}{(\alpha^2+i(\omega_0+\delta_k))(\beta^2+i(\omega_0+\delta_k))(\gamma^2+i(\omega_0+\delta_k))}+$$
$$+\frac{(\alpha\beta+\alpha\gamma+\beta\gamma-i(\omega_0+\delta_k))\sqrt{i(\omega_0+\delta_k)}\times\sin[\sqrt{i(\omega_0+\delta_k)}t]}{(\alpha^2+i(\omega_0+\delta_k))(\beta^2+i(\omega_0+\delta_k))(\gamma^2+i(\omega_0+\delta_k))}, \quad (3.63)$$

where

$$U(\alpha,\beta,\gamma) = \frac{\alpha e^{\alpha t}}{(\beta-\alpha)(\gamma-\alpha)(\alpha^2+i(\omega_0+\delta_k))} \quad (3.64)$$

Substituting this into Eq. (3.61), we obtain an expression for $M_k(t)$ which involves evaluating an integral for each of the terms in Eq. (3.63) above.

Upon evaluating these integrals (see Appendix B) we obtain

$$\begin{aligned} M_k(t) = \frac{e^{-i\Delta_k t}}{\omega_k\Delta_k^2-\Gamma^2c^2}\Bigg[&\frac{-e^{i\omega_k t}\, i\sqrt{i}\Gamma c}{\sqrt{\pi t}} \\ &+i\omega_k\Delta_k+\frac{1}{2}\sqrt{\frac{\pi}{t}}i\sqrt{i}\Gamma c L_{1/2}^{-1/2}(i\omega_k t)\Bigg] \\ &+V(\alpha,\beta,\gamma)+V(\beta,\alpha,\gamma)+V(\gamma,\beta,\alpha), \end{aligned} \quad (3.65)$$

where

$$V(x,y,z) = \frac{x^2\exp[(x^2+i\omega_0)t]}{(y-x)(z-x)(x^2+i\omega_k)}(1+\mathrm{Erf}(x\sqrt{t}))$$

and we have defined $\omega_k = \hbar k^2/(2m)$ and $\Delta_k = \omega_k - \omega_0$. The function $L_{\frac{1}{2}}^{-\frac{1}{2}}(x)$ is related to the Laguerre polynomial.

In fact, it is usual for Laguerre polynomials to only have integer indices. Here we have an index of $1/2$ which we have introduced as a generalized form of the Laguerre polynomial. In general, the Laguerre polynomial with integer indices, $L_n^a(x)$ is defined by the solution to the equation

$$xy''+(a+1-x)y'+ny = 0, \quad (3.66)$$

and an orthogonality condition.

Our definition of the function $L_{1/2}^{1/2}(x)$ is defined in analogy to the integer case as the solution to Eq. (3.66). For the case of n=1/2, and a=-1/2 (see Eq. (3.65)) the function, $L_{1/2}^{-1/2}(x)$ is given by

$$L_{1/2}^{-1/2}(x) = \frac{2e^x}{\pi}-2\sqrt{\frac{x}{\pi}}\times\mathrm{Erfi}[\sqrt{x}]. \quad (3.67)$$

where Erfi is the imaginary error function, given by $\mathrm{Erfi}[z] = -i\times\mathrm{Erf}[iz]$.

Substituting Eq. (3.65) into Eq. (3.44) gives an analytic expression for the output spectrum from an atom laser using broadband coupling. In the next section we consider the behaviour of this output spectrum as a function of time and coupling strength.

3.5 Output spectrum

We mentioned earlier that the time dependence of the output spectrum is given purely by the behaviour of the term $|M_k(t)|^2$ in Eq. (3.44). Fig. 3.2 shows the behaviour of $|M_k(t)|^2$ given by Eq. (3.65), as a function of ω_k and time after we turn on the output coupling interaction.

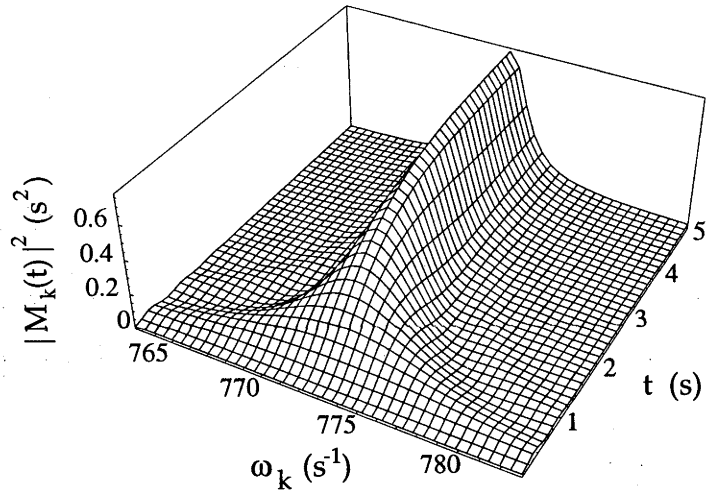

Figure 3.2: Plot of $|M_k(t)|^2$ as a function of ω_k and time for $t = 0$s to $t = 5$s, and ω_k ranging from 762s^{-1} to 783s^{-1} about the single mode trap frequency, $\omega_0 \approx 772\text{s}^{-1}$. $\Gamma = 1.8 \times 10^3\text{s}^{-2}$.

3.5.1 Short time limit

Initially $|M_k(t)|^2$ is small, and for short enough times, arbitrarily broad in k-space (see Fig. 3.3). This agrees with the perturbative solutions presented by Hope [54] which are only valid for short time and for low coupling strengths, $\Gamma^{1/2}$. For weak coupling or strong coupling for very small times, t, we can take a series expansion of the expression for $M_k(t)$ in Γ. The zeroth order term in Γ is found to be given by $|M_k|^2 = (2 - 2\cos[(\omega_k - \omega_0)t])/(\omega_k - \omega_0)^2$. This agrees with the perturbative expressions obtained by Hope. In particular,

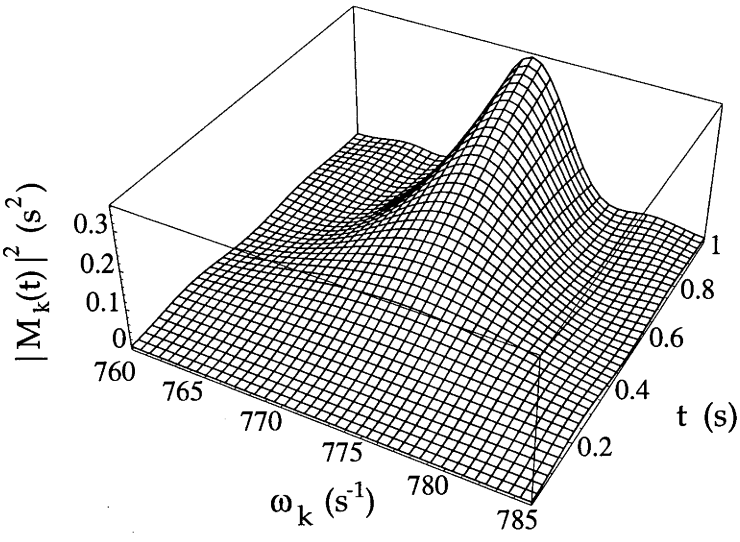

Figure 3.3: Plot of $|M_k(t)|^2$ as a function of ω_k and time for $t = 0$s to $t = 1$s. This shows the initial evolution of Fig. 3.2 in more detail before the steady state has been reached.

when $|M|^2$ is broad at small times, the shape of the output spectrum $\langle b_k^\dagger b_k \rangle$ given by Eq. (3.44) is given by $|\kappa(k,t)|^2$.

3.5.2 Long time limit

For longer times or stronger coupling a perturbative solution is no longer valid. However, the analytic solution presented above allows the long time limit to be investigated. Eq. (3.65) shows that the spectrum reaches a stable shape. The analytic solution allows the long time shape to be investigated as a function of other parameters, such as coupling strength.

We consider here a continuous coupler, turned on at time $t = 0$, and examine the resulting long time spectrum in the external modes described by $b_k^\dagger$. We observe in Fig. 3.3 that for longer times $|M_k(t)|^2$ narrows into a sinc^2 function centered about the trap ground state frequency, ω_0. Eventually $|M_k(t)|^2$ reaches a stationary state with a lorentzian like profile as shown in Fig. 3.2. We can obtain an analytic form for the long time output spectrum profile by taking the limit of Eq. (3.65) as $t \to \infty$. This longtime behaviour is given by

$$\lim_{t\to\infty} M_k(t) = \frac{i\sqrt{\omega_k}e^{-i\Delta_k t}}{\sqrt{\omega_k}\Delta_k - \Gamma c} + V(\gamma,\beta,\alpha), \tag{3.68}$$

where α, β and γ are the particular solutions to the cubic discussed above,

given by the expressions

$$\alpha = e^{-i\frac{5\pi}{12}}\left(2^{\frac{1}{3}}\omega_0/\xi^{\frac{1}{3}} + e^{i\frac{\pi}{3}}\xi^{\frac{1}{3}}/54^{\frac{1}{3}}\right) = i\beta^*, \tag{3.69}$$

$$\gamma = e^{i\frac{\pi}{4}}\left(2^{\frac{1}{3}}\omega_0/\xi^{\frac{1}{3}} - (4\xi)^{\frac{1}{3}}/6\right), \tag{3.70}$$

$$\xi = -27i\Gamma c + \left(-(27\Gamma c)^2 + 108\omega_0^3\right)^{\frac{1}{2}}. \tag{3.71}$$

In obtaining this limit we have used the fact that the limit as $t \to \infty$ of the our generalized Laguerre function, $L_{1/2}^{-1/2}$ (defined in Eq. (3.67) above) is given by

$$\lim_{t\to\infty}\sqrt{\frac{\pi}{t}}L_{1/2}^{-1/2}(i\omega_k t) = \sqrt{-4i\omega_k}. \tag{3.72}$$

Only one of the three terms in Eq. (3.65) is nonzero in the limit $t \to \infty$. This is given by $V(\gamma, \beta, \alpha)$ where we have used the notation that γ corresponds to the solution of the cubic which has equal real and imaginary parts.

The longtime expression for $M_k(t)$, Eq. (3.68) contains two terms. The first of these terms dominates in the case of small Γ, while the second dominates for very large Γ. As a result, the long time spectrum has two distinct behaviours depending on the strength of the coupling. For intermediate coupling both of the two terms in Eq. (3.68) are of similar magnitude and there is a complex interplay between these terms which leads to a differing spectral shape from either of the two regimes we present below.

3.5.3 Small Γ

We consider the case of slow coupling (small Γ) initially. In this case, the long time expression for $M_k(t)$ is dominated by the first term in Eq. (3.68) above, and the resulting long time spectrum is given by

$$\langle b_k^\dagger b_k\rangle = \Gamma\,|\psi(k)|^2\,\frac{1}{(\Delta_k^2 + |\Gamma c|^2/\omega_k)}. \tag{3.73}$$

Plots of the long time spectrum, Eq. (3.73) as a function of ω_k are presented in Fig. 3.4 for various coupling strengths. Fig. 3.4 shows that for increasing coupling strength the linewidth of the long time spectrum increases. The values for Γ chosen lie about $\Gamma = 4 \times 10^4 \mathrm{s}^{-2}$, which corresponds approximately to values of Raman laser Rabi frequencies, $\Omega_1 \approx 2\pi \times 50$ kHz and $\Omega_2 \approx 2\pi \times 1.6$ MHz and detuning, $\Delta_1 \approx 2\pi \times 2.5$ GHz similar to values presented in Chapter 1. However, much smaller or larger coupling strengths can be achieved by suitably adjusting the intensities of the lasers and their detunings. The figures assume a trap with ground state frequency $\omega_0 = 2\pi \times 123\ \mathrm{s}^{-1}$,

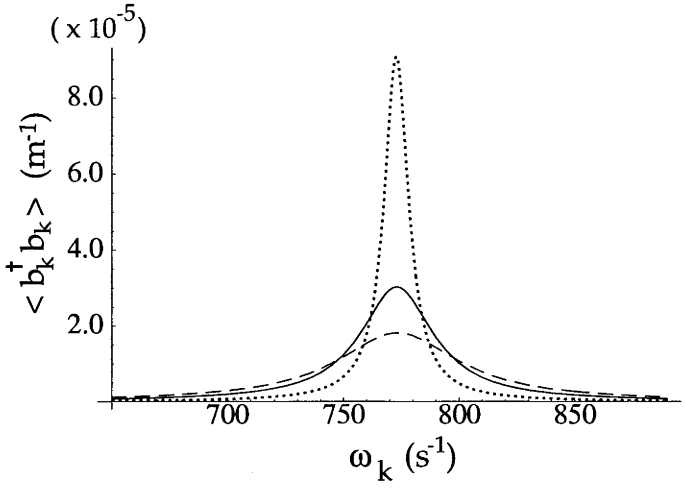

Figure 3.4: Plot of long time behaviour of $\langle b_k^\dagger b_k \rangle$ as a function of ω_k for various coupling strengths, $\Gamma = 10^4 s^{-2}$ (dotted line), $\Gamma = 3 \times 10^4 s^{-2}$ (solid line) and $\Gamma = 5 \times 10^4 s^{-2}$ (dashed line).

typical of magnetic traps for ultra cold atoms [4]. A ground state gaussian with width $\sigma_k \approx 10^6 m^{-1}$ has been assumed, which corresponds to a position space wavefunction of size of the order of $2\mu m$. This value of σ_k corresponds to a full width at half maximum in ω_k space of $\sigma_{\omega_k} \approx 10^4 s^{-1}$.

For each of the graphs shown in Fig. 3.4, the lorentzian like spectrum is centred about ω_0, the ground state frequency of the single mode trap, with the width of the spectrum dependent on the strength of the coupling as mentioned above. In all cases, however, the linewidth is much less than that which would be obtained if the trap was rapidly turned off, that is $\sigma_{\omega_k} \approx 10^4 s^{-1}$. We see from Eq. (3.73) that the distribution isn't exactly lorentzian due to the presence of ω_k in the second part of the denominator. However over a large range of ω_k the spectrum is well approximated by a lorentzian distribution of width $|\Gamma c|/\sqrt{\omega_0}$. The values of ω_k for which this approximation fails is given by the condition ($\omega_k >> \omega_0$ and $\omega_k << |\Gamma c|^{3/2}$), or ($\omega_k << \omega_0$ and $\omega_k << |\Gamma c|^2/\omega_0^2$). Typically, however, we are interested in the distribution about $\omega_k \approx \omega_0$ where the spectrum is approximately lorentzian.

The full width at half maximum of the lorentzian distribution is $2|\Gamma c|/\sqrt{\omega_0}$. This estimate does not give exactly the width of the function $|M_k|^2$ found in the equation for the spectrum. In fact, $|M_k|^2$ is not lorentzian due to the dependence of ω_k in the bottom line of Eq. (3.73). Fig. 3.5 shows a comparison of the "lorentzian" linewidth and the correct full width of $|M_k|^2$ as a function of coupling strength. The full width at half maxima of the function $|M_k|^2$ has been obtained by directly solving for the two half maximum points as a function of

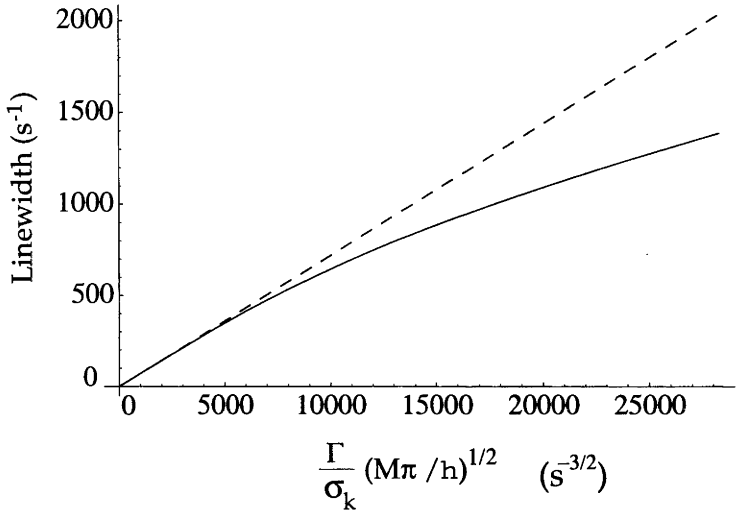

Figure 3.5: Comparison of the "lorentzian" linewidth to the correct full width of $|M_k|^2$ as a function of coupling strength. The limiting Lorentzian linewidth curve is given by $2\frac{\Gamma}{\sigma_k}\sqrt{\frac{M\pi}{\hbar\omega_0}}$.

ω_0 and Γ. The distance in ω_k space between these two solutions is taken to be the linewidth. In the regimes where this differs from the lorentzian linewidth the shape of the spectrum will not be symmetrical about the maximum. Due to this non-lorentzian lineshape, the width of the spectrum is not directly proportional to the coupling strength, even in this small Γ regime. This contrasts with the typical results for an optical cavity in the broadband regime and will be discussed further in section 3.6. As Γ gets even larger the small Γ approximation we have used here to obtain the approximately lorentzian spectrum will fail. We discuss this regime in the next section.

3.5.4 Large Γ

We have already mentioned that the exact nature of the long time limit for $|M_k(t)|^2$ depends on the strength of the coupling. For very large values of the coupling strength, the long time limit becomes very broad in k-space. As a result, the shape of the output spectrum, as given by Eq. (3.44), simply reflects the momentum distribution of the cavity wave-function, $\psi(k)$. As a result there is no narrowing of linewidth in momentum space. The recent MIT experiments [4, 12] are an example of an output coupling with an extremely large coupling strength. In these experiments a short, 5μs RF pulse was used to couple atoms out of a BEC, making a pulsed atom laser.

For the width of $M_k(t)$ to be large compared with $\kappa(k,t)$ we require that Γ, the coupling strength, must be sufficiently large so that $|\Gamma c|/\sqrt{\omega_0} >> \sigma_{\omega_k}$. This expression comes from Eq. (3.73) which gives an approximate width of the first term in Eq. (3.68)). When this is sufficiently large, the spectrum becomes dominated by the cavity momentum spread $\psi(k)$. Thus, for sufficiently fast coupling (large Γ) the output spectrum changes significantly from the lorentzian shape considered above, and instead reflects the momentum spread of the cavity (see Fig. 3.6). The spectrum is centred about zero, and falls away exponentially in ω_k space, as required for a gaussian distribution in momentum space given by $\psi(k)$.

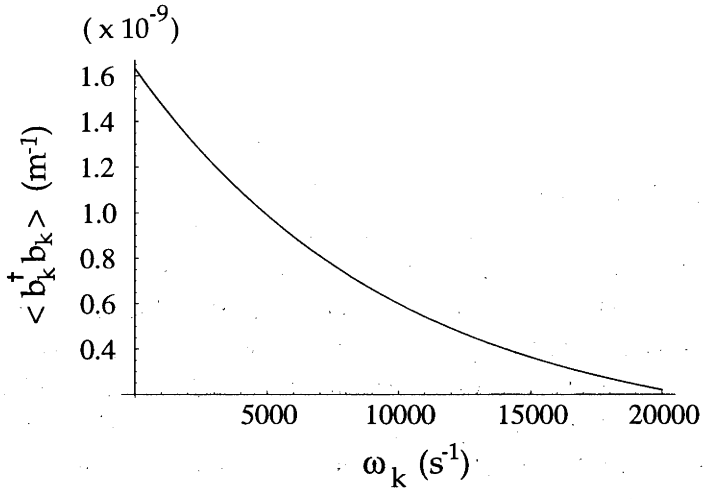

Figure 3.6: Plot of the steady state behaviour of $\langle b_k^\dagger b_k \rangle$ as a function of ω_k for the large coupling limit ($\Gamma \approx 10^{13}\mathrm{s}^{-2}$).

3.6 Comparison with optics

We have already mentioned that the Hamiltonian, given by Eq. (3.30) - Eq. (3.33) is equivalent to that used in the standard optical input-output theory. The solution we have produced for the spectrum, however, differs from the optical result. We mention that Eq. (3.42) is equivalent to that which would be obtained in the optical case. The solution method in optics, however, is based on the fact that $\omega_k = c_L|k|$ is proportional to the wavenumber k in optics, whereas it is proportional to k^2 in our atom case. By assuming a large ω_0 and broadband coupling, the integral over k space (usually ω space is used in the optics formalism) can be approximated by a Dirac delta function. Making

these assumptions in Eq. (3.45) leads to the "optical" equation for $|M_k(t)|^2$,

$$|M_k|^2(t) = \frac{1}{\Delta_k^2 + 4|\kappa|^2}\left(1 + e^{-4|\kappa|^2 t} - e^{(-2|\kappa|^2 + i\Delta_k)t} - e^{(-2|\kappa|^2 - i\Delta_k)t}\right). \quad (3.74)$$

From this it is clear that the long time behaviour is given by

$$\lim_{t\to\infty} |M_k|^2(t) = \frac{1}{\Delta_k^2 + 4|\kappa|^2}. \quad (3.75)$$

Thus the spectrum in this case is purely lorentzian in shape with the linewidth being always directly proportional to the coupling strength, contained in κ. In fact, this result relies on a number of approximations in the optical case which are generally found to be true. We will discuss the differences between optics and the atom case and the regimes of validity of such approximations further in Chapter 4.

3.7 Conclusions

We have shown how the longtime spectrum from an output coupler based on state change depends on the strength of the output coupling. For very strong coupling, the output spectrum is given by the cavity spectrum, and is very broad in momentum space. As the strength of the coupling is reduced, however, the long time linewidth is correspondingly reduced. For small coupling strengths the linewidth is effectively lorentzian, centred about the energy of the cavity with a linewidth proportional to Γ.

Chapter 4

An atom laser master equation and the Born-Markov approximation

Overview

In the previous chapter we discussed the output spectrum which is obtained by coupling a single mode of an atomic trap to a continuum of free space modes. The usual way in which such a coupling is described in the optical theory is through a Born-Markov Master equation term. This allows a master equation description of the atom laser to be obtained. Here, we discuss the use of the Born and Markov approximations in describing the dynamics of output coupling atoms from a cavity. We present conditions based on the atomic reservoir, and atom dispersion relations for when the Born-Markov approximations are valid and discuss parameter regimes where these approximations fail in our atom laser model. Differences between the standard optical laser model and the atom laser are due to a combination of factors, including the parameter regimes in which a typical atom laser would operate, the different reservoir state which is appropriate for atoms, and the different dispersion relations between atoms and photons. We present results based on an exact method in the regimes in which the Born-Markov approximation fails. We also discuss the effects of gravity and atom-atom interactions in the system.

4.1 Introduction

In Chapter 1 we mention that many of the atom laser schemes which have been presented to date are based around a master equation description for the dynamics of the system [1,8,9,23,24]. These models describe the atom laser output by a Born-Markov master equation. Making the Born-Markov approximation involves assuming that reservoir correlations decay rapidly compared with the system damping time and that the reservoir does not change significantly with time due to the effect of the system. We discuss these approxima-

tions in the context of atom output coupling.

Born-Markov master equations were initially derived for optical systems [7,51,56,57]. There they are used to describe a system (for instance an optical laser mode) coupled to a large, unchanging reservoir (the external modes). In optics the Born-Markov approximations allow an equation containing only system variables to be derived. One of the fundamental assumptions involved in deriving such a Born-Markov master equation is that the reservoir correlation functions decay rapidly. This allows the reservoir to be approximated as unchanging in time. While it is assumed the system does not affect the reservoir, the reservoir does affect the system.

An equation in terms of system variables alone is also an important goal for describing atom lasers. However, atom and photon devices work in substantially different parameter regimes. Moreover, atoms and photons have different dispersion relations, which affects the behaviour of the reservoir correlation functions. Furthermore, typically the reservoir for an optical cavity is taken to be at thermal equilibrium at a nonzero temperature. For atoms, a vacuum reservoir with all modes initially empty is often more appropriate.

The reservoir is described as a continuum of free-space modes. As in Chapter 3 our description of the coupling will be quite general. We have already described one method of output coupling which is based on state change. This method uses either a Raman transition [58] or an RF transition [4,12,59] to change the atoms to an untrapped state. We will also discuss the effects of gravity on output coupling. In the latter part of the paper we will focus on broadband coupling. This allows a comparison with exact results [54,58]. We also present numerical, finite coupling results which more accurately describe output coupling through a change of state. We will discuss exact equations along with some numerical results which can be obtained in regimes where the Born-Markov approximations fail.

4.2 The Born-Markov master equation term

As we have discussed in Chapter 1, dilute gas Bose Einstein Condensates (BEC) are now available in the laboratory. To produce a continuously running atom laser from a BEC requires the addition of a suitable pumping mechanism, and an output coupler. The output coupling from a single mode to a large reservoir is sometimes described by a Born-Markov master equation of the form

$$\frac{d\rho(t)}{dt} = C(2a\rho(t)a^\dagger - a^\dagger a\rho(t) - \rho(t)a^\dagger a), \tag{4.1}$$

where C describes the strength of the coupling and a ($a^\dagger$) is the annihilation (creation) operator for the single mode system. Two important approximations involved in such a description are that the evolution is Markovian and that it depends only on the system operators. The Markovian property means that the rate of change of the state depends only on the state at that time. There is no explicit dependence on the state at previous times. The equation is a function of system variables only, due to tracing over the reservoir. This is appropriate if the reservoir remains uncorrelated with the system.

We wish to investigate these two approximations, and their validity for describing atomic output coupling. In this work we do not consider pumping. We model a single populated mode coupled to a continuum of free space modes. Experimentally this corresponds to output coupling a BEC, or a pulsed atom laser. In a continuously pumped atom laser model, which we do not consider here, a pumping term would also be included.

4.3 Exact solutions

We begin by considering the generic output coupling mechanism which we have previously analysed in Chapter 3. We consider a single mode system (the lasing mode with creation operators $a^\dagger$) coupled to a one-dimensional continuum of free space modes. The free space modes are labeled by their momentum, $\hbar k$ (creation operators $b_k^\dagger$). The Hamiltonian describing the system is given by Eq. (3.30) - Eq. (3.33). In these equations the function $\kappa(k)$ describes the shape of the coupling in k space. We leave this general here. By appropriately choosing $\kappa(k)$ we may simulate a wide range of practical output coupling mechanisms, including position dependent coupling and the effect of momentum kicks. Choosing $\kappa(k)$ as constant over a broad region corresponds to broadband coupling. This model is used for optical input-output theory [7], and in proposed atom laser theories which result in Born-Markov master equations. For the atom case this model ignores potentially important effects such as gravity and atom-atom interactions. For now, we neglect these effects in order to investigate the Born-Markov approximations. We will extend the model in section 4.8.

We use the Hamiltonian presented above to write Heisenberg equations of motion for the operators a, b_k. We can also obtain equations for combinations of these operators which may be of more interest, such as the number of atoms in the system, $a^\dagger a$. These equations can be difficult to solve in general. However, since they include the output and system explicitly, they describe the dynamics of the model exactly [54, 58]. Exact solutions can be compared with Born-Markov master equations.

We have already discussed equations for $a^\dagger$ and a in Chapter.3. These are

given by Heisenberg equations,

$$\frac{d}{dt}\langle a^\dagger(t)\rangle = i\omega_0\langle a^\dagger(t)\rangle - \int_0^t d\tau\, f'^*(\tau)\langle a^\dagger(t-\tau)\rangle e^{i\omega_0\tau}, \tag{4.2}$$

$$\frac{d}{dt}\langle a^\dagger(t)a(t)\rangle = -\int_0^t d\tau\, f'(\tau)\,\langle a^\dagger(t)a(t-\tau)\rangle e^{-i\omega_0\tau} + \text{h.c.} \tag{4.3}$$

As in Chapter 3, we have the following solutions for $\langle a^\dagger(t)\rangle$ and $\langle a^\dagger(t)a(t)\rangle$:

$$\langle a^\dagger(t)\rangle = \langle a^\dagger(0)\rangle e^{i\omega_0 t}\,\mathcal{L}^{-1}\left\{\frac{1}{s+\mathcal{L}\{f'(t)^*\}(s)}\right\}(t), \tag{4.4}$$

$$\langle a^\dagger(t)a(t)\rangle = \langle a^\dagger(0)a(0)\rangle \times \left|\mathcal{L}^{-1}\left\{\frac{1}{s+\mathcal{L}\{f'(t)\}(s)}\right\}(t)\right|^2. \tag{4.5}$$

To obtain these we assume (as we will do in the master equation descriptions to follow) that the reservoir is initially empty, $\langle b_k^\dagger(0)b_k(0)\rangle = 0$. We do not place any further restrictions on $\langle b_k^\dagger(t)b_k(t)\rangle$. This is the first fundamental difference between the atom and photon case. An empty reservoir for photons is inappropriate at finite temperatures [56]. In experiments where a Bose-Einstein condensate is allowed to leak out of a trap, however, the most appropriate initial state for the outside atom modes is a vacuum. Similarly, for an atom laser in a hollow fibre, which we discussed in Chapter 2 [58], the initial output modes would be empty.

In Eq. (4.5) we have reintroduced the function, $f'(t)$ defined by

$$f'(t) = \int_{-\infty}^{\infty} dk|\kappa(k)|^2 e^{-i(\omega_k-\omega_0)t}. \tag{4.6}$$

The function $f(t) = f'(t)e^{-i\omega_0 t}$ is the "reservoir correlation function" in the master equation picture which we describe in the next section. Here $\omega_k = \hbar k^2/(2m)$ for atoms, in contrast to $\omega_k = c_L|k|$ for photons. Here m is the mass of the atoms, and c_L is the speed of light.

For the output coupling from a condensate through state change described in Chapter 3, $\kappa(k)$ is a Gaussian of width σ_k, Eq. (3.36). In Eq. (3.36) the strength of the coupling is given by the coupling constant, Γ. Using this form of coupling $f'(t)$ may be evaluated as:

$$f'(\tau) = \frac{e^{i\omega_0\tau}\Gamma}{\sqrt{1+i\alpha\tau}}, \tag{4.7}$$

where we have defined

$$\alpha = \hbar\sigma_k^2/m. \tag{4.8}$$

For the broadband limit of Eq. (4.8) (discussed in section 4.5) we may use methods similar to those outlined in Chapter 3 to obtain an analytical form for the inverse Laplace transform,

$$\mathcal{L}^{-1}\left\{\frac{1}{s+\mathcal{L}\left\{f'(t)\right\}(s)}\right\}(t) = e^{i\omega_0 t} \times \left(W(a,b,c)+W(b,a,c)+W(c,b,a)\right), \tag{4.9}$$

$$W(a,b,c) = \frac{a^2 e^{a^2 t}\left(1+\mathrm{erf}[a\sqrt{t}]\right)}{(a-b)(a-c)}. \tag{4.10}$$

The variables, a,b and c are the three solutions of the equation $s^3+i\omega_0 s+\Gamma c\sqrt{i}=0$. Note that Eq. (4.4) gives that $\langle a(t)\rangle$ will always remain zero if $\langle a(0)\rangle = 0$. For the case of damping of a BEC which we consider here, the initial state corresponds to a BEC in an atom trap. According to spontaneous symmetry breaking arguments BECs are in coherent states with a definite global phase [60], so that $\langle a(0)\rangle \neq 0$. This is a useful assumption. Nevertheless, even if $\langle a\rangle = 0$, the form of the equation for $\langle a(t)\rangle$ must be as given.

The solutions to the Heisenberg equations of motion given by Eq. (4.4) and Eq. (4.5) are exact for the system under consideration. In specific cases it is very difficult to solve for these inverse Laplace transforms. Moreover, the Heisenberg equations for system operators depend on the external operators, $b_k(0)$ in general. We next investigate equations of motion based on the Born and Markov approximations. These are compared with the exact solutions given above.

4.4 Deriving the Born-Markov master equation

Derivations of the Born-Markov master equation for a general system reservoir interaction are given in references [56,57,61] and we provide a review of the general derivation in Appendix C. Here we present a derivation for the specific model of Eq. (3.30) to Eq. (3.33). We assume that the atom reservoir is initially in a vacuum state - that is, there are initially no atoms outside the system. This assumption was also made in the exact solutions presented in section 2.5. We make the Born approximation. This involves ignoring correlations which may arise between the system and reservoir and ignoring any time evolution of the reservoir density operator. We use the interaction Hamiltonian in Eq. (3.33). This leads to the non-Markovian master equation:

$$\frac{d\tilde{\rho}}{dt} = -\int_0^t d\tau \left\{a^\dagger a\tilde{\rho}(t-\tau) - a\tilde{\rho}(t-\tau)a^\dagger\right\} \times f'(\tau) + \mathrm{h.c}, \tag{4.11}$$

where, $\tilde{\rho}$ is the density operator in the interaction picture. The function, $f'(\tau)$, defined as $f'(\tau) = f(\tau)\, e^{i\omega_0\tau}$ is the same as defined in Eq. (4.6) and Eq. (4.7). Here $f(\tau)$ is the reservoir correlation function.

Eq. (4.11) is non-Markovian, and corresponds to Eq. (C.4), given in appendix 1 for a general interaction Hamiltonian. The second major approximation required to produce a Born-Markov master equation is the Markov approximation. The Markov approximation is made on the assumption that the reservoir correlation function, $f(\tau)$ goes to zero rapidly compared with the time scale on which $\tilde{\rho}(t)$ changes. Making the Markov approximation thus involves replacing the terms $\tilde{\rho}(t-\tau)$ in Eq. (4.11) with $\tilde{\rho}(t)$. In the optics case, this approximation is also usually accompanied with the extension of the upper limit of the integral from t to infinity. Making these approximations gives

$$\dot{\tilde{\rho}} = \left\{(c+c^*)a\tilde{\rho}(t)a^\dagger - c\, a^\dagger a\tilde{\rho}(t) - c^*\tilde{\rho}(t)a^\dagger a\right\}, \tag{4.12}$$

where

$$\begin{aligned} c &= \int_0^{t\to\infty} d\tau \int_{-\infty}^{\infty} |\kappa(k)|^2 e^{-i(\omega_k-\omega_0)\tau} dk \\ &= \int_0^{\infty} f'(\tau) d\tau \\ &= \frac{\Gamma\sqrt{2\pi}\exp\left[-\omega_0/\alpha\right]}{\sqrt{2\omega_0\alpha}} \left(1 + \mathrm{Erf}\left[i\sqrt{\frac{\omega_0}{\alpha}}\right]\right). \end{aligned} \tag{4.13}$$

The upper integration limit t has been extended to ∞, as is done in the optical case. This produces the Born-Markov master equation term. We note that we could redefine c to be real without loss of generality by incorporating the imaginary part of c in with the free part of the system Hamiltonian. This reduces the form of the loss term to the familiar $C(2a\rho a^\dagger - a^\dagger a\rho - \rho a^\dagger a)$, with $C = \mathcal{R}e[c]$ the (real) coupling strength.

The value of the constant c depends on the form of $f'(\tau)$. In the following, we consider $f'(t)$ to be either that resulting from the Gaussian coupling presented in this section, or the broadband limit of this function which we discuss in the next section.

4.5 Timescale conditions

The Born-Markov master equation, Eq. (4.12), is of the form used recently in various discussions of atom laser dynamics [1,8,9,23,24]. This Born-Markov master equation is used ubiquitously in quantum optics. Like in the optical case, the validity of the Markov approximation depends on the interplay between the reservoir correlation timescale, the system timescale, and the timescale on which the system decays.

The condition for the validity of the Born-Markov approximations is given in standard optics texts by the timescale separation condition [56,57,61]

$$t_R << \Delta t << t_D \tag{4.14}$$

where t_R is the reservoir correlation time, and t_D is the cavity decay time. Δt defines a coarse grained timescale on which the equations of motion are valid. Generally t_R is defined as the "timescale on which the reservoir correlations are non-zero". t_D is the decay timescale of the system which can be obtained by solving the equations for system and reservoir self consistently. In the Markov approximation this timescale goes as $1/(c + c^*)$ for c similar to that defined in Eq. (4.13) except with the optics dispersion relation.

Both t_R and t_D depend on the function $f'(\tau)$, and thus in turn on the form of ω_k as a function of k. For atoms $\omega_k = \hbar k^2/(2m)$, whereas for photons $\omega_k = c_L|k|$, where c_L is the speed of light. It also depends on factors such as the nature of the reservoir and the parameter regime in which atom lasers operate.

A second timescale condition for the Born-Markov approximation which is discussed in some treatments [57,61] of the optical Born-Markov approximation is that the system timescale, defined as $t_s = 1/\omega_0$ must satisfy

$$t_s << \Delta t. \tag{4.15}$$

This is equivalent to requiring ω_0 to be very large. A large ω_0 condition is required in optics for a number of reasons. First, the initial coupling Hamiltonian, of the form $(ab_k^\dagger + a^\dagger b_k)$, is in the rotating wave approximation and ignores terms of the form ab_k and $a^\dagger b_k^\dagger$. This rotating wave approximation in optics can only be made in the case of large ω_0. For the atom coupling, however, the correct form of the coupling does not include such (non atom number conserving) terms, even for small ω_0. The terms which are eliminated in the optics case [57,61] through the assumption of large ω_0 are already zero for our model, due to the assumption of an atom vacuum reservoir. Thus, one may be led from these treatments to suppose that the Born-Markov approximation is made independently of ω_0 for an atom-vacuum reservoir. This however is not the case as we will discuss later.

In optics, these timescale conditions are usually satisfied. For a coupling based on a mirror it is standard to assume that the coupling is broadband [7]. That is, we assume $\kappa(k)$ is flat in k-space. In this case the reservoir correlation function, $f'(\tau)$, given by Eq. (4.6) becomes

$$\begin{aligned} f'(\tau) &\approx |\kappa(k_0)|^2 e^{i\omega_0\tau} \int_{-\infty}^{\infty} e^{-i\omega_k\tau}\, dk \\ &= 2|\kappa(k_0)|^2 \int_{-\omega_0/c_L}^{\infty} e^{-ic_L k\tau}\, dk \end{aligned}$$

$$\approx 2|\kappa(k_0)|^2\,\delta(\tau). \tag{4.16}$$

In the final equation the Dirac delta function, $\delta(\tau)$, is obtained by extending the frequency integral into physically unrealistic negative frequencies. This is a standard technique in optics [7] where ω_0 is typically large compared with the output coupling rate.

Typically, for a laser, $\omega_0 \approx 10^{15}\mathrm{s}^{-1}$ is large compared with the output coupling rate, and the assumption of a Dirac delta function decay is very good. Atom traps work in rather different parameter regimes with $\omega_0 \approx 10^{3}\mathrm{s}^{-1}$ which is much closer to typical atom output coupling rates. If we avoid using negative frequencies, with the assumption of the empty reservoir considered here, we obtain the sum of a Dirac delta function, and an imaginary part corresponding to the Cauchy principal value of the integral in Eq. (4.16).

$$f'(\tau) = \frac{2\pi}{c_L}|\kappa(k_0)|^2 e^{i\omega_0\tau}\left(\delta(\tau) - \frac{i}{\pi\tau}\right). \tag{4.17}$$

However, for an optical reservoir this estimate of correlation function decay based on our reservoir model is not strictly valid. This is because, while we have considered here the photonic dispersion relation, a vacuum is unrealistic for an optical reservoir at finite temperatures. More appropriate is a thermal reservoir, which leads to a decay time of order $\hbar/k_BT \approx 10^{-13}\mathrm{s}$ [56].

These reservoir correlation times must be short compared with the decay time, t_D. The system timescale, $1/\omega_0$ must also be short compared with t_D for a standard optical reservoir. t_D is the timescale of exponential decay, given by $e^{-(c+c^*)t}$ in the Born-Markov limit. From an equivalent derivation of the optical master equation to that given in section 4.2, the decay timescale is given by $t_D = 1/(c+c^*) \propto (\sigma_k/\Gamma)$. That is t_D is inversely proportional to the strength of the coupling, given by Γ/σ_k in the broadband limit. We will see later that for the atom coupling, the different dispersion relation makes t_D depend on ω_0 and the parameters relating to the coupling function, $\kappa(k)$. For optical systems this decay time is typically of the order $10^{-8}\mathrm{s}$. Thus, in typical optical systems, the Born-Markov approximation holds for a number of reasons. The condition $t_R << t_D$ holds, because in the large ω_0 limit the reservoir correlations decay as a Dirac delta function. t_D does not depend on ω_0 and is typically many orders of magnitude larger than the reservoir decay times. Similarly, the system timescale t_s for realistic optical cavities is very much shorter than the decay timescale, t_D.

In contrast, the large ω_0 limit is not necessarily valid for realistic atom traps. Moreover, even in the limit of infinitely large ω_0, the atom correlation function $f'(\tau)$ does not tend towards a Dirac delta function. This is due to the atomic dispersion relations, which lead to a dependence of t_D on parameters other than the coupling strength. Furthermore, the assumption of an initially empty

reservoir is realistic for atoms. For atoms, the broadband limit of the function $f'(t)$ is given by

$$\begin{aligned} f'(\tau) &\approx |\kappa(k_0)|^2 e^{i\omega_0\tau} \int_{-\infty}^{\infty} e^{-i\omega_k\tau}\, dk \\ &= 2|\kappa(k_0)|^2 e^{i\omega_0\tau} \int_{0}^{\infty} e^{-i\hbar k^2/(2m)\tau}\, dk \\ &= |\kappa(k_0)|^2\, e^{i\omega_0\tau}\, \frac{\sqrt{m\pi}\,(1-i)}{\sqrt{\hbar\tau}}. \end{aligned} \tag{4.18}$$

This is the broadband limit of the general reservoir correlation function, Eq. (4.7) given in section 4.2. Both broadband and Gaussian coupling give forms for $f'(\tau)$ which fall off as inverse $\sqrt{\tau}$. The broadband limit of Eq. (4.7) is obtained as both σ_k and Γ tend to infinity, with $\Gamma/\sigma_k = \text{const.} = \sqrt{2\pi}|\kappa(k_0)|^2$. σ_k and Γ are both defined in section 4.2 with σ_k giving the width of the Gaussian coupling, $\kappa(k)$. We note that the broadband limit of Eq. (4.7) is not correctly obtained by taking $\sigma_k \to \infty$ while keeping Γ constant. If $\sigma_k \to \infty$ then the coupling function $\kappa(k)$ and the constant c in the master equation, Eq. (4.12), go to zero everywhere due to the normalisation of our coupling, Eq. (3.36).

We may now highlight three points relating to the validity of the Born-Markov approximations and the differences between optical and atomic systems. Firstly, the system timescale, $1/\omega_0$, is significantly larger compared with the output coupling rates for atom traps than for optical cavities. Secondly, the atomic reservoir correlation function decays as $1/\sqrt{\tau}$ for broadband coupling as shown by Eq. (4.18). The decay form is also different from the optical case for more general coupling (for example, Eq. (4.7)), and will lead to different behaviour of the exact equations. Thirdly, the timescale on which the system decays is given by $t_D \approx 1/(c + c^*)$ where c is related to the integral of the correlation function, f', given in Eq. (4.13).

The optical dispersion relation causes the system decay time to depend only on the coupling strength, Γ/σ_k, and the speed of light, c_L. For the atom dispersion relation, t_D also depends on the system frequency, ω_0 and parameters relating to the output coupling, $\kappa(k)$. For gaussian output coupling, t_D is given by

$$t_D = 2\sqrt{\frac{\omega_0\hbar}{m\pi}}\left(\frac{\sigma_k}{\Gamma}\right) \tag{4.19}$$

The validity of the Born-Markov approximation for both optical and atomic systems depends on the interplay of these (or similarly derived optical) timescales. Indeed, the optical Born-Markov theory is not universally valid for optics, either. In a photonic band gap material the dispersion relation for the photons and the radiation reservoir may be modified. Bay *et al.* [62] have discussed fluorescence into a radiation continuum in which a band gap with

dispersion relation near the band edge, $\omega_k = \omega_e + A(k - k_0)^2$, similar to the atomic dispersion relation, is present. They find behaviour which cannot be described using the Born-Markov theory.

In the next section, we discuss equations of motion obtained from the Born-Markov master equation for $\langle a^\dagger(t)\rangle$ and $\langle a^\dagger(t)a(t)\rangle$.

4.6 The validity of the Born-Markov approximation.

We consider first the Born-Markov master equation, Eq. (4.12). Using the relation,

$$\frac{d\langle\tilde{o}\rangle}{dt} = \mathrm{Tr}\left[\tilde{o}\frac{d\tilde{\rho}}{dt}\right], \tag{4.20}$$

where $\tilde{o}$ is any system operator in the interaction picture, we obtain the following equations of motion for $\langle a^\dagger\rangle$ and $\langle a^\dagger a\rangle$ from the Markovian master equation, Eq. (4.12).

$$\frac{d\langle a^\dagger(t)\rangle}{dt} = [i\omega_0 - c^*]\langle a^\dagger\rangle(t), \tag{4.21}$$

$$\frac{d\langle a^\dagger(t)a(t)\rangle}{dt} = -(c + c^*)\langle a^\dagger(t)a(t)\rangle. \tag{4.22}$$

We compare the exact equations, Eq. (4.2) and Eq. (4.3) with Eq. (4.21) and Eq. (4.22) respectively. The equations derived from the Born-Markov master equations are equivalent to the exact equations under the approximation that the term $\langle a^\dagger(t-\tau)\rangle e^{i\omega_0\tau} = \langle a^\dagger(t)\rangle$ and $\langle a^\dagger(t)a(t-\tau)\rangle e^{-i\omega_0\tau} = \langle a^\dagger(t)a(t)\rangle$. That is, if we ignore the effect of the output coupling on the system evolution. Alternatively, the exact and Born-Markov equations will agree if $f'(\tau)$ can be approximated by a Dirac delta function. While there is no exact limit in which $f'(\tau)$ tends to a Dirac delta function this does not mean that we cannot replace $\langle a^\dagger(t-\tau)\rangle e^{i\omega_0\tau}$ by $\langle a^\dagger(t)\rangle$ in Eq. (4.2) any parameter regimes. Rather, if we consider the exact equation, Eq. (4.3), and the solutions obtained from the Heisenberg equations of motion, we can see that the exact equation can be rewritten as

$$\frac{d}{dt}\langle a^\dagger(t)a(t)\rangle = -\langle a^\dagger(t)a(t)\rangle \times \int_0^t f'(\tau) \times \frac{\mathcal{L}^{-1}\left\{\frac{1}{s+\mathcal{L}\{f'(t)\}(s)}\right\}(t-\tau)}{\mathcal{L}^{-1}\left\{\frac{1}{s+\mathcal{L}\{f'(t)\}(s)}\right\}(t)}\, d\tau + \text{h.c.} \tag{4.23}$$

From this form of the exact equation, the Born-Markov equation is obtained by the assumption that $f'(\tau)$ decays rapidly on the timescale on which the other

(inverse Laplace transform) terms in the integral change with τ. For parameters in which the Born-Markov approximation is valid, we know that this ratio, given exactly from Eq. (4.9), is approximately exponential with a timescale of order t_D. This fact can be motivated by considering Eq (4.5). This equation shows that the number of atoms in the cavity as a function of time is given by the square of the absolute value of the inverse Laplace transform term, identical to that found in Eq. (4.23) above. In the Born-Markov regime we know the number of atoms in the cavity must decay approximately exponentially on the timescale t_D. Thus, for the Born-Markov approximation to hold we require that the the timescale on which $f'(t)$ decays must be small compared to t_D.

For the non-broadband case, we can define a timescale on which $f'(t)$ decays by the width at half maximum of the absolute value of the reservoir correlation function $|f(\tau)|$

$$t_R = \frac{\sqrt{15}m}{\hbar\sigma_k^2} = \frac{\sqrt{15}}{\alpha}. \tag{4.24}$$

Here m is the mass of the atoms and σ_k is the width of the Gaussian lasing mode in momentum space. This timescale must be small compared with the decay timescale, t_D discussed earlier. This condition, by itself, would suggest that as the coupling becomes increasingly broadband the Born-Markov approximations become increasingly good. However, this is not the case. Although the function $f'(\tau)$ becomes infinite at zero in the broadband limit and therefore must have a zero half width, t_R, there are significant contributions to the integral in Eq. (4.23) away from $\tau = 0$. Instead of the half width of the reservoir correlation function, t_R, we are more interested in the half width of the integral of $f'(\tau)$. This timescale is defined in terms of the reservoir correlation function, $f(\tau)$, and the system frequency, ω_0.

We define t_s such that

$$\int_0^{t_s} f'(\tau)d\tau = 1/2 \int_0^{\infty} f'(\tau)d\tau. \tag{4.25}$$

We have used the symbol, t_s here, because for broadband coupling the quantity defined by Eq. (4.25) is $t_s = 1/\omega_0$. The atomic dispersion relations make t_D also depend on ω_0, Eq. (4.19) which means that the condition $t_s << t_D$, can be written as

$$\omega_0^{3/2}\sqrt{\frac{\hbar}{m\pi}}\left(\frac{\sigma_k}{\Gamma}\right) >> 1. \tag{4.26}$$

For broadband coupling, this timescale condition determines the parameter regimes in which the Born-Markov approximation is valid. The dependence on $\omega_0^{3/2}$ and on the mass in this condition comes from the dependence

of t_D on the coupling shape, $\kappa(k)$, which we have expressed here in terms of m and ω_0. In the equivalent model with optical dispersion relations, t_D only depends on the strength of the coupling, given by Γ/σ_k.

We now compare the results of the exact and Born-Markov equation. We initially consider Gaussian coupling with similar parameters to those discussed in [58]. For atoms, $m \approx 5 \times 10^{-26}$kg. Atom traps in which BEC has been achieved have frequencies of $\omega_0 \approx 2\pi \times 123\text{s}^{-1}$ [4]. Values for the coupling strength, Γ depend on the method used. For Raman coupling, for instance, Γ depends on the intensity of the lasers [58], so a range of values down to zero can be achieved. The Born-Markov approximations become increasingly good for smaller coupling strengths. However, in output coupling which has occurred experimentally to date, the output coupling have been in the strong coupling regime. We choose a value in this regime, $\Gamma \approx 10^6\text{s}^{-2}$ which can be achieved with laser intensities similar to those discussed in [58].

In Fig. 4.1 a the solution for the expectation value of the number of atoms in the system at time t is plotted for the parameters quoted above. The exact solution is given by Eq. (4.5). The solution derived from the Born-Markov master equation in which the reservoir cannot couple back into the system is also shown. This is given by

$$\langle a^\dagger(t)a(t)\rangle \;=\; \langle a^\dagger(0)a(0)\rangle\, e^{-(c+c^*)t}. \tag{4.27}$$

Fig. 4.1 demonstrates that the results for the number of atoms using the Born-Markov approximations disagree with the exact solutions in the case of Gaussian output coupling. For these parameters, $t_R \approx 2.0 \times 10^{-3}$s, $t_s \approx 1.4 \times 10^{-3}$s and $t_D \approx 5.0 \times 10^{-4}$s, so that both the inequalities $t_R < t_D$ and $t_s < t_D$ fail.

We have presented results in terms of the Gaussian coupling discussed in section 4.2. From the inequality $t_s < t_D$ we see that in the broadband limit, atoms are not lost exponentially from the system for parameters which correspond to the ones we consider above. Fig. 4.1b compares the exact and Born-Markov solutions to our model in the broadband limit. In this limit the timescale, t_R as defined above tends to zero, thus the first inequality is satisfied. However, the inequality, Eq. (4.26), fails. The parameters chosen are the same as those for the Gaussian coupling, with a strength of coupling in the exact solutions given by

$$|\kappa(k_0)|^2 = \frac{\Gamma}{\sqrt{2\pi}\,\sigma_k} \approx 0.4\text{m s}^{-2}, \tag{4.28}$$

In this case the Born-Markov solution again gives exponential decay. However, the decay constant is now given as the broadband limit of Eq. (4.13).

The timescale considerations we have presented here, along with Fig. 4.1, demonstrate that for large output coupling rates, correct results for the number

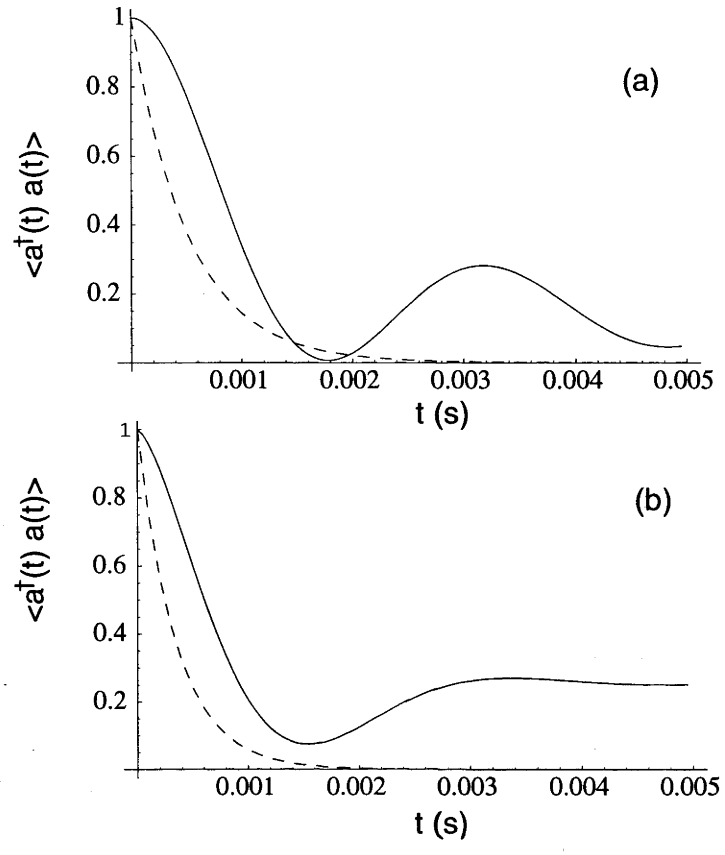

Figure 4.1: A comparison between $\langle a^\dagger(t)a(t)\rangle$ found using the Born-Markov master equation (dashed line) and the exact solution (solid line). Parameters are (a) $\Gamma = 1 \times 10^6 \mathrm{s}^{-2}$, $\sigma_k \approx 10^6 \mathrm{m}^{-1}$ for Gaussian coupling and (b) $|\kappa(k_0)|^2 = 1.0/\sqrt{2\pi}\mathrm{m\,s}^{-2}$ for broadband coupling. Other parameters are $m = 5 \times 10^{-26}\mathrm{kg}$, $\omega_0 = 2\pi \times 123\mathrm{s}^{-1}$.

of atoms in a trap which is coupled to free space can not be obtained using the Born-Markov approximation. One of the effects of not being able to ignore the back-action from the reservoir is that for the model we are considering the number of atoms in the cavity does not tend to zero for long times (Fig. 4.1). We discuss reasons for this behaviour in the section 4.8. If effects such as gravity and repulsive interactions are included the cavity number will tend to zero. However, even with these effects included the loss is not exponential and the conclusion that the Born-Markov approximation fails to describe the output coupling remains.

Here, we have demonstrated the failure of the Born-Markov approximation by the use of the particular system variable, $\langle a^\dagger a\rangle$. However, the problems with using the Born-Markov approximations are not confined to this

particular example. For instance, if the output from a BEC is described using a Born-Markov master equation, the resulting long time energy spectrum is Lorentzian. However, if we avoid making the Born-Markov approximations for atoms the exact spectrum may be non-Lorentzian for some values of coupling strength, Γ, and frequency, ω_0 [58].

4.7 Non-Markovian master equation

In the previous section we show that the standard master equation does not correctly describe the dynamics of our model for particular parameters. However a master equation, in terms of only the system variables, would be an important tool for describing an atom laser. We now consider whether a non-Markovian master equation can give a correct description of the atom laser. To do this, we continue to make the Born approximation, but do not make a Markov approximation.

The master equation with the Born approximation only is given in Eq. (4.11). Again, we check the validity of the Born approximation by comparing the results obtained from this Born master equation with the exact solutions. We begin by considering the resulting equation for the expectation value $\langle a^\dagger \rangle$,

$$\frac{d\langle a^\dagger(t)\rangle}{dt} = i\omega_0\langle a^\dagger\rangle(t) - \int_0^t dt'\langle a^\dagger(t')\rangle \times \int |\kappa(k)|^2 e^{i\omega_k(t-t')}dk, \qquad (4.29)$$

Eq. (4.29) is the same as that obtained through the full system plus reservoir equations given in Eq. (4.2). This can be seen by making the transformation $\tau = t - t'$ in Eq. (4.29) to obtain the alternative form, Eq. (4.2). Despite this success, the density operator equation with the Born approximation, Eq. (4.11) is not correct. In particular, the Born approximation does not give correct values for higher order expectation values, such as $\langle a^\dagger a\rangle$.

The equation derived from the non-Markovian master equation, Eq. (4.11) for the number operator expectation value is

$$\frac{d\langle a^\dagger(t)a(t)\rangle}{dt} = -\int_0^t d\tau\langle a^\dagger a\rangle(t-\tau) \times \int |\kappa(k)|^2 e^{i(\omega_0-\omega_k)\tau}dk + \text{h.c}, \qquad (4.30)$$

with solution

$$\langle a^\dagger(t)a(t)\rangle = \langle a^\dagger(0)a(0)\rangle \times \mathcal{L}^{-1}\left\{\frac{1}{s + \mathcal{L}\{f'(t)\}(s) + \mathcal{L}\{f'(t)^*\}(s)}\right\}(t). \qquad (4.31)$$

These do not agree with the corresponding exact equations given in Eq. (4.3) and Eq. (4.5), as is shown in Fig. 4.2. This figure compares the ex-

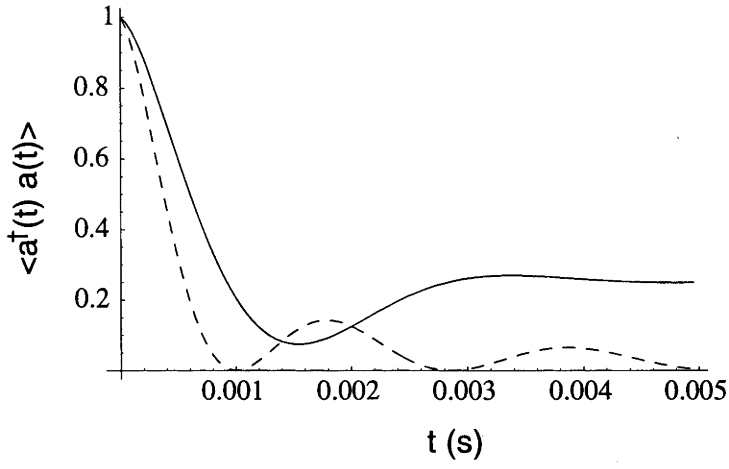

Figure 4.2: A comparison between $\langle a^\dagger(t)a(t)\rangle$ found using the Born (non-Markovian) master equation (dashed line) and the exact solution (solid line) respectively in the broadband regime. Parameters are the same as in Fig. 4.1.

act results for $\langle a^\dagger(t)a(t)\rangle$ with the solution in the Born approximation only, Eq. (4.31). The parameter values chosen are the same as those discussed in section 4.6 and the comparison is made for broadband coupling.

4.8 Effects of gravity and interactions

In this section we present a quasi-single particle model which allows us to consider the effects of gravity on our output coupling. This model is equivalent to a mean-field model of output coupling from a BEC. We will extend the model and include pumping in Chapter 5. Mean field models cannot be extended to show interesting effects, such as noise suppression due to gain saturation if pumping is added to the model as it does not give information about the general quantum statistics of the output atom field. However, it shows that the inclusion of gravity causes the atom number to asymptote to zero. It does this in a non-exponential way, however, and therefore cannot be modeled by a damping term based on the Born-Markov approximation. Moreover, we demonstrate that the short time behaviour predicted by the models with gravity agree with the exact solutions we have presented earlier which ignore the effects of gravity.

The previous section demonstrated qualitative differences between the exact solution of our model and the solution which uses the Born-Markov ap-

proximation. In fact, the exact solution of the model has a stable, nondispersing state which means that not all of the atoms leave the cavity, whereas the approximate solution shows an exponential decay of atoms from the cavity. The presence of the stable state is due to a coherence between the atoms in the cavity and the output modes. The Born-Markov approximation ignores any coherence between the cavity mode and the output modes, and therefore cannot describe any model which produces such features. We now show that such features would be destroyed by gravity.

For coherent dynamics without atom-atom interactions, the multiparticle evolution is identical to the evolution of a single particle [63]. The gravitational term makes it impossible to derive analytical results as in section 2.5, so here we solve the corresponding time-dependent Schrödinger equation numerically. This was done in the position basis for convenience. The Hamiltonian for our system with the inclusion of a gravitational potential is

$$
\begin{aligned}
H &= H_s + H_r + H_{sr} + H_g, && (4.32)\\
H_s &= \hbar\omega_0 |\psi_a\rangle\langle\psi_a|, && (4.33)\\
H_r &= \frac{\hat{P}^2}{2M}, && (4.34)\\
H_{sr} &= \int dx\ \left(g^*(x)|\psi_a\rangle\langle x| + g(x)|x\rangle\langle\psi_a|\right), && (4.35)\\
H_g &= Mg\hat{x}\sin(\theta), && (4.36)
\end{aligned}
$$

where the coupling function, $g(x)$ is related to $\kappa(k)$ by a Fourier transform,

$$
\begin{aligned}
g(x) &= \int dk \frac{i\hbar\kappa^*(k)\, e^{ikx}}{\sqrt{2\pi}}. && (4.37)\\
&= -\Gamma^{\frac{1}{2}}\hbar e^{i(\omega_{2L}-\omega_{1L})t} \left(\frac{2\sigma_k^2}{\pi}\right)^{\frac{1}{4}} e^{ik_0x}\, e^{-\sigma_k^2x^2}, && (4.38)
\end{aligned}
$$

and Eq. (4.38) is obtained from the definition of $\kappa(k)$ given in Eq. (3.36) and Eq. (3.49). $\hat{P}$ is the momentum operator.

We numerically solve this model using a standard split operator method for solving linear and non-linear Schrödinger equations. If we write the Hamiltonian, Eq. (4.32) - Eq. (4.36) as

$$
\begin{aligned}
H &= H_A + H_B, && (4.39)\\
H_A &= H_s + H_r, && (4.40)\\
H_B &= H_{sr} + H_g, && (4.41)
\end{aligned}
$$

and consider a general state of the system given by

$$|\psi(t)\rangle \;=\; c_a(t)\,|\psi_a\rangle + \int dx\; C_x(t)\,|x\rangle \tag{4.42}$$

then the time evolution of this state is given by

$$|\psi(t+\Delta t)\rangle \;=\; e^{-i(H_A+H_B)\Delta t/\hbar}\,|\psi(t)\rangle = U(\Delta t)\,|\psi(t)\rangle. \tag{4.43}$$

In the split operator method we separate this evolution so that

$$U(\Delta t) \;=\; U_A\left(\frac{\Delta t}{2}\right) U_B(\Delta t)\, U_A\left(\frac{\Delta t}{2}\right) \;+\; O(\Delta t^3). \tag{4.44}$$

The term $U_A(\Delta t/2)$ is evaluated to infinite order in Δt. The term $U_B(\Delta t)$ is approximated to second order as

$$U_B(\Delta t)\,|\psi\rangle \;=\; |\psi(t)\rangle \;+\; \frac{\Delta t}{i\hbar} H_B|\psi\rangle \;+\; \frac{1}{2}\left(\frac{\Delta t}{i\hbar}\right)^2 H_B^2|\psi\rangle \;+\; O(\Delta t^3). \tag{4.45}$$

This is found to be a good approximation. We do not evaluate U_B to infinite order because the interaction term H_{sr} does not act in a simple manner in the exponential on a momentum or position state basis. With the term $H_g = 0$, this model is equivalent to a single particle version of our earlier many particle description, Eq. (3.30), and produces a time dependence for the probability of finding an atom in the cavity which is identical to $\langle a^\dagger(t)a(t)\rangle$, found previously. These show a long time steady state in the number of atoms in the cavity which does not tend towards zero. With the inclusion of gravity ($H_g \neq 0$), however, the number of atoms decays to zero in a non-exponential manner. This behaviour is shown in Fig. 4.3.

In Fig. 4.3 we can see collapses and revivals in the number of atoms in the cavity. This is due to the evolving phase relationship between the atoms in the cavity and the atoms which have been coupled into the output field modes. There is no version of the Born-Markov approximation that can describe behaviour such as this, as such an approximation requires that there be no entanglement between the lasing mode and the output modes.

The presence of gravity changes the long time behaviour of our model so that the number of atoms asymptotes to zero, while the short time behaviour remains the same. Other effects may also lead to the long time decay of atom number. Repulsive interactions, for instance, would be expected to destroy the thin stable structure in position space which leads to the long time non-zero population of the cavity mode. The effect of repulsive interactions in the output can be included in this model by including the effects of a nonlinear

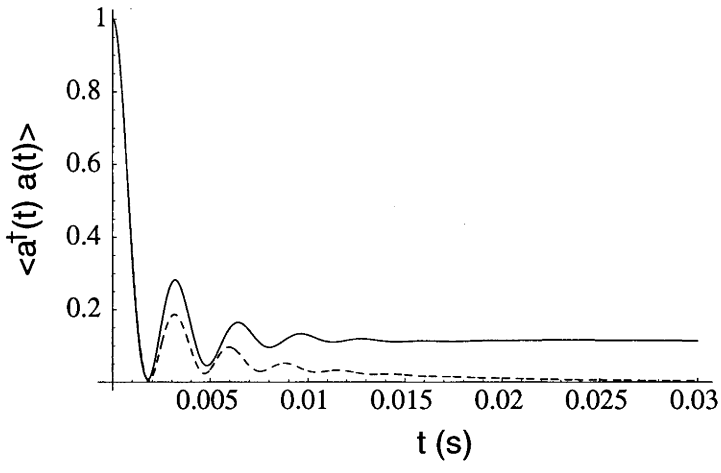

Figure 4.3: The effect of introducing gravity into the model on the number of atoms in the cavity, $\langle a^\dagger(t)a(t)\rangle$. The solid line shows the figure with gravity turned off and agrees with the results presented in Fig. 4.1a. The dashed line includes gravity, $g\sin(\theta)$, $g = 9.8\mathrm{m\,s^{-1}}$, $\theta = \pi/20$.

term given by

$$NU_0|\psi(x)|^2. \tag{4.46}$$

Including such interactions into our model produces a Gross-Pitaevskii type equation [64], where N is the number of atoms in the system and U_0 an interaction strength (see Chapter 5). We find that introducing such an interaction term does cause the atom number to go below the nonzero steady state predicted in the interaction free model.

4.9 Multimode model in the trap basis

In section 4.8 above, we consider a quasi-single particle model of output coupling from a trap to a continuum of free space modes. For coherent dynamics this is identical to the atom number evolution obtained in the many particle input-output theory presented earlier in this chapter. In both of these models, however, we make a single-mode approximation in which we ignore all but the ground state level of the trap. We extend the model here to a multimode model and show that the addition of these extra levels does not greatly change the output dynamics. We still do not consider atom-atom interactions in the trap mode here, however. We introduce these effects in the mean-field model outlined in Chapter 5.

We begin by defining a multi-mode version of the total Hamiltonian, Eq. 4.32. This modified Hamiltonian is given by

$$H_{\text{multimode}} = H_A + H_B, \tag{4.47}$$

where

$$H_A = \sum_j \hbar\omega_j \, |\psi_j\rangle\langle\psi_j| + \int dk \, \frac{(\hbar k)^2}{2m} \, |k\rangle\langle k| \tag{4.48}$$

$$H_B = \sum_j \int dk' \, \tilde{g}_j(k') \, |k\rangle\langle\psi_j| + \sum_j \int dk' \, \tilde{g}_i^*(k') \, |\psi_j\rangle\langle k| + H_g, \tag{4.49}$$

$$\tilde{g}_i(k) = -\hbar\Gamma^{\frac{1}{2}} \left(e^{i(\omega_{2L}-\omega_{1L})t} \psi_j(k - k_{1L} - k_{2L}) \right), \tag{4.50}$$

and

$$\psi_n(k) = \frac{i^{-n} 2^{-\frac{n}{2}} (n!)^{-\frac{1}{2}}}{(2\pi\sigma_k^2)^{\frac{1}{4}}} \exp\left[\frac{-k^2}{4\sigma_k^2}\right] H_n\left[\frac{k}{\sqrt{2}\sigma_k}\right]. \tag{4.51}$$

$H_n[z]$ is the n^{th} order Hermite polynomial.

The output coupling term $\tilde{g}_j(k)$ is most easily expressed in the position basis. In the position basis the output coupling part of the Hamiltonian is written as

$$H_{\text{sr}} = \sum_j \int dx \, g_j^*(x) \, |\psi_j\rangle\langle x| + g_j(x) \, |x\rangle\langle\psi_j|, \tag{4.52}$$

where the coupling function in position space, $g_j(x)$, is related to $\tilde{g}_j(k)$ through a Fourier transform and is given by

$$g_n(x) = \frac{-\Gamma^{\frac{1}{2}} \hbar e^{i(\omega_{2L}-\omega_{1L})t} 2^{\frac{-n+1}{2}} (n!)^{-\frac{1}{2}} e^{ik_0 x} \sigma_k}{(2\pi\sigma_k^2)^{\frac{1}{4}}} \, e^{-\sigma_k^2 x^2} H_n[\sqrt{2}\sigma_k x]. \tag{4.53}$$

Fig. 4.4 shows the number of atoms in the various modes of the cavity as a function of time. These results were obtained by considering the first ten modes of the trap. All modes other than the two plotted in this figure have negligible population. These results show that higher order modes of the cavity do not become significantly populated due to the output coupling mechanism and help to verify the use of the single mode approximation in the general input-output theory.

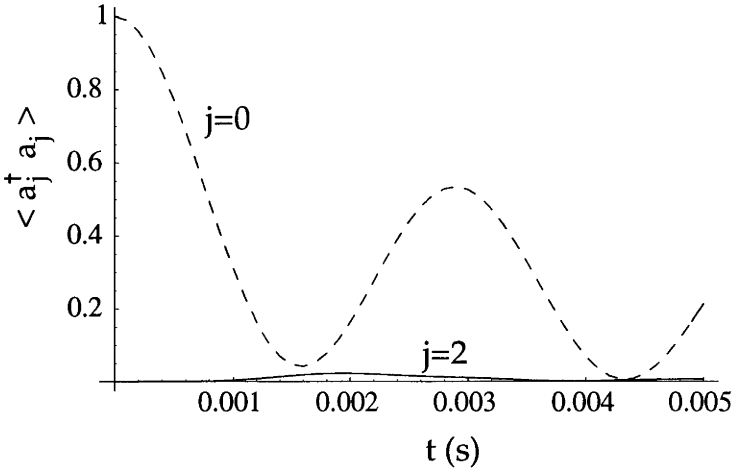

Figure 4.4: Plot of the number of atoms in the ground state ($j = 0$) and the next highest even mode, ($j = 2$) as a function of time. Other modes have negligible population.

4.10 Conclusions

We have discussed the use of master equations and other density operator equations for describing output coupling from a single mode to a continuum of free space modes. We find that the Born-Markov master equation is not valid in some parameter regimes in which atoms are coupled out of a trap. These regimes correspond to large coupling rates, which are similar to the experimental output coupling methods produced to date. In a continuously pumped atom laser, however, smaller output coupling rates would be possible while still providing a reasonable output flux if a suitably large number of atoms could be built up in the lasing mode.

The Born-Markov approximations must be made self consistently. In regimes where the Born-Markov approximations fail, the system can be solved in the Heisenberg picture, treating the output modes fully [54, 58]. For broadband coupling, the parameter regimes in which the Born-Markov approximation is valid is given in Eq. (4.26). Another possibility for describing such systems involves the use of quantum trajectories. These have been found to be useful for other systems in which no Born-Markov master equation exists [62].

While many practical atom lasers may work in regimes in which the Born and Markov approximations are valid, the failure of these approximations also opens up the possibility of finding new properties of atom lasers significantly different from those found in the optical laser.

Chapter 5

Pumping, loss, and the atom laser

Overview

In the previous two chapters we have discussed output coupling from a BEC in an atomic trap. In these considerations, however, we do not consider any pumping mechanism. In the following chapter we consider a pumping mechanism which could be combined with output coupling to produce a continuous atom laser. We consider generalizations of the equations presented in Chapter 2 and 3 with the inclusion of pumping. We also present a mean-field theory model of a pumped and damped atom laser.

5.1 Introduction

Our focus in the last two chapters has been on output coupling from a BEC. A beam of atoms obtained by coherently coupling a BEC to free space can be considered to be a pulsed atom laser. However, to obtain a continuous atom laser which is the analogue of a cw optical laser, we require a suitable pumping mechanism. Furthermore, higher order coherences in the output beam require that the pumping mechanism is strongly depleted.

Along with pumping, a complete model of an atom laser must include the effect of interatomic interactions. The effects of atom-atom interactions are naturally included in models which describe atom fields using the nonlinear Schrödinger equations. Such models (see Chapter 1) have been proposed by Steck and Naraschewski [31, 65] , Kneer [33] and Ballagh [30]. We have already presented a non-pumped version of output coupling which is equivalent to a mean field model in Chapter 4. Later we will include pumping into our model to produce a pumped and damped mean-field model of the atom laser. Models based on the NLSE do not consider the effect of the coherences between the lasing mode and the external modes, and they assume that the cavity modes are in a coherent state of some spatial wavefunction. These models cannot be extended to show interesting effects, such a noise suppression due to gain

saturation if pumping added. Nevertheless, such models are a useful tool towards understanding the atom laser where other full quantum statistics models are intractable.

Before we discuss our NLSE model further, we consider the problem of extending the input-output formalism presented in chapters 2 and 3 to include pumping. Using this formalism, we have assumed that atom-atom interactions are negligible. This assumption may not necessarily be valid in some parameter regimes. However, the inclusion of atom-atom interactions in full generality would be a difficult process. For instance, the energy levels of the cavity would depend on the number of atoms which were trapped in the cavity. In the limit of weak interactions, it would be necessary to add an extra dephasing term to the master equation, which may also limit the coherence of the output. The strength of the coupling between the cavity mode and the external modes depends on the spatial overlap as we discussed in Chapter 2, so it will become time dependent as the shape of the spatial wavefunction changes with the intracavity atom number. A complete description of these effects would, thus, require a multimode description of the intracavity field.

Of course, it is expected that well above threshold the single mode approximation for the cavity will be a good one. This was indicated by the rate equations presented in Chapter 2. This is indeed the case in the equivalent optical theory, where we find that well above threshold the number of atoms in the cavity is reasonably well defined and the complicated dynamics of the pumping process can be approximated by a linearised master equation term [7]. We derive such a term for the atom laser here.

5.2 Model

The basis of our model for a pumped and damped cavity has been discussed in Chapter 3 and 4. We consider a single mode cavity, with Hamiltonian H_{sys} (Eq. (3.31)), coupled through the interaction term H_{int} (Eq. (3.33)) to a continuum of free space modes described by H_{ext} in Eq. (3.32). Here we consider the addition of a pump term, H_{pump} so that the total Hamiltonian is given by

$$H_{tot} = H_{sys} + H_{ext} + H_{int} + H_{pump}. \tag{5.1}$$

The pump does not directly couple to the external modes, described by creation operators $b_k^\dagger$, so that the appropriate commutation relations are given by

$$[b_k^\dagger, H_{pump}] = [b_k, H_{pump}] = 0. \tag{5.2}$$

However, the pump term does couple the pump modes to the cavity modes, described by the creation operator $a^\dagger$. Nevertheless, it is clear from

Eq. (5.2) that the Heisenberg equations of motion for $b_k(t)$ are unaffected by the pump term, except through their affect on $a(t)$. That is, the solution to the Heisenberg equations of motion for $b_k(t)$,

$$\frac{db_k(t)}{dt} = -i\omega_k b_k(t) + \sqrt{\Gamma}\kappa'(k)^* a(t), \tag{5.3}$$

is given by

$$b_k(t) = e^{-i\omega_k t} b_k(0) + \sqrt{\Gamma}\kappa'(k)^* \int_0^t \mathrm{d}u e^{-i\omega_k(t-u)} a(u). \tag{5.4}$$

This is the same as that obtained in the absence of pumping and leads to the solution when the external field is initially empty given by

$$\langle b_k^\dagger(t) b_k(t)\rangle \;=\; |\kappa(k)|^2 \int_0^t dt' \int_0^t dt''\, e^{-i\omega_k(t'-t'')} \langle a^\dagger(t') a(t'')\rangle. \tag{5.5}$$

Again, this is exactly equivalent to the non-pumping solution for the spectrum given in Eq. (3.44) using Eq. (3.48) to express the term $M_k(t)$ in terms of the system variables, a, $a^\dagger$. Of course, with the addition of pumping the solution for $\langle a^\dagger(t')a(t'')\rangle$ is no longer given simply by solutions to the Heisenberg equations of motion outlined in Chapter 3. The importance of Eq. (5.4), however, is that the output operators, $b_k(t)$ can be expressed in terms of $b_k(0)$ and the cavity modes, $a(t)$. Thus any property of the output field including the spectrum, $\langle b_k^\dagger(t)b_k(t)\rangle$ can be obtained from the solution for $a(t)$ and initial conditions. For this reason we now focus on the equations of motion and solutions for $a(t)$ and $a^\dagger(t)$ in the presence of a pumping term.

5.3 Motivation of the pumping term

In this section we use a similar method to that used in the optics case to derive a master equation term describing the pumping of an atom laser through spontaneous emission. To derive a master equation description of pumping we trace over the pump states. This produces a master equation for a reduced density matrix which describes only the cavity and output fields. To be able to trace over the pump states, the pumping process must be irreversible so that any backaction from the reservoir can be ignored. Spontaneous emission has already been suggested as an irreversible pumping method by a number of authors [20–22, 58]. In this model, we continue to avoid tracing over the output states in general. The output coupling must be coherent so we cannot use spontaneous emission to provide an irreversible output coupling term which obeys the Born-Markov equations. However, even if we avoid tracing over the output modes, there are regimes in which the Born-Markov approximation is

valid.

The basic approach to pumping is similar to that followed by Scully and Lamb [66] and found in standard Quantum Optics texts [7]. In the optics case, pumping is modelled by the injection of a poissonian sequence of inverted atoms into the laser cavity. Each injected atom changes the bosonic field through the possible emission of a photon into the field.

For the atom laser, we also consider atoms prepared in the excited state and injected into an atom cavity. The atom field is changed by a process in which the atom spontaneously emits a photon, causing it to change transfer into the atom-laser mode. As for the derivation of the pumping term for an optical laser [7], we begin by considering the effect on the boson field of a single atom injected into the system. Here we wish to describe an atom in an excited state, interacting with the quantized electromagnetic field in terms of the atomic variables only. The master equation is given by Cirac *et al.* [36]:

$$\dot{\rho} = -i\hbar H_{\text{eff}}\rho + i\hbar\rho H_{\text{eff}}^{\dagger} + J\rho, \tag{5.6}$$

where

$$H_{\text{eff}} = \omega_e e^{\dagger}e + \sum_{k=0}^{\infty}\omega_k a_k^{\dagger}a_k - i\frac{\Gamma}{2}e^{\dagger}e\left[1 + \sum_{k,j=0}^{\infty}\alpha_{kj}a_k^{\dagger}a_j\right], \tag{5.7}$$

$$J\rho = \Gamma\sum_{k,j=0}^{\infty}\alpha_{kj}^{R}a_j^{\dagger}e\rho e^{\dagger}a_k. \tag{5.8}$$

Here, e and a_k are the annihilation operators for atoms in the internal excited level and k^{th} ground level respectively. Γ is the spontaneous emission rate from the excited level. $\hbar\omega_e$ and $\hbar\omega_k$ are the energies of the excited and k^{th} ground level respectively. A detailed description of the α_{ij} is given in [67] where this master equation is also used as the starting point in the context of spontaneous emission into a Bose-Einstein condensate.

Cirac *et al.* restrict themselves to the Bose accumulation regime and consider in this regime what the effect of a single atom spontaneous emission event will be on the system. In particular they consider the possible reabsorptions of photons. Here we further simplify the equation by considering an optically thin medium. Doing this we ignore much of the interesting behaviour found by Cirac *et al.* regarding the effect of reabsorption of photons and atom-atom collisions. However, if we do not ignore these effects, the decay of a single excited state atom can lead (through multiple absorptions and emissions) to an arbitrarily large change in the number of atoms in the lasing mode after the introduction of a single excited state atom.

Moreover, for simplicity we consider a model in which the infinitely many trap levels in the above Hamiltonian are replaced with only two effective lev-

els. One of these levels is the lasing level, into which we wish to pump a large number of bosons. The second level is a notional "non-lasing level". This provides the loss channel required in a pumping mechanism, as outlined in Chapter 1. In a more realistic model, this single level would be replaced by an infinite number of higher levels in the trap. We further assume that this second level always has a negligible population compared with the lasing mode. For a single level this could be achieved by having it leak irreversibly at a rate which is large compared to the atomic injection rate. In reality, however, this notional level consists of many levels, each of which will remain unpopulated compared to the lasing level if the probability for an atom to spontaneously emit into the lasing level is greater than the probability to emit into any of the other levels [22]. In considering an effective two level system, we redefine $\alpha_{11} = 1 - \alpha_{00}$ as the probability that the excited atom decays into "non-lasing" mode. Typically α_{11} may be larger than α_{00}, as α_{11} does not describe the probability of an atom decaying into a single state, but into any one of an infinite collection of higher modes of the trap.

We proceed in a manner similar to the optics case [7] and assume the system has N atoms in the lasing mode at some time, t. We then calculate the effect on this system of introducing an excited state atom which may decay into either the lasing mode or into the non-lasing level. If $\rho_N^e = |1\rangle_e\langle 1| \otimes \rho_N$ is the initial state of the system, with N atoms in the ground state and one atom in the excited state, then the state of the system after this atom has decayed is formally given by [67]

$$\rho' = \int_0^\infty dt\, J\left[e^{-iH_{\rm eff}t}\,\rho_N^e\, e^{iH_{\rm eff}^\dagger t}\right], \tag{5.9}$$

$$\approx \int_0^t dt_1 \Gamma \sum_{r=0}^{1} \alpha_{rr}\, a_r^\dagger \Bigg[\sum_{n_0,n_1,m_0,m_1} \rho_{n_0,n_1,m_0,m_1} \tag{5.10}$$

$$\exp\left[\frac{-\Gamma(1+\alpha_{00}a_0^\dagger a_0)t_1}{2}\right] |n_0,n_1\rangle\langle m_0,m_1| \exp\left[\frac{-\Gamma(1+\alpha_{00}a_0^\dagger a_0)t_1}{2}\right]\Bigg] a_s.$$

In arriving at Eq. (5.10) we have used the approximations discussed above. In particular we have assumed an effective two mode system, and ignored interactions between different energy levels. We have also ignored the possibility of absorbing the emitted photon, which is the process that Cirac *et al.* investigate. Tracing over the non-lasing mode (labeled as $|n_1\rangle\langle m_1|$) in Eq. (5.10), we obtain:

$$\rho' = \sum_{n,m} \rho_{nm} \int_0^\infty dt'\, \Gamma\, e^{-\Gamma t'(1+\alpha_{00}{}'n/2+\alpha_{00}{}'m/2)} \times$$

$$\left(\alpha_{00}\sqrt{n+1}\sqrt{m+1}\,|n+1\rangle\langle m+1| + \alpha_{11}\,|n\rangle\langle m|\right). \tag{5.11}$$

Upon evaluating the integral in Eq. (5.11) above, we obtain

$$\begin{aligned} \rho' &= \sum_{n,m=0}^{\infty} \rho_{n,m}(0)\left(A_{nm}|n\rangle\langle m| + B_{nm}|n+1\rangle\langle m+1|\right). \\ &= \mathcal{P}(\rho) \end{aligned} \tag{5.12}$$

This is of the same form as that obtained for the optical case, though here we calculate A_{nm} and B_{nm} to be

$$A_{nm} = \frac{\alpha_{11}}{1+\alpha_{00}n/2+\alpha_{00}m/2} \tag{5.13}$$

$$B_{nm} = \frac{\sqrt{(n+1)(m+1)}\alpha_{00}}{1+\alpha_{00}n/2+\alpha_{00}m/2}. \tag{5.14}$$

Finally we assume atoms are injected at a rate given by r [7]. Thus, the density operator at a time $t+\Delta t$ is given by

$$\rho(t+\Delta t) = r\Delta t\mathcal{P}\rho(t) + (1-r\Delta t)\rho(t) \tag{5.15}$$

where $r\Delta t$ gives the probability an atom will be injected into the system between times t and $t+\Delta t$. Taking the limit as $\Delta t \to 0$, we obtain

$$\frac{d\rho_{nm}}{dt} = \frac{G}{\alpha_{00}}\left(\frac{\sqrt{nm}\rho_{n-1,m-1}}{\frac{\alpha_{11}}{\alpha_{00}}+\frac{m+n}{2}} - \frac{(m+n+2)/2\rho_{nm}}{\frac{\alpha_{11}}{\alpha_{00}}+\frac{m+n+2}{2}}\right), \tag{5.16}$$

where $G = \alpha_{00}r$ and α_{00} is the probability of an atom decaying into the lasing mode. $\alpha_{11} = 1-\alpha_{00}$ is the probability of an atom decaying into the non-lasing modes. Eq. (5.16) is similar in form to the standard optical equation in Fock number representation. This equation can be expressed in standard operator notation as

$$\dot{\rho} = \frac{G}{\alpha_{00}}\mathcal{D}[a^\dagger]\left(\frac{\alpha_{11}}{\alpha_{00}}+\mathcal{A}[a^\dagger]\right)^{-1}\rho. \tag{5.17}$$

$$\mathcal{D}[c] = \mathcal{J}[c]-\mathcal{A}[c], \tag{5.18}$$

$$\mathcal{J}[c]\rho = c\rho c^\dagger, \tag{5.19}$$

$$\mathcal{A}[c]\rho = \frac{1}{2}(c^\dagger c\rho + \rho c^\dagger c). \tag{5.20}$$

This is of the same form as presented for a generic master equation by Wiseman [8] with the saturation number, n_s, in Wiseman's model being given by α_{11}/α_{00}, here. We stress, however, that in deriving this result we have used a particularly simple model which ignores much of the interesting physics which would typically occur in a spontaneous emission process. However, it follows closely the derivation given for an optical pumping mechanism, and

is likely to be a good approximation in regimes where reabsorption of emitted photons can be ignored.

5.4 Equations of motion

The Hamiltonian which describes the pumped and damped atom laser system consists of a pump term, H_{pump} along with H_{sys},H_{int} and H_{ext}. While H_{sys}, H_{int} and H_{ext} only depend on system and external "output" operators the pump term, H_{pump} contains, in principle, a full description of the pump modes including coupling to the photon reservoir and other specifics of the pump scheme. Using such a Hamiltonian description of the full pumping process is unwieldy. However, using the master equation pump term, Eq. (5.17) we effectively trace over the pump modes to obtain the following equation for the cavity dynamics,

$$\frac{d\rho}{dt} = \frac{G}{\alpha_{00}}\mathcal{D}[a^\dagger]\left(\frac{\alpha_{11}}{\alpha_{00}} + \mathcal{A}[a^\dagger]\right)^{-1}\rho + \frac{i}{\hbar}[\rho, H_{sys} + H_{int} + H_{ext}] \quad (5.21)$$

Equations of motion for $\langle a^\dagger(t)\rangle$ due to pump

In Chapter 3, we consider equations of motion for $\langle a^\dagger(t)\rangle$ and use these to solve for the output spectrum and higher order properties of an output beam. To do this, we use the fact that the equation of motion for the two time correlation is related to equations of motion for the expectation value of the field operator, $\langle a^\dagger(t)\rangle$. We now wish to consider what terms we must add to these unpumped equations of motion to include the effects of the pumping term, Eq (5.21). Previously we have shown that the pumping term dynamics can be written in the Fock basis as

$$\frac{d\rho^{pump}_{n,m}}{dt} = r\left(\frac{\sqrt{nm}}{n_s + (n+m)/2}\rho_{n-1,m-1} - \frac{(n+m+2)/2}{n_s + (n+m+2)/2}\rho_{n,m}\right). \quad (5.22)$$

Here we have used the notation, n_s for the saturation atom number given by $n_s = \alpha_{11}/\alpha_{00}$. Using Eq (5.22) to obtain the evolution of $\langle a^\dagger(t)\rangle$ due to the pump term, we get

$$\left(\frac{d\langle a^\dagger(t)\rangle}{dt}\right)_{\text{pump}} = \sum_{n=0}^{\infty}\sqrt{n+1}\dot{\rho}_{n,n+1}, \quad (5.23)$$

$$= \sum_{n=0}^{\infty}\left(\frac{r}{2n+2n_s+1}\right)\sqrt{n}\rho_{n-1,n}. \quad (5.24)$$

We approximate Eq. (5.24) further in section 5.4.1. Now, however, we consider the photon statistics and linewidth in the Born and Markov approxima-

tions.

5.4.1 Pumping - in the Born and Markov approximations

In Chapter 4 we have described a damping term which is obtained in the Born approximation. This involves tracing over the output field to obtain a master equation, Eq. (4.11), for the lasing mode which describes the output coupling. Tracing over the output field does not affect the pumping term, which is given in Eq. (5.21) above. Combining these terms the master equation which describes the pumped and damped atom laser is given by

$$\begin{aligned} \frac{d\rho}{dt} &= \dot{\rho}_{\text{pump}} + \dot{\rho}_{\text{damp}} \qquad (5.25) \\ &= r\mathcal{D}[a^\dagger](n_s + \mathcal{A}[a^\dagger])^{-1}\rho \\ &\quad - \int_0^t d\tau \left(f'(\tau)(a^\dagger a \rho(t-\tau) - a\rho(t-\tau)a^\dagger) + \text{h.c} \right). \qquad (5.26) \end{aligned}$$

This density equation now describes only the cavity mode in parameter regimes where the Born approximation is valid.

We now consider the photon number obtained from this model, following directly the optics case as outlined by Walls *et al.* [7].

Photon number - Born approximation

Taking the $\langle n|$, $|n\rangle$ matrix element of Eq. (5.26) we obtain an equation for the photon number distribution, $p_n = \rho_{nn}$. This is given by

$$\begin{aligned} \frac{dp_n}{dt}(t) &= \frac{rn}{n+n_s} p_{n-1}(t) - \frac{r(n+1)}{n+n_s+1} p_n(t) \\ &\quad -2n \int_0^t du\, \text{Re}[f(u)e^{i\omega_0 t}]\, p_n(t-u) \; + \\ &\quad +2(n+1) \int_0^t du\, \text{Re}[f(u)e^{i\omega_0 t}]\, p_{n+1}(t-u). \qquad (5.27) \end{aligned}$$

We make the assumption that $p_n(t)$ reaches a steady state, p_n^{ss} for long time, t. Using the fact that the time derivative of this steady state is zero, and rearranging the resulting equations we can obtain the following relation between p_n^{ss}, p_{n-1}^{ss} and p_{n+1}^{ss}

$$p_n^{ss}\left(\frac{r(n+1)}{n+n_s+1} - n(c+c^*) \right) = \frac{rn}{n+n_s} p_{n-1}^{ss} + (n+1)(c+c^*)p_{n+1}^{ss}. \qquad (5.28)$$

Here c is derived in Eq. (4.13) in Chapter 4. For convenience we will use $\gamma = c + c^*$ from here on, as this describes the output loss strength in the Born-

Markov approximation. Eq. (5.29) is a recursion relation which can be solved to give a steady state for the atom number distribution in the cavity,

$$p_n^{ss} = \mathcal{N}\frac{(r/\gamma)^n}{(n+n_s)!}. \tag{5.29}$$

$\mathcal{N}$ is a normalisation constant. As we have written this here, this is almost identical to the steady state optical laser photon number. As for the optical case, such a distribution looks thermal for $r/\gamma < n_s$ (this is the below threshold regime), and for $r/\gamma > n_s$ the distribution becomes increasingly well approximated by a Poissonian distribution as r/γ increases, with the mean atom number, $\bar{n}$ and variance, V given by

$$\bar{n} = \frac{r}{\gamma} - n_s, \tag{5.30}$$

$$V = \bar{n} + n_s. \tag{5.31}$$

Atom Laser linewidth

The statistics obtained in the previous section show that the number distribution above threshold becomes localised about $\bar{n}$. For a laser operating well above threshold, this allows us to approximate Eq. (5.24) by replacing the factor, n in the denominator of this equation by $\bar{n}$, the mean atom number. This follows the outline given for the optics case in Walls *et al.* [7]. Explicitly,

- We assume that the number distribution is well localised about a (large) mean value, $\bar{n}$.

With this assumption, the pump term can be written as

$$\left(\frac{d\langle a^\dagger(t)\rangle}{dt}\right)_{\text{pump}} \approx \frac{r}{2(\bar{n}+n_s)+1}\langle a^\dagger\rangle. \tag{5.32}$$

By expanding the exact expression as a Taylor series in $1/\bar{n}$, we see that there is an error term of the order $1/\bar{n}^2$. However, in the case where the first order terms cancel, the linewidth will actually be of this order. Indeed this will be the case if we obtain linenarrowing, in which the spectrum becomes increasingly narrow as we increase the pumping of the laser. However, if this does occur, then we may approximate the magnitude of the off-diagonal elements of ρ as though it were a coherent state. This then shows that the expression given in Eq. (5.32) is correct to third order in $1/\bar{n}$.

Eq. (5.32) gives the time dependence of $\langle a^\dagger(t)\rangle$ due to the pump term. The atom laser linewidth is dictated by the interplay between this pump term and the damping term. In the discussion above we have made the Born approximation, in which the damping term is given by Eq. (4.11). Due to the time

dependence of $\rho(t-u)$ on times other than t in the Born approximation, the equations for $\langle \dot{a}^\dagger(t)\rangle$ are non Markovian. This makes solving for the output spectrum difficult. Later we will investigate output coupling without tracing over the output field and hence consider non-Markovian (and non-Born) output coupling. For now however we consider a more simple system in which we make use of the Markov approximation. This is valid in parameter regimes with sufficiently slow output coupling rates. In these cases the damping term is given by a term of the form $\gamma(a\rho a^\dagger - 1/2a^\dagger a\rho - 1/2\rho a^\dagger a)$, with γ (defined in the previous section) giving the strength of the coupling. Using this form for the damping and Eq. (5.32) for the pump term we obtain the following equation of motion for the expectation value of the system operator, $a^\dagger$,

$$\frac{d\langle a^\dagger(t)\rangle}{dt} = \left(\frac{r}{2(\bar{n}+n_s)+1} - \frac{\gamma}{2}\right)\langle a^\dagger(t)\rangle, \tag{5.33}$$

$$= \left(\frac{r}{2(\bar{n}+n_s)+1} - \frac{r}{2(\bar{n}+n_s)}\right)\langle a^\dagger(t)\rangle, \tag{5.34}$$

$$\approx -\frac{r}{4\bar{n}^2}\langle a^\dagger(t)\rangle. \tag{5.35}$$

where we have used the fact that in the Born-Markov approximation, the steady state number distribution is given by $\bar{n} = r/\gamma - n_s$ to obtain Eq. (5.34), above. Eq. (5.35) is obtained under the assumption that $\bar{n} >> n_s$ and $\bar{n} >> 1$ and using the series expansion to first order

$$\frac{1}{1+\frac{(n_s+1/2)}{\bar{n}}} \approx 1 - \frac{n_s+1/2}{\bar{n}}. \tag{5.36}$$

The time dependence of the solution to Eq. (5.35) is given by exponential decay. This is an important feature of the atom laser with Born-Markov output coupling which also occurs for the optical laser. We have noted that well above threshold we obtain Poisson photon statistics. This suggests that we may have a coherent state, however the decay of $\langle a^\dagger(t)\rangle$ shows that this is not the case. Indeed, while the intensity of the atom laser is stable the phase undergoes diffusion until it is uniformly distributed over 2π. This rate of amplitude decay, $\Gamma = r/(4\bar{n}^2)$ is a measure of the phase diffusion rate. From the quantum regression theorem we can show that the two time correlation function also decays exponentially at rate Γ and hence that the spectrum is Lorentzian with a width 2Γ. This width, $2\Gamma = r/(2\bar{n}^2)$ can be written in terms of γ as $\Gamma = \gamma/(2\bar{n})$ where γ is the output coupling strength and corresponds to the bare linewidth of the trap due to the output coupling. Thus, the linewidth, $\gamma/(2\bar{n})$ tends to zero as we pump the laser more strongly. This is gain narrowing, and also occurs in many optical laser models.

The above results show the atom laser working in a similar manner to the optical laser for our pumping mechanism and for damping in a parameter regime in which the Born-Markov approximation holds. In the following section we consider the affect of pumping on the atom laser without the Born and Markov approximations.

5.5 Pumping - without tracing over the output field

Without the Born or Markov approximations it is still possible to produce a general equation of motion for $\langle a^\dagger(t)\rangle$ which includes both pumping and (exact) damping terms. The pumping term is given in Eq. (5.32). We stress again, here, that this form is derived under the assumption of a large steady state population, $\bar{n}$ which is well localised. Using this pumping term we obtain the following equation of motion

$$\frac{\partial}{\partial t}\langle a^\dagger\rangle = \left(i\omega_o + \frac{r}{2(\bar{n}+n_s)+1}\right)\langle a^\dagger\rangle(t) + \Gamma\int_{-\infty}^{\infty}\kappa'(k)^*\langle b^\dagger\rangle(t). \tag{5.37}$$

We introduce the parameter

$$P = \frac{r}{2(\bar{n}+n_s)+1}, \tag{5.38}$$

to simplify the notation for the pump term in Eq. (5.37). Using Eq. (5.37) we can obtain information about the spectrum and higher order correlation functions using the quantum regression theorem. This gives an equation of motion for the higher order correlation function,

$$\begin{aligned}\frac{\partial}{\partial\tau}\ \langle a^\dagger(t+\tau)a(t)\rangle &= (i\omega_o + P)\langle a^\dagger(t+\tau)a(t)\rangle \\ &\quad -\Gamma\textstyle\int_0^{t+\tau}\mathrm{du}\ f(t+\tau-u)^*\langle a^\dagger(u)a(t)\rangle\end{aligned} \tag{5.39}$$

where $\tau > 0$, and $f(t)$ is defined in Eq. (3.46). We can compare this equation with the equation in the Born-Markov approximation, discussed previously. In the Born-Markov approximation we find that both $\langle a^\dagger(t)\rangle$ and the corresponding correlation function, $\langle a^\dagger(t+\tau)a(t)\rangle$ decay exponentially leading to a lorentzian spectrum. This is not the case here. Indeed, Eq. (4.21) by itself is not sufficient to specify the dynamics of the cavity, as it is only a single partial integro- differential equation in a two dimensional space. We can obtain a second equation from the integro–differential equation for the intracavity number. This is given by

$$\frac{\partial}{\partial t}\langle a^\dagger a\rangle \ = \ r - \Gamma\int_0^t \mathrm{du}\ 2Re\{f(t-u)^*\langle a^\dagger(u)a(t)\rangle\}. \tag{5.40}$$

The second term of this equation is due to the output coupling and is derived in Chapter 4. The pumping term, r is obtained in a similar manner to the term, P in the above equations from

$$\begin{aligned}
\frac{\partial}{\partial t}\langle a^\dagger a\rangle_{\text{pump}} &= \text{Tr}\left\{\dot{\rho} a^\dagger a\right\}_{\text{pump}} \\
&\approx \sum_{n=0}^{\infty} r\frac{n+1}{n_s+n+1}\rho_{n,n} \qquad (5.41)\\
&= \sum_{n=0}^{\infty} r\frac{\bar{n}+1}{n_s+\bar{n}+1}\rho_{n,n} \qquad (5.42)\\
&\approx r\left(\frac{\bar{n}+1}{n_s+\bar{n}+1}\right) = \bar{r}. \qquad (5.43)
\end{aligned}$$

The pair of equations, Eq. (5.39) and Eq. (5.40) can be solved for the dynamics and output spectrum of the pumped and damped atom laser. We consider two solutions to these equations in the following two sections.

Solution in the case of rapid decay of reservoir correlations

Eq. (5.39) and Eq. (5.40) can be solved for the case $f(t) = |\kappa(k_0)|^2\,\delta(t)$. In Chapter 4 we have show that this function is the reservoir correlation function. In some parameter regimes, this function may be well approximated by a Dirac delta function. Indeed this is also the typical case in optics, where the dispersion relation, $\omega_k = c_L|k|$ allows the function $f(t)$ to be approximated as the fourier transform of a constant (a delta function) in the broadband regime. With $f(t)$ given by a Dirac delta function, equations Eq. (5.39) and Eq. (5.40) become local. The solutions are given by

$$\begin{aligned}
\langle a^\dagger(t)a(t)\rangle &= \langle a^\dagger(0)a(0)\rangle e^{-|\kappa(k_0)|^2 t} + \frac{\bar{r}}{|\kappa(k_0)|^2}(1-e^{-|\kappa(k_0)|^2 t}), \qquad (5.44)\\
\langle a^\dagger(t+\tau)a(t)\rangle &= \langle a^\dagger(t)a(t)\rangle\, e^{i\omega_0\tau} e^{(P-|\kappa(k_0)|^2/2)\tau}. \qquad (5.45)
\end{aligned}$$

From these equations we can see that there is a steady state number, $\langle a^\dagger(t)a(t)\rangle = \bar{n}$ given by

$$\bar{n} = \lim_{t\to\infty}\langle a^\dagger(t)a(t)\rangle = \frac{\bar{r}}{|\kappa(k_0)|^2}. \qquad (5.46)$$

That is the steady state number is the ratio of the pumping and damping rates. Furthermore, Eq. (5.45) shows that the two time correlation decays exponentially at a rate given by $P - |\kappa(k_0)|^2/2$ which corresponds to a competition between the pump and damping terms. We can express the term $P - |\kappa(k_0)|^2/2$

as

$$P - \frac{|\kappa(k_0)|^2}{2} = \frac{r}{2(\bar{n}+n_s)+1} - \frac{\bar{r}}{2\bar{n}}, \tag{5.47}$$

$$\approx -\frac{r}{4\bar{n}(\bar{n}+n_s)} \approx -\frac{r}{4\bar{n}^2}, \tag{5.48}$$

so that we once again gain the standard optical results which lead to gain narrowing well above threshold. The atom laser spectrum in this case is lorentzian.

The above solutions are based on the assumption that the function $f(t)$ can be well approximated by a Dirac delta function and are therefore only valid in the regime in which the Born-Markov approximations are valid. We now consider a more general solution for the equations, Eq. (5.39) and Eq. (5.40) where we do not make this approximation.

General solution

The equations, Eq. (5.39) and Eq. (5.40) can be solved in general for a pump term of the form we have considered here. Indeed, Eq. (5.39) is equivalent to the unpumped equation of motion solved in Chapter 4 with the addition of the pumping term, P. It is easy to show, using similar methods to those presented in Chapter 3 and Chapter 4, that the formal solution to Eq. (5.39) is given by

$$\langle a^\dagger(t+\tau)a(t)\rangle = \langle a^\dagger(t)a(t)\rangle e^{(i\omega_0+P)\tau} \frac{\mathcal{L}^{-1}\left\{\frac{1}{s+\mathcal{L}\{f_1'(t)\}(s)}\right\}^*(t+\tau)}{\mathcal{L}^{-1}\left\{\frac{1}{s+\mathcal{L}\{f_1'(t)\}(s)}\right\}^*(t)}, \tag{5.49}$$

where

$$f_1'(t) = f'(t)e^{-Pt}. \tag{5.50}$$

Using this solution in Eq. (5.40) we can rewrite the equation of motion for $\langle a^\dagger(t)a(t)\rangle$ as

$$\frac{\partial}{\partial t}\langle a^\dagger(t)a(t)\rangle = r - \int_0^t du\, 2\mathrm{Re}\left\{ f^*(t-u)\, e^{(-i\omega_0+P)(t-u)} \frac{\mathcal{L}^{-1}\left\{\frac{1}{s+\mathcal{L}\{f_1'(t)\}(s)}\right\}(t)}{\mathcal{L}^{-1}\left\{\frac{1}{s+\mathcal{L}\{f_1'(t)\}(s)}\right\}(u)} \right\} \times \langle a^\dagger(u)a(u)\rangle. \tag{5.51}$$

For simplicity of notation we introduce the definitions

$$M(t,u) = \frac{\mathcal{L}^{-1}\left\{\frac{1}{s+\mathcal{L}\{f_1'(t)\}(s)}\right\}(t)}{\mathcal{L}^{-1}\left\{\frac{1}{s+\mathcal{L}\{f_1'(t)\}(s)}\right\}(u)}, \tag{5.52}$$

$$M'(t,u) \;=\; M(t,u)\, e^{-(i\omega_0 - P)(t-u)}. \tag{5.53}$$

In the broadband limit these functions can be obtained analytically, as outlined in Chapter 4 and $M'(t,u)$ is given by

$$M'(t,u)_{\text{broadband}} = \frac{W(\alpha,\beta,\Gamma)(t)\,(\beta-\gamma) + W(\beta,\alpha,\gamma)(t)\,(\gamma-\alpha) + W(\gamma,\beta,\alpha)(t)\,(\alpha-\beta)}{W(\alpha,\beta,\Gamma)(u)\,(\beta-\gamma) + W(\beta,\alpha,\gamma)(u)\,(\gamma-\alpha) + W(\gamma,\beta,\alpha)(u)\,(\alpha-\beta)}, \tag{5.54}$$

where

$$W(\alpha,\beta,\gamma)(t) \;=\; \alpha^2 e^{\alpha^2 t}(1 + \text{Erf}[\alpha\sqrt{t}]), \tag{5.55}$$

and α, β and γ are the three solutions to the equation $s^3 + (i\omega_0 - P)s + \Gamma c\sqrt{i} = 0$, with Γ and c as defined in Eq. (3.37) and Eq. (3.54) respectively. Using the definition in Eq. (5.53) we can rewrite Eq. (5.51) as

$$\frac{\partial}{\partial t}\langle a^\dagger(t)a(t)\rangle \;=\; r - \int_0^t du\, \text{Re}\left\{2f^*(t-u)M'(t,u)\right\} \;\times \langle a^\dagger(u)a(u)\rangle. \tag{5.56}$$

In this form we can recognize Eq. (5.56) as a linear first order Volterra integro–differential equation. In general such an equation can be solved as outlined in appendix D [68]. The solution is given by

$$\langle a^\dagger(t)a(t)\rangle \;=\; \langle a^\dagger(0)a(0)\rangle + rt + \int_0^t \Gamma(t,s)\left(\langle a^\dagger(0)a(0)\rangle + rs\right) ds, \tag{5.57}$$

where

$$\Gamma(t,s) \;=\; \sum_{i=1}^{\infty} k_i(t,s) \tag{5.58}$$

$$k_n(t,s) \;=\; \int_s^t k_1(t,\tau)k_{n-1}(\tau,s)\, d\tau \tag{5.59}$$

$$k_1(t,s) \;=\; \int_s^t \text{Re}\left\{-2f^*(\tau-s)M'(\tau,s)\right\} d\tau. \tag{5.60}$$

While the above solution is analytic, the integrals involved in Eq. (5.60) are difficult to evaluate, even in the broadband case. It is more practical to solve Eq. (5.51) numerically. A computer program was written implementing NAG routines to solve a Volterra equation of the second kind. Either this program, or the analytic solution above gives solutions to $\langle a^\dagger(t)a(t)\rangle$.

5.6 Failure of the steady state assumption

A consideration of the general solutions, Eq. (5.49) and Eq. (5.57) in the case of broadband coupling (Eq. (5.53)) gives the results,

$$\lim_{t\to\infty}\langle a^\dagger(t+\tau)a(t)\rangle = \infty \tag{5.61}$$

$$\lim_{t\to\infty}\langle a^\dagger(t)a(t)\rangle = \infty, \tag{5.62}$$

for any pumping rate, $P \neq 0$. As a result, any nonzero pumping into the lasing mode will lead to unbounded growth in the number of atoms in the lasing cavity. This result invalidates one of the assumptions made in deriving this result - that there is a well localized, steady state number distribution about a mean value, $\bar{n}$. Specifically, the use of Eq. (5.38) in the equations for $\langle a^\dagger(t+\tau)a(t)\rangle$ is only justified if these equations ultimately lead to a narrow steady state. As an example where this is the case, we saw in section 5.4.1 that the assumption of a narrow steady state is self-consistently justified in the Born-Markov approximation.

If we use non-Morkovian output coupling, however, the steady state assumption is invalid. Physically we can understand this in the context of the results presented in Chapter 4. There we find that in the non-pumped case the output coupling mechanism does not empty the cavity for arbitrarily long times. Instead, there is a stable, non-dispersing state of the system which is an eigenstate of the total system Hamiltonian. As a result, with the inclusion of pumping into the cavity dynamics, the number of atoms which are never lost from the cavity grows without bound for increasing time.

In Chapter 4 we introduced gravitational acceleration into the system using a quasi-single particle theory. This destroyed the stable state and lead to an atom number which decayed to zero for sufficiently long times. Similarly we would expect physically that the presence of gravitational acceleration, or repulsive atom-atom interactions in the pumped system may lead to a finite steady state atom number, $\bar{n}$.

Solution methods similar to those described here may prove useful for describing output coupling in a full quantum mechanical input-output theory which also includes the effects of gravitational acceleration or atom-atom interactions.

A simpler theoretical description of loss and pumping from an atomic cavity makes use of a mean field theory of a pumped and damped cavity. In such a model, the condensate mode is described by a nonlinear Schrödinger equation. Gravitational acceleration and atom-atom interactions may then be included relatively easily into the model. In section 5.7 we present an extension of the model of Chapter 4 to produce a mean-field model of the pumped and damped atom laser.

5.7 Mean-field atom laser model

In section 4.9 we described output coupling from a trap to a continuum of free space modes using a quasi-single particle Hamiltonian. There we showed that the single mode approximation was a good one for our output coupling model. However, the inclusion of atom-atom interactions between trapped atoms will mean that the atoms occupy a self consistent mode of the many particle system which does not correspond to a single trap mode.

In the absence of atom-atom interactions, the single particle evolution we described is indentical to the multiparticle evolution. If we wish to consider the multi-particle evolution including interactions in full generality, then we begin with an atom field theory. We then assume that the atom-field, represented by a field operator, $\hat{\psi}(x,t)$ is in a coherent state, and consider the evolution of the scalar mean field, $\psi(x,t) = \langle\hat{\psi}(x,t)\rangle$. The evolution of the two coupled coherent matter waves, describing the trapped and untrapped atoms, is given by

$$i\hbar\frac{\partial\psi^a}{\partial t} = -\frac{\hbar^2}{2m}\frac{\partial^2}{\partial x^2}\psi^a + \frac{1}{2}m\omega^2x^2\psi^a + U_0^a|\psi^a|^2\psi^a - \hbar\Gamma^{\frac{1}{2}}e^{-ik_0x}\psi^b(x) \quad (5.63)$$

$$i\hbar\frac{\partial\psi^b}{\partial t} = -\frac{\hbar^2}{2m}\frac{\partial^2}{\partial x^2}\psi^b + mgx\sin(\theta)\psi^b + U_0^b|\psi^b|^2\psi^b - \hbar\Gamma^{\frac{1}{2}}e^{-ik_0x}\psi^a(x) \quad (5.64)$$

Here $\psi^a(x)$ and $\psi^b(x)$ denote the trapped and untrapped mean-fields respectively. The first three terms is Eq. (5.63) are the standard Gross-Pitaevskii (GP) equation and describe the evolution of a mean-field in a trapping potential. The third term describes the harmonic trapping potential of frequency ω. The fourth term in Eq. (5.63) describes the coupling to free space. Eq. (5.64) describes the evolution of the free space wavefunction under the effects of gravity, atom-atom interactions, and back coupling, respectively. Similar equations have been used by other authors to describe coupling between two traps [30], or between a trap and free space [31,32]

Eq. (5.63) and Eq. (5.64) are formally equivalent to the single-particle evolution presented in Chapter 4 in the case where $U_0^a = U_0^b = 0$ and the trap potential in Eq. (4.48) is assumed to be harmonic with trap frequency, ω.

We can solve Eq. (5.63)-Eq. (5.64) using the split operator method. If we begin with the initial condition

$$\psi^a(x) = \frac{-\Gamma^{\frac{1}{2}}\hbar\sqrt{2}\sigma_k}{(2\pi\sigma_k^2)^{\frac{1}{4}}}\,e^{-\sigma_k^2x^2}, \quad (5.65)$$

$$\psi^b(x) = 0, \quad (5.66)$$

and assume that $U_0^a = U_0^b = 0$. we obtain the plot shown in Fig. 5.1 for the number of atoms in the trap state at time t given by $\int|\psi^a(x,t)|^2\,dx$

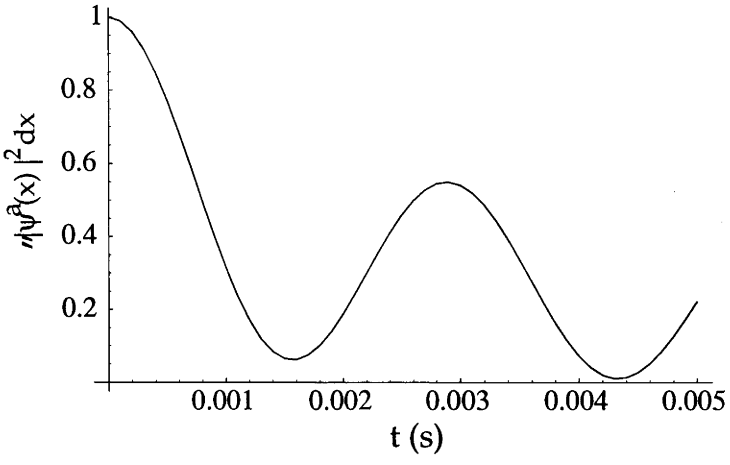

Figure 5.1: Plot of the number of atoms in the condensate mode, $N_c = \int |\psi^a(x)|^2 \, dx$ as a function of time. This plot is obtained by solving two coupled GP equations, without pumping and agrees with the results obtained using a multimode trap model, Fig 4.4.

The results shown in Fig. 5.1 agree with those obtained using the multimode split operator method shown in Fig. 4.4.

5.7.1 Addition of pumping to the model

Recent work by Kneer *et al.* provides a generic model of the atom laser using a modified Gross-Pitaevskii equation [33]. In this they add phenomenological gain and loss terms to the Gross-Pitaevskii equation. Here we have already modelled loss through the coupling terms between $\psi^a(x)$ and $\psi^b(x)$. We avoid reducing this loss term to a phenomenological exponential loss term here. Doing so is equivalent to making the Born-Markov approximation and is valid in regimes in which the output coupling rate is sufficiently small. Using the more general equations allows the behaviour of the system to be examined both in the Born-Markov regime and in regimes with higher coupling rate. However, as discussed in section 5.3, it is often possible trace over the pump modes in many realistic situations. This is because the pumping term is irreversible, due to coupling to the photon reservoir, so the effect of back action can be ignored.

We introduce into our equations a phenomenological pump term, identical to that used by Kneer *et al.* [33]. As we mentioned earlier, a pumping mechanism involves both a channel which pumps the lasing mode and a loss channel. In our earlier pump model, we considered injecting a series of excited state atoms at rate, r into a system. We assume here this injects the atoms into

uncondensed states. These then decayed into either the lasing mode or were lost into uncondensed modes at rates Γ_p and γ_u respectively. The number of uncondensed atoms at a given time, t is given by $N_u(t)$. Using these definitions [33], the pumping term is

$$H_{\text{gain}} = \frac{i\hbar}{2}\Gamma_p N_u \psi^a. \tag{5.67}$$

This is coupled to a rate equation, similar to those we discuss in Chapter 2 for the number of uncondensed atoms, $N_u(t)$:

$$\frac{dN_u}{dt} = r - \gamma_u N_u - \Gamma_p N_c N_u. \tag{5.68}$$

N_c is the number of condensed atoms, and can be expressed in terms of $\psi^a(x)$ as

$$N_c = \int |\psi^a(x)|^2 \, dx. \tag{5.69}$$

The full set of equations which describe the pumped and damped atom laser are

$$i\hbar\frac{\partial\psi^a}{\partial t} = -\frac{\hbar^2}{2m}\frac{\partial^2}{\partial x^2}\psi^a + \frac{1}{2}m\omega^2 x^2\psi^a + U_0^a|\psi^a|^2\psi^a - \hbar\Gamma^{\frac{1}{2}}e^{-ik_0x}\psi^b(x) + \frac{i\hbar}{2}\Gamma_p N_u\psi^a \tag{5.70}$$

$$i\hbar\frac{\partial\psi^b}{\partial t} = -\frac{\hbar^2}{2m}\frac{\partial^2}{\partial x^2}\psi^b + mgx\sin(\theta)\psi^b + U_0^b|\psi^b|^2\psi^b - \hbar\Gamma^{\frac{1}{2}}e^{-ik_0x}\psi^a(x) \tag{5.71}$$

$$\frac{dN_u}{dt} = r - \gamma_u N_u - \Gamma_p N_c N_u. \tag{5.72}$$

The description of pumping in these and the trap potential are identical to the model outlined in Kneer *et al* [33]. There however, they do not consider the evolution of the output level, $\psi^b(x)$, and assume that the loss mechanism is well described by exponential decay.

There are two main advantages in using the approach we present here. First, these equations allow us to investigate some simple features, such as the spectrum in momentum space of the output coupled atoms. We can also predict, and investigate the spatial distribution of these output coupled atoms for various coupling mechanisms. For instance, by considering the effect of a momentum kick, k_0 on the output. The second advantage is that, as we have noted in Chapter 4, the dynamics of the system become less and less Markovian as the output coupling rate increases. In practice, it may be simpler to produce atom lasers in a regime in which the coupling rate is small, and rely on a large build up of atom number in the condensate mode to provide a large

total flux of atoms. However, practically, this atom number build up is limited by the size of the trap. It may be important to run atom lasers in regimes which break or are close to breaking the standard Born-Markov approximations.

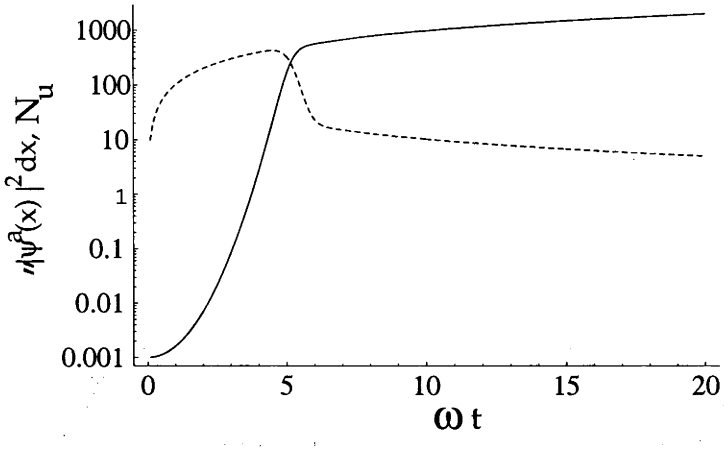

Figure 5.2: Plot of the number of atoms, N_c in the condensate mode (solid line) and the number of non-condensed atoms, N_u (dashed line) as a function of time (scaled by ω).

Fig. 5.2 shows a plot of the number of atoms in the condensate mode, given by $N_c = \int |\psi^a(x)|^2 \, dx$, versus time, t. The parameters used correspond to those presented in [33]. The initial state has $N_u = 0$, and $N_c = 10^{-3}$. The small initial seed state in the condensate is necessarily, as discussed by Kneer *et al.* to avoid the system settling on the unstable steady state solution in which there are zero atoms in the condensate. Other parameters are given in terms of ω, the trap frequency. The injection rate of uncondensed atoms is $r/\omega = 10^2$. The pump rate Γ_p into the condensate and the loss rate, γ_u are given by $\Gamma_p/\omega = \gamma_u/\omega = 10^{-2}$. The atom-atom interaction strength is given by $U_0/(\hbar\omega a) \approx 0.008$. The final parameter they give is the loss rate, γ_c out of the condensate. They give $\gamma_c/\omega = 10^{-2}$. In our case we do not have Markovian damping, however, from Eq. (4.13) in Chapter 4, we can obtain Γ in terms of γ_c. We use

$$\Gamma \approx 1.47 \, \gamma_c \omega_0. \tag{5.73}$$

We can investigate the behaviour of the condensate mode using this model. We are also able to investigate the output coupled state, for the various output coupling mechanisms. This allows us to consider the effect of momentum k_0 kicks and coupling rate on the output momentum spectrum. Using an out-

put coupling mechanism which does not make use of the Born and Markov approximations also allows effects due to the backaction of the reservoir to be taken into account in the case of large output coupling rates.

5.8 Conclusions

We have discussed the introduction of a pumping term into the output coupling theory presented in earlier chapters. We consider the input-output relations discussed in Chapter 3 with the addition of this pumping term. We also present a mean-field model of a pumped and damped atom laser which corresponds to an extension of the model proposed in Chapter 4. This model is similar in nature to a model proposed by Kneer *et al.* [33], however we model the output coupling explicitly here. This allows us to investigate the effect of various coupling rates and momentum kicks on the output spectrum, as well as the potential to describe output coupling in regimes where non-Markovian behaviour becomes significant. Further work will continue to analyse the consequences of this model in various parameter regimes and the comparison of these results with other atom laser models.

Chapter 6

Conclusions

With the production of Bose-Einstein condensates in alkali atoms, many experimental groups around the world are now focusing attention towards the goal of producing an atom laser [12, 13, 69–72]. In this thesis we have developed a number of theoretical models for describing the output coupling of atoms from a Bose-Einstein condensate and continuous atom lasers. We have also considered the pumping of BECs using spontaneous emission.

Three main methods have been used to describe atom lasers. These are rate equation models, quantum operator (master equation) models and mean-field models. Each of these have various advantages and disadvantages in terms of explaining the physics behind, and examining the characteristics of, an atom laser.

In this thesis, we have presented a rate equation model for an atom laser. We used this to demonstrate the presence of some fundamental features of a typical optical laser in our atom laser model. We have found a threshold condition on the pumping rate. Above threshold a large number of atoms build up in the lasing mode through Bose enhancement at the expense of higher order modes. We considered one possible physical implementation of this model involving hollow optical fibres. We also considered the use of a Raman transition to provide the output coupling mechanism from the atom laser. The lasers change the atoms to an untrapped state with the possibility of imparting a momentum kick to the atoms, providing an output direction for the beam. The pumping method involves spontaneous emission from an exited state to the lasing state. We calculated overlap factors and transition rates explicitly for the model.

The rate equation analysis presented, however, is limited in its ability to describe the output from an atom laser. We investigated the output properties of a single mode system coupled to a continuum of free space modes. In this work we developed solution methods for describing the output field obtained from an output coupling method based on state change. We demonstrated that the standard optical coupling Hamiltonian can be used to describe this output coupling, and developed analytic methods which produce solutions for the

output field in the broadband case. We also produced numerical solutions for non-broadband coupling. We discussed the output spectral width in free space in terms of the coupling rate and found, as dictated by the Heisenberg uncertainty principle, that slow coupling leads to a narrow spectral width.

In experiments which have been performed to date on output coupling atoms from BECs, the output coupling rates have been typically very large. The most obvious example of a coupling rate which is large occurs in switching off the trap. In the limit of large output coupling we found that the Born-Markov approximation becomes invalid. While the Born-Markov approximation is an extremely useful tool, this limit of small coupling rates may prove to be a significant one in a continuous atom laser. In an atom laser, the output flux will, for small coupling rates, be limited by the number of atoms which can be stored in an atom trap. We investigated the regimes of validity of the Born-Markov approximation and found that timescale conditions, similar to those required in optics, dictate the validity of the approximation. In atoms, however, these approximations fail for some realistic output coupling parameters. The differences in dynamics between the optical and atom cases are due to a combination of factors. These include the different parameters regimes in which atom lasers operate, the different dispersion relations between atoms and photons, and the nature of the atom reservoir. We have presented techniques in this thesis which describe the behaviour of a BEC output coupled to free space without having made the Born and Markov approximations. These techniques are also valid when the Born-Markov approximation is applicable.

Another important aspect of a continuous atom laser is a pump source. We considered a simple derivation of a pump term which is based on spontaneous emission. This derivation follows closely the optical pump derivation, and helps to provides an understanding of the physical processes which lead to the master equation term we use. We have discussed the nature of the output field in the Born-Markov regime. We also found that, in the exact equations, the presence of a stable, non-dispersing state of the system leads to a continuous build up in the number of atoms in the lasing mode, for long times. We found that the presence of gravitational acceleration or atom-atom repulsive interactions destroys this non-dispersing state. Future directions of this work may lead to the addition of gravitational effects and atom-atom interactions into the full input-output equations for a pumped and damped cavity.

We presented an alternative description of the pumped and damped atom laser using a mean-field theory approach. These techniques do not allow the consideration of the quantum statistics of the atom laser output, however they do allow a description of the output field to be obtained without the use of the Born-Markov approximation. The output of the atom laser is treated explicitly using a nonlinear Schrödinger equation, so that, unlike for techniques which model output coupling through a phenomenological damping term, the out-

put coupled atom dynamics are included explicitly.

In the future, experiments will almost certainly lead to the development of further pulsed and continuous atom laser sources. The possibility that an atom laser may be guided or created in a hollow optical fibre seems a very real one. Similarly, pumping mechanisms which involve spontaneous emission into a lasing mode are likely to be developed in future experimental work. To provide large output fluxes, output coupling methods may need to be developed which provide large coupling rates, and thus avoid making the Markov approximation. In regimes where the Born-Markov approximations are valid, the methods described in this thesis are useful for describing, explicitly, the nature of the output field. Furthermore, the investigation of the physics in the regime in which non-Markovian dynamics dominates, may lead to other new devices with uses and behaviour vastly different from the optical or atom lasers.

Volterra solution method.

In Chapter 3, Eq. (3.40) provides a general solution for the operator, $a(t)$ in terms of an inverse Laplace transform. This solution, however, is strictly only valid if this Laplace transform exists. We write the inverse Laplace transform here as

$$\mathcal{L}^{-1}\left\{\frac{a(0)}{s+\mathcal{L}[f'(t)](s)}\right\}(t), \tag{A.1}$$

using the derivation of $f'(t)$ given in Chapter 3. The existence of this inverse Laplace transform is related to the positions of the poles of

$$\frac{1}{s+\mathcal{L}[f'(t)](s)}, \tag{A.2}$$

and hence the zeros of $s+\mathcal{L}[f'(t)](s)$. In the work in Chapter 3, we assume broadband coupling to obtain an analytic expression for the output spectrum. More generally we can obtain the expression for $\mathcal{L}[f'(t)](s)$ in the case of a coupling function, $\kappa(k)$ which is gaussian, with standard deviation of σ_k. We also include a momentum kick of size k_0. The general result is then

$$\mathcal{L}(f')(s) \;=\; \Gamma c\frac{\sqrt{i}}{\sqrt{s-i\omega_0}}\,G_2(s), \tag{A.3}$$

where

$$\begin{aligned} G_2(s) = e^{-k_0^2/(2\sigma_k^2)}\,\exp\left[\frac{-im}{\hbar\sigma_k^2}\,(s-i\omega_0)\right]\,\times \\ \frac{1}{2}\left\{\exp\left[-\sqrt{\frac{2imk_0^2}{\hbar\sigma_k^4}}\,\sqrt{s-i\omega_0}\right]\left(1-\operatorname{erf}\left[\sqrt{\frac{-im}{\hbar\sigma_k^2}}\,\sqrt{s-i\omega_0}-\sqrt{\frac{-k_0^2}{2\sigma_k^2}}\right]\right)\right. \\ \left.+\exp\left[\sqrt{\frac{2imk_0^2}{\hbar\sigma_k^4}}\,\sqrt{s-i\omega_0}\right]\left(1-\operatorname{erf}\left[\sqrt{\frac{-im}{\hbar\sigma_k^2}}\,\sqrt{s-i\omega_0}+\sqrt{\frac{-k_0^2}{2\sigma_k^2}}\right]\right)\right\} \end{aligned} \tag{A.4}$$

This expression reduces to Eq. (3.51) in the broadband limit, $\sigma_k \to \infty$. In the broadband case, or in the finite coupling case with $k_0 = 0$, the expression $s + \mathcal{L}[f'(t)](s)$ tends towards s as $\mathrm{Re}[s] \to \infty$. That is, there is a value of s above which corresponds to the largest zero of $s + \mathcal{L}[f'(t)](s)$ and hence the largest pole of Eq. (A.2). In contrast, however, for $k_0 \neq 0$, the expression $s + \mathcal{L}[f'(t)](s)$, as given by Eq. (A.3), oscillates continuously through zero, for large s. As a result, there is no largest pole of Eq. (A.2) and the inverse Laplace transform does not exist.

Physically, the case of finite coupling with a k_0 kick is nevertheless a valid one. In this case, a solution can be obtained through a general volterra equation solver. If we consider the general equation, Eq. (3.42), given in Chapter 3, we can write this in the form of a linear Volterra equation of the second kind,

$$F(t) = G(t) + \int_0^t K(t,s)F(s)\,ds, \tag{A.5}$$

where

$$\begin{aligned} K(t,s) &= -A'(t-s) \\ &= -\int_0^{t-s} dt' \int_{-\infty}^{\infty} |\kappa(k)|^2\, e^{i(\omega_0-\omega_k)t'}, && \text{(A.6)} \\ F(t) &= a'(t), && \text{(A.7)} \\ G(t) &= a(0) - \int_0^t dt' \int_{-\infty}^{\infty} |\kappa(k)|^2\, e^{i(\omega_0-\omega_k)t'}\, b_k(0). && \text{(A.8)} \end{aligned}$$

We discuss the solution of equations of this form in Chapter 5 and in Appendix D.

Appendix B

Integrals for $M_k(t)$

To obtain the expression for $M_k(t)$ we given in Eq. (3.65) we must evaluate the integral

$$\int_0^\infty u e^{-u^2/(4t)} \mathcal{L}^{-1}\{h(s)\}\, du, \tag{B.1}$$

for each of the terms in the expression for $\mathcal{L}^{-1}\{h(u)\}(t)$. These integrals are given as follows. The first three terms are obtained from the integral

$$\int_0^\infty u e^{-u^2/(4t)}\, e^{\alpha u} \;=\; 2t \;+\; 2\alpha t^{3/2}\sqrt{\pi}\, e^{\alpha^2 t}\,(1 - \mathrm{Erf}[-\alpha\sqrt{t}]). \tag{B.2}$$

The fourth term in the expression for $M_K(t)$ is obtained upon evaluating

$$\int_0^\infty u e^{-u^2/(4t)} \cos[\sqrt{c}t] \;=\; \pi t L_{1/2}^{-1/2}(ct) e^{-ct}, \tag{B.3}$$

where we have introduced a generalized Laguerre polynomial, $L_{1/2}^{-1/2}(ct)$ here as defined in Chapter 3. Finally the integral

$$\int_0^\infty u e^{-u^2/(4t)} \sin[\sqrt{c}t] \;=\; 2\sqrt{\pi c} t^{-3/2}\, e^{-ct}, \tag{B.4}$$

gives the final term in the expression for $M_k(t)$, Eq. (3.65).

Appendix C

Derivation of Born-Markov master equation

We provide a review of the derivation of the Born-Markov master equation for a general system [7,51,56,57]. We consider a general interaction Hamiltonian, given by H_{sr}. This describes both the atom and optical case.

We begin with a general Hamiltonian of the form given in Eq. (3.22). From this Hamiltonian one can obtain an equation of motion for the density operator of the system plus reservoir, ρ_{tot}. This is equivalent to the Heisenberg (or Schrödinger) equations of motion. We transform the equations into the interaction picture, separating the motion generated by $H_s + H_r$ from the motion generated by the interaction H_{sr}. Thus we have

$$\tilde{\rho}_{\text{tot}}(t) = e^{i(H_s+H_r)t/\hbar}\, \rho_{\text{tot}}(t)\, e^{-i(H_s+H_r)t/\hbar}, \tag{C.1}$$

and similarly for $\widetilde{H}_{sr}(t)$. This leads to the following equation which is exact.

$$\begin{aligned} \frac{d\tilde{\rho}_{\text{tot}}}{dt} &= \frac{-i}{\hbar}\left[\widetilde{H}_{sr}(t), \rho_{\text{tot}}(0)\right] - \\ &\quad \frac{1}{\hbar^2}\int_0^t dt' \left[\widetilde{H}_{sr}(t), \left[\widetilde{H}_{sr}(t'), \tilde{\rho}_{\text{tot}}(t')\right]\right] \end{aligned} \tag{C.2}$$

We now wish to produce a master equation in the Born and Markov approximations. The first assumption we make regards the nature of the reservoir when the interaction is turned on at time $t = 0$. We assume that at $t = 0$ no correlations exist between the system and reservoir. This means that $\rho_{\text{tot}}(0) = \rho(0) \otimes R(0)$, where we use $\rho(0)$ and $R(0)$ to describe the initial system and reservoir density operators respectively. We then trace over the reservoir (using $\tilde{\rho} = \text{Tr}_R\{\tilde{\rho}_{\text{tot}}\}$) in Eq. (C.2), leading to,

$$\begin{aligned} \frac{d\tilde{\rho}}{dt} &= \frac{-1}{\hbar^2}\int_0^t dt' \,\text{Tr}_R\{ \\ &\quad \left[\widetilde{H}_{sr}(t), \left[\widetilde{H}_{sr}(t'), \tilde{\rho}_{\text{tot}}(t')\right]\right]\}, \end{aligned} \tag{C.3}$$

where we have eliminated the term

$$\mathrm{Tr}_R\left\{\left[\widetilde{H}_{sr}(t), \rho_{\mathrm{tot}}(0)\right]\right\}$$

with the assumption that $\mathrm{Tr}_R\left\{\widetilde{H}_{sr}R(0)\right\} = 0$. This can be arranged by including $\mathrm{Tr}_R(H_{sr}R(0))$ in the system Hamiltonian.

We are now ready to make our first major approximation - the Born approximation. We have stated previously that ρ_{tot} factorizes at $t = 0$ into a system and reservoir part. At later times, however, correlations between the system and reservoir may arise due to their coupling via the interaction Hamiltonian. The Born approximation involves assuming that this coupling is sufficiently weak that at all times $\rho_{\mathrm{tot}}(t)$ should only show deviations of order H_{sr} from an uncorrelated state. We also assume that the reservoir is a large system which is not affected by its coupling to the system. Thus the Born approximation involves neglecting terms higher than second order in H_{sr}, and writing $\widetilde{\rho}_{\mathrm{tot}}(t') = \widetilde{\rho}(t') \otimes R(0)$ in Eq. (C.3) above. This gives

$$\begin{aligned}\frac{d\widetilde{\rho}}{dt} &= \frac{-1}{\hbar^2}\int_0^t dt' \,\mathrm{Tr}_R\{ \\ &\quad \left[\widetilde{H}_{sr}(t), \left[\widetilde{H}_{sr}(t'), \widetilde{\rho}(t') \otimes R(0)\right]\right]\Big\}, \end{aligned} \tag{C.4}$$

This equation is non-Markovian due to the dependence of $\widetilde{\rho}$ on t'. It is the general form of the non-Markovian master equation given in Eq. (4.11). The second major approximation is the Markov approximation, in which we replace $\widetilde{\rho}(t')$ by $\widetilde{\rho}(t)$. Thus, the master equation in the Born-Markov approximation becomes

$$\begin{aligned}\frac{d\widetilde{\rho}}{dt} &= \frac{-1}{\hbar^2}\int_0^t dt' \,\mathrm{Tr}_R\{ \\ &\quad \left[\widetilde{H}_{sr}(t), \left[\widetilde{H}_{sr}(t'), \widetilde{\rho}(t) \otimes R(0)\right]\right]\Big\}, \end{aligned} \tag{C.5}$$

This equation is the general form of Eq. (4.12).

Appendix D

Solution to Volterra equation

In Chapter 5 we solve a linear first order Volterra integro-differential equation of the form

$$\frac{df(t)}{dt} - \int_0^t k(t,s)f(s)ds = g(t). \tag{D.1}$$

In writing the equation in this general form we identify $f(t)$ in the equation above with $\langle a^\dagger(t)a(t)\rangle$ in our equations. $k(t,s)$ is the kernal of the integral and is given in our particular equation by $-2\mathrm{Re}\,[f^*(t-s)\,M'(t,s)]$. The function $g(t)$ in the general form above corresponds to r in our equations and is a constant.

To solve Eq. (D.1) we first write this first order equation as a Volterra equation of the second kind. That is, we integrate and rearrange the terms in Eq. (D.1) to obtain

$$F(t) = G(t) + \int_0^t K(t,s)F(s)\,ds, \tag{D.2}$$

where, now we have

$$K(t,s) = \int_s^t k(\tau,s)d\tau, \tag{D.3}$$

$$F(t) = f(t), \tag{D.4}$$

$$G(t) = f(0) + rt. \tag{D.5}$$

Next, we observe that both $K(t,s)$ and $G(t)$ are continuous. In particular, we note that this is trivially true for the broadband case we examine in Chapter 5 in which have an analytic solution for each of these functions. Having written the equation in the form given above, we now make use of the following general theorem of Volterra equations, [68].

Theorem 1 *If $K(t,s)$ and $G(t)$ are continuous then the unique continuous solution*

to the equation

$$F(t) = G(t) + \int_0^t K(t,s)F(s)ds, \tag{D.6}$$

is given by

$$F(t) = G(t) + \int_0^t \Gamma(t,s)G(s)ds \tag{D.7}$$

where

$$\Gamma(t,s) = \sum_{i=1}^{\infty} K_i(t,s), \tag{D.8}$$

$$K_1(t,s) = K(t,s), \tag{D.9}$$

$$K_n(t,s) = \int_s^t K(t,\tau)\, K_{n-1}(\tau,s)\, d\tau. \tag{D.10}$$

This theorem leads to the solution quoted in Eq. (5.57) for our case.

Bibliography

[1] A.M. Guzman M. Moore and P. Meystre, *'Theory of a coherent atomic-beam generator'*, Phys. Rev. A **53**, 977 (1996).

[2] M.H. Anderson, J.R. Ensher, M.R. Matthews, C.E. Wieman, and E.A. Cornell, *'Observation of Bose-Einstein condensation in a dilute atomic vapor'*, Science **269**, 198 (1995).

[3] K.B. Davis, M.O. Mewes, M.R. Andrew, N. J. van Druten, D.S. Durfee, D.M. Kurn, and W. Ketterle, *'Bose-Einstein condensation in a gas of sodium atoms'*, Phys. Rev. Lett. **75**, 3969 (1995).

[4] M.-O. Mewes, M.R. Andrews, N.J. van Druten, D.M. Kurn, D.S. Durfee, and W. Ketterle, *'Bose-Einstein condensation in a tightly confining DC magnetic trap'*, Phys. Rev. Lett. **77**, 416 (1996).

[5] C.C. Bradley, C.A. Sackett, J.J. Tollett, and R.G. Hulet, *'Evidence of Bose-Einstein condensation in an atomic gas with attractive interactions'*, Phys. Rev. Lett. **75**, 1687 (1995).

[6] A. E. Siegman, *Lasers*, University Science Books, California, 1986.

[7] D.F. Walls and G.J. Milburn, *'Quantum Optics'*, Springer-Verlag, Berlin, 1994.

[8] H.M. Wiseman, *'What is an atom laser'*, Phys. Lett. A **56**, 2068 (1997).

[9] M. Holland, K. Burnett, C. Gardiner, J.I. Cirac, and P. Zoller, *'Theory of an atom laser'*, Phys. Rev. A **54**, R1757 (1996).

[10] C.M. Savage, J.J. Hope, and G.M. Moy, 'An atom laser based on Raman Transitions', in *Satellite meeting on Atom Optics, Cairns, IQEC*, 1996.

[11] V.I. Yukalov, E.P. Yukalova, and V.S. Bagnato, *'Non-ground-state Bose-Einstein condensates of trapped atoms'*, Phys. Rev. A **56**, 4845 (1997).

[12] M.-O. Mewes, M.R. Andrews, D.M. Kurn, D.S. Durfee, C.G. Townsend, and W. Ketterle, *'An output coupler for Bose condensed atoms'*, Phys. Rev. Lett. **78**, 582 (1997).

[13] M.R. Andrews, C.G. Townsend, H.J. Miesner, D.S. Durfee, D.M. Kurn, and W. Ketterle, *'Observation of interference between two Bose condensates'*, Science **275**, 637 (1997).

[14] R. Glauber, *'Optical coherence and photon statistics'*, Quantum Optics and Electronics. (1965).

[15] R.J. Dodd, C.W. Clark, M. Edwards, and K. Burnett, *'Characterizing the coherence of Bose-Einstein condensates and atom lasers'*, Optics Express **1**, 284 (1997).

[16] W. Ketterle and Hans-Joachim Miesner, *'Coherence properties of Bose-Einstein condensates and atom lasers'*, Phys. Rev. A **56**, 3291 (1997).

[17] E.A. Burt, R.W. Ghrist, C.J. Myatt, M.J. Holland, E.A. Cornell, and C.E Wieman, *'Coherence, Correlations and Collisions: What one learns about Bose-Einstein Condensates from their Decay'*, Phys. Rev. A **79**, 337 (1997).

[18] K. Molmer, *Optical coherence, a convenient fiction*, Phys. Rev. A **55**, 3195 (1997).

[19] S. M. Barnett, K. Burnett, and J. A. Vaccaro, *'Why a condensate can be thought of as having a definite phase'*, Journal of Research of the National Institute of Standards and Technology **101**, 593 (1986).

[20] R.J.C. Spreeuw, T. Pfau, U. Janicke, and M. Wilkens, *'Laser-like scheme for atomic-matter waves'*, Europhys. Lett. **32**, 469 (1995).

[21] M. Olshanii, Y. Castin, and J. Dalibard, 'A model for an atom laser', in *'Proceedings of the XII conference on laser spectroscopy'*, World Scientific, New York, 1995.

[22] G.M. Moy, J.J. Hope, and C.M. Savage, *'An atom laser based on Raman transitions'*, Phys. Rev. A **55**, 3631 (1997).

[23] H.M. Wiseman and M.J. Collett, *'An atom laser based on dark-state cooling'*, Phys. Lett. A **202**, 246 (1995).

[24] H.M. Wiseman, A. Martins, and D. Walls, *'An atom laser based on evaporative cooling'*, Quant. Semiclass. Optics **8**, 737 (1996).

[25] N. Davidson, H. Lee, M. Kasevich, and S. Chu, *'Raman cooling of atoms in 2-dimensions and 3-dimensions'*, Phys. Rev. Lett. **72**, 3158 (1994).

[26] J. Dalibard and C. Cohen-Tannoudji, J. Opt. Soc. Am. B **2**, 1707 (1985).

[27] C. Cohen-Tannoudji, 'Atomic motion in laser light', in *Fundamental systems in quantum optics: Les Houches session LIII*, North-Holland, Amsterdam, 1992.

[28] W. Petrich, M. Anderson, J.R. Ensher, and E.A. Cornell, *'Stable, tightly confining magnetic trap for evaporative cooling of neutral atoms'*, Phys. Rev. Lett. **74**, 3352 (1995).

[29] D. M. Stamper-Kurn, M. R. Andrews, A. P. Chikkatur, S. Inouye, H.-J. Miesner, J. Stenger, and W. Ketterle, *'Optical confinement of a Bose-Einstein condensate'*, Phys. Rev. Lett. **80**, 2027 (1998).

[30] R.J. Ballagh, K. Burnett, and T.F. Scott, *'Theory of an output coupler for Bose-Einstein condensed Atoms'*, Phys. Rev. Lett. **78**, 1607 (1997).

[31] H. Steck, M. Narashewski, , and H. Wallis, *'Output of a pulsed atom laser'*, Phys. Rev. Lett **80**, 1 (1998).

[32] W. Zhang and D.F. Walls, *'Gravitational and collective effects in an output coupler for a Bose-Einstein condensate in an atomic trap'*, Phys. Rev. A **57**, 1248 (1998).

[33] B. Kneer, T.Wong, K. Vogel, W.Schleich, and D.Walls, 'Generic model of an atom laser', 1998.

[34] N. Davidson, H. Lee, C.S. Adams, M. Kasevich, and S. Chu, *'Long atomic coherence times in an optical dipole trap'*, Phys. Rev. Lett. **74**, 1311 (1995).

[35] D. J. Harris and C.M. Savage, *Atomic gravitational cavities from hollow optical fibers*, Phys. Rev. A **51**, 3967 (1995).

[36] J.I. Cirac and M. Lewenstein, *'Pumping atoms into a Bose-Einstein condensate in the boson-accumulation regime'*, Phys. Rev. A **53**, 2466 (1996).

[37] S. Marksteiner, C.M. Savage, P. Zoller, and S.L. Rolston, *'Coherent atomic waveguides from hollow optical fibers - quantized atomic motion'*, Phys. Rev. A **50**, 2680 (1994).

[38] C.M. Savage, S. Marksteiner, and P. Zoller, 'Atomic waveguides and cavities from hollow optical fibers', in *Fundamentals of Quantum Optics III*, Springer-Verlag, Berlin, 1993.

[39] H. Ito et al., *'Optical potential for atom guidance in a cylindrical-core hollow fiber'*, Opt. Comm. **115**, 57 (1995).

[40] M.J. Renn, E.A Donley, E.A. Cornell, C.E. Wieman, and D.Z. Anderson, *'Evanescent-wave guiding of atoms in hollow optical fibers'*, Phys. Rev. A **53**, 648 (1996).

[41] H. Ito, T. Nakata, K. Sakaki, M. Ohtsu, K.I. Lee, and W. Jhe, *'Laser spectroscopy of atoms guided by evanescent waves in micron-sized hollow optical fibers'*, Phys. Rev. Lett. **76**, 4500 (1996).

[42] J.P. Dowling and J. Gea-Banacloche, *'Evanescent light-wave atom mirros, resonators, waveguides and traps'*, Adv. At. Mol. Opt. Phys. **36** (1996).

[43] M.A. Ol'Shanii, Y.B. Ovchinnikov, and V.S. Letokhov, *'Laser guiding of atoms in a hollow optical fibre'*, Opt. Comm. **98**, 77 (1993).

[44] M.J. Renn, D. Montgomery, O. Vdovin, D.Z. Anderson, C.E. Wieman, and E.A. Cornell, *'Evanescent-wave guidin of atoms in hollow optical fibres'*, Phys. Rev. Lett. **75**, 3253 (1995).

[45] J.J Hope and C.M. Savage, 'Hollow optical fibre atom waveguides', in *Coherence and Quantum Optics VII*, Plenum, New York, 1996.

[46] G.P. Agrawal, *'Nonlinear Fibre Optics'*, Academic Press, London, 1989.

[47] T. Pfau, S. Spälter, Ch. Kurtsiefer, C.R. Ekstrom, and J. Mylnek, *'Loss of spatial coherence by a single spontaneous emission'*, Phys. Rev. Lett. **73**, 1223 (1994).

[48] J.J. Hope and C.M. Savage, *'Mechanical Potentials Due to Raman Transitions'*, Phys. Rev. A **53**, 1697 (1996).

[49] J.J. Hope and C.M. Savage, *'Stimulated Enhancement of Cross-Section by a Bose-Einstein Condensate'*, Phys. Rev. A **54**, 3117 (1996).

[50] C. Cohen-Tannoudji, B. Diu, and F. Laloe, *Quantum Mechanics*, Wiley, New York, 1977.

[51] R. Loudon, *'The quantum theory of light'*, Clarendon Press, Oxford, 1983.

[52] K. Moler, D. Weiss, M. Kasevich, and S. Chu, *'Theoretical analysis of velocity-selective Raman transitions'*, Phys. Rev. A **45**, 342 (1992).

[53] A.L. Fetter and J.D. Walecka, *'Quantum Theory of Many-Particle Systems'*, McGraw-Hill, New York, 1971.

[54] J.J. Hope, *'A Theory of Input and Output of Atoms from an Atomic Trap'*, Phys. Rev. A **55**, R2531 (1997).

[55] F.Oberhettinger and L.Badii, *Tables of Laplace Transforms*, Springer Verlag, NewYork, 1973.

[56] H. Carmichael, *'An open systems approach to quantum optics'*, Springer Verlag, New York, 1991.

[57] C. Cohen-Tannoudji, J. Dupont-Roc, and G. Grynberg, *Atom-photon interations*, Wiley, New York, 1992.

[58] G. Moy and C.M. Savage, 'Output coupling from an atom laser by state change', 1997.

[59] M.-O. Mewes, M.R. Andrews, N.J. van Druten, D.M. Kurn, D.S. Durfee, C.G. Townsend, and W. Ketterle, *'Collective excitations of a Bose-Einstein condensate in a magnetic trap'*, Phys. Rev. Lett. **77**, 988 (1996).

[60] K. Huang, *'Statistical Mechanics'*, Wiley, New York, 1987.

[61] W. Louisell, *'Quantum statistical properties of radiation'*, Wiley, Oxford, 1990.

[62] P.Lambropoulos S. Bay and K. Molmer, *'Fluorescence into flat and structured radiation continua: An atomic density matrix without a master equation')*, Phys. Rev. Lett. **79**, 14 (1997).

[63] M. Kasevich and S. Harris, *'non-linear optical properties of a non interacting Bose gas'*, Optics Letters. **21**, 677 (1996).

[64] E.M. Lifshit and L.P. Pitaevskii, *'Statistical Physics'*, Pergamon Press, Oxford, 1980.

[65] A.Schenzle M. Naraschewski and H. Wallis, Phys. Lett. A **56**, 603 (1997).

[66] M.O. Scully and W.E. Lamb, *'Quantum theory of an optical Maser, I. General theory.'*, Phys. Rev.A **159**, 208 (1967).

[67] J.I. Cirac, C.W. Gardiner, M. Naraschewski, and P. Zoller, *'Continuous observation of interference fringes from Bose condensates'*, Phys. Rev. A **54**, 3714 (1996).

[68] P. Linz, *'Analytical and Numerical methods for Volterra equations'*, Siam, Philadelphia, 1985.

[69] T. Hansch I. Bloch and T. Esslinger, *An atom laser with a cw output coupler*, Phys. Rev. Lett. **82**, 3008 (1999).

[70] B.P. Anderson and M.A. Kasevich, *'Macroscopic Quantum interference from atom tunnel arrays'*, Science **282**, 1686 (1998).

[71] E.W. Hagley, L. Deng, M. Kozuma, J. Wen, K. Helmerson, S.L. Rolston, and W.D Phillips, *'A well-collimated quasi-continuous atom laser'*, Science **283**, 1706 (1999).

[72] J.L. Martin, C.R. McKenzie, N.R. Thomas, J.C. Sharp, D.M. Warrington, P.J. Manson, W.J. Sandle, and A.C. Wilson, *'Output coupling of a Bose-Einstein condensate formed in a TOP trap'*, J. Phys. B **32**, 3065 (1999).